Photoconductivity studies on some semiconducting thin films for photovoltaic applications

Thesis submitted to
Cochin University of Science and Technology
for the award of the degree of

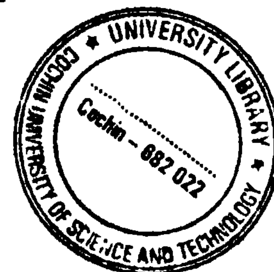

DOCTOR OF PHILOSOPHY

By

S. B. SYAMALA

Thin Film Photovoltaic Division
Department of Physics
Cochin University of Science and Technology
Kochi 682022
India

January 2004

Dr. C.Sudha Kartha
Reader

Department of Physics
Cochin University of
Science and Technology
Cochin-682 022, India

19th January 2004

Certificate

This is to certify that this thesis entitled **"Photoconductivity studies on some semiconducting thin films for photovoltaic applications"** is a report of the original work carried out by **Smt. S.B. Syamala** under my supervision and guidance in the Department of Physics, Cochin University of Science and Technology, Kochi. No part of the work reported in this thesis has been presented for any other degree from any other institution.

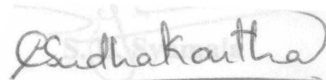

Dr. C.Sudha Kartha

Ph(off):+91484-2577404 Fax:+91484-2577595 Email : csk@cusat.ac.in

Declaration

I hereby declare that the present work entitled **"Photoconductivity studies on some semiconducting thin films for photovoltaic applications"** which will be submitted is based on the original work done by me under the guidance of **Dr. C. Sudha Kartha**, Reader, Dept. of Physics, Cochin University of Science and Technology, Kochi-682 022 has not been included in any other thesis submitted previously for the award of any degree.

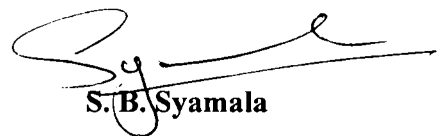

S. B. Syamala

Kochi-22
19th January 2004

Acknowledgements

At the very outset I would like to express my deep indebtedness to Dr. C. Sudha Kartha, Reader, Department of Physics whose invaluable guidance made this study possible. Prof. Dr. K.P. Vijayakumar, Professor and Head of the Department of Physics lent me his unstinted support during the course of my research and gave this study new dimension. Let me place on record my deep sense of gratitude to him.

I place on record my sincere appreciation to all the members of the faculty of Physics, Cochin University of Science and Technology for all the support given to me to complete this study successfully.

My research colleagues in the Department of Physics, Cochin University of Science and Technology deserve to be acknowledged with gratitude for their endless and untiring support during all the stages of this study. The Non-Teaching staff in the Department of Physics were all helpful and I thank one and all for their support.

Prof. Dr. Y. Kashiwaba of Department of Electrical and Electronic Engineering of the Iwate University, Morioka, Japan needs special mention of thanks for his contribution in conducting XPS analysis.

My study made lots of progress during my Faculty Improvement Programme and I acknowledge with gratitude the timely support of The University Grants Commission for sanctioning the fellowship. The Principals of N.S.S. College, Cherthalla and N.S.S. College for Women, Trivandrum, who were holding posts during my period of study, are gratefully remembered. The encouragement given to me by my colleages (teaching and non teaching) at the NSS College, Cherthalla and N.S.S. College for Women, Thiruvananthapuram deserve special mention.

Prof. Baby Thomas [Retired], Department of English, Newman College, Thodupuzha needs to be mentioned individually for fine tuning this report to enhance the quality of its presentation. I also place on record my gratitude to Mr. N. Jaykrishnan who has spared his valuable time in presenting this thesis in its final form.

I thank each and every one connected with me personally and officially for the moral support they rendered to me during the past years.

S. B. SYAMALA

CONTENTS

Preface

Chapter 1

Introduction

1.1 Introduction to electrical and optical properties of semiconducting thin films. 1
1.2 Lifetime measurements- different techniques. 22
1.2.1 Steady state methods
1.2.2 Transient methods
1.2.3 Modulation method
1.2.4 Stored charge method
1.3 Effects of dopants and temperature on lifetime 35
1.4 Importance of lifetime measurements 41

Chapter 2

Photoconductivity Studys on CBD CdS thin films

2.1 Introduction 47
2.2 Preparation of CBD CdS thin films 49
2.3 Photoconductive decay measurements 50
2.3.1 Experimental setup
2.3.2 Photoconductivity decay time measurements at room temperature in air and vacuum
2.3.3 Decay time variation with temperature
2.3.4 Effect of thickness
2.4 Conclusion 65

Chapter 3

Photoconductivity studies on γ-In_2Se_3 thin films

3.1 Introduction 69
3.2 Preparation of γ-In_2Se_3 thin films 71
3.3 Steady state photoconductivity studies at room temperature 74

3.4 Variation of decay time at room temperature for samples prepared at different temperatures 74
3.5 Variation of decay time with sample temperature 77
3.6 Effect of Indium concentration on decay time 81
3.7 Dark conductivity measurements 83
3.8 Thermally stimulated current measurements (TSC) 83
3.9 Conclusion 85

Chapter 4

Photoconductivity studies on $CuInSe_2$ thin films

4.1 Introduction 89
4.2 Preparation of $CuInSe_2$ thin films 91
4.3 Experimental set up 93
4.4 Variation of nature of photoconductivity with Cu concentration in the film 93
4.5 Conclusion 101

Chapter 5

Photoconductivity studies on $CuInS_2$ thin films

5.1 Introduction 105
5.2 Preparation of $CuInS_2$ thin films 106
5.3 Experimental set up 107
5.4 Nature of photoconductivity in $CuInS_2$ thin films 107
5.5 Variation of photoconductivity with Cu/In and S/Cu molar ratio in the solution 114
5.6 Conclusion 114

Chapter 6

Conclusion 117

List of publications 123

List of symbols and abbreviations 125

PREFACE

With the advent of characterization techniques, a number of materials reached the advanced state of development when their properties were in demand to provide specific functions. Photoconductivity (PC) processes may be the most suitable technique for obtaining information about the states in the gap. It finds applications in photovoltaics, photo detection and radiation measurements. The main task in the area of photovoltaics, is to increase the efficiency of the device and also to develop new materials with good opto-electronic properties useful for energy conversion, keeping the idea of cost effectiveness. Photoconduction includes generation and recombination of carriers and their transport to the electrodes. So thermal relaxation process, charge carrier statistics, effects of electrodes and several mechanisms of recombination are involved in photoconductivity.

A major effect of trapping is to make the experimentally observed decay time of photocurrent, longer than carrier lifetime. If no trapping centers are present, then observed photocurrent will decay in the same way as the density of free carriers and the observed decay time will be equal to carrier lifetime. If the density of free carriers is much less than density of trapped carriers, the entire decay of photocurrent is effectively dominated by the rate of trap emptying rather than by the rate of recombination.

In the present study, the decay time of carriers was measured using photoconductive decay (PCD) technique. For the measurements, the film was loaded in a liquid Helium cryostat and the temperature was controlled using Lakshore Auto tuning temperature controller (Model 321). White light was used to illuminate the required area of the sample. Heat radiation from the light source was avoided by passing the light beam through a water filter. The decay

current, after switching off the illumination, was measured using a Kiethely 2000 multimeter. Sets of PCD measurements were taken varying sample temperature, sample preparation temperature, thickness of the film, partial pressure of Oxygen and concentration of a particular element in a compound. Decay times were calculated using the rate window technique, which is a decay sampling technique particularly suited to computerized analysis. For PCD curves with two well-defined regions, two windows were chosen, one at the fast decay region and the other at the slow decay region. The curves in a particular window were exponentially fitted using Microsoft Excel 2000 programme. These decay times were plotted against sample temperature and sample preparation temperature to study the effect of various defects in the film. These studies were done in order to optimize conditions of preparation technique so as to get good photosensitive samples, useful for photovoltaic applications.

Materials selected for the study were CdS, In_2Se_3, $CuIn_2Se_3$ and $CuInS_2$. Photoconductivity studies done on these samples are organised in six chapters including introduction and conclusion. The chapter wise description of the content is as follows.

First chapter includes an introduction to electrical and optical properties of semi conducting thin films, different techniques of lifetime measurements, effects of dopants and temperature on lifetime and importance of lifetime measurements. The first part of the chapter pictures the theory of photoconductivity. In the later section, the measurement of decay time and the study of its variation with temperature and dopants, as a tool to characterize a photoconducting material, are explained.

The second chapter describes photoconductivity studies on CBD CdS thin films. CdS is a wide band gap material. It is used as a window material in different solar cells. Polycrystalline CdS thin film used for this study is prepared

using Chemical bath deposition (CBD), which is simple, low cost and large area deposition is possible through this method. Experimental set up to measure the decay time of carriers in this material is explained in this chapter. Photoconductivity and decay time variation with three different thicknesses of CdS thin film are studied at room temperature in air. It is found that as thickness increases, photoconductivity also increases. When measurements were taken with the sample in air, photocurrent was very low which was attributed to the presence of recombination centers formed by chemisorbed oxygen. It is also confirmed from the XPS analysis. The decay time variation with temperature shows the presence of various defects like grain boundary defect, the presence of Chlorine in sulphide ion vacancy and Cadmium Sulphur vacancy complexes. These defects were detected using Thermally Stimulated Current measurement (TSC) technique also.

In third chapter, PC studies on γ-In_2Se_3 thin film are described. It includes introduction, preparation of the film, and steady state and transient PC studies on this film. γ-In_2Se_3 is an n-type semiconductor with high absorption coefficient and its energy gap is 1.8 eV. A brief explanation of the preparation of this film is given in this chapter. Steady state PC studies show that PC decreases with sample preparation temperature. The decay time of charge carriers also decreased with sample preparation temperature. Decay time variation study with sample temperature shows that there are two defects, which release charge carriers at 200 K and 300 K. Activation energies of these defects were obtained from TSC and dark conductivity studies. As the sample preparation temperature is increased, the defect releasing charge carrier at 300 K is decreased. The other one existed in all the samples. The defect corresponding to 300 K increased as Indium concentration in the film increased. From dark conductivity measurements only the defect corresponding to 300 K could be identified, whereas the other defect could be identified using TSC technique.

Fourth chapter describes photoconductivity studies on $CuInSe_2$ thin films. It includes introduction to material, preparation of thin film and transient photoconductivity studies done on this material by varying Cu concentration. $CuInSe_2$ film is prepared using Stacked Elemental Layer (SEL) technique. The thickness of the layers of Selenium, Indium and Copper were chosen in such a way that the film formed will be nearly stoichiometric with Cu:In:Se ratio 1:1:2. PC studies are done on a set of samples by varying Cu:In ratio from 1.3 to 0.45. In Copper rich film (sample having Cu:In ratio 1.3) photoconductivity decreased on illumination. This property of negative photoconductivity decreased as concentration of Copper in the film decreased. Photoconductivity became positive for samples having Cu:In ratio 0.9. Decay time vs. sample temperature study showed an increase in decay time around room temperature. The maximum decay time at this temperature was around 1000 ms. As Cu:In ratio decreased to 0.45, this decay time at room temperature decreased to 400 mS and the decay time vs. sample temperature studies show an additional peak around 150 K for this sample.

Fifth chapter pictures photoconductivity studies done on spray pyrolised $CuInS_2$ thin films. Introduction and preparation of the material is also described in the first part of the chapter. Photoconductivity studies were done on samples varying Cu:In ratio from 0.5 to 1.5 in the solution keeping S:Cu molar ratio constant at 4. Photo response was found only in the sample prepared from the solution containing Cu:In molar ratio 0.5. On varying S:Cu ratio from 3 to 8 keeping Cu:In ratio at 0.5, photoconductivity was maximum for the sample prepared from a solution containing S:Cu ratio5. Another observation was that photocurrent was high when the sample was in air and it reduced on keeping the sample in vacuum for longer time.

Sixth chapter is a summary of the whole work done for this thesis. The major results obtained in this study are highlighted.

Chapter 1

Introduction

1.1 Introduction to semiconductor optical and electrical properties

After the invention of bipolar transistor there was a significant development in the material characterization as well as device fabrication, based on the optical and electrical properties of semi conducting materials. With the advent of the characterization techniques a number of materials reached the advanced state of development, when their properties are in demand to provide specific functions (1). First and foremost of these materials is silicon. Other examples are GaAs, AlAs, GaP and InP.

Optical and electrical properties of semiconductors are determined by :

1. The chemical composition of the pure perfect crystal – This determines intrinsic properties such as the fundamental energy gap and effective masses of the carriers.

2. Lattice defects such as vacant and interstitial sites and complexes there of, which introduce electron states within the band gap of the material – Such defects occur as a consequence of the way in which the crystal is grown, its thermal history and as a by product of doping by ion implantation.

3. Chemical impurities, which introduce electron states within the band gap. (These states may be near one of the band edges.)

4. Dimensions of the structure – When the dimensions become similar to or less than de Broglie wavelength of electron, the energy levels of the structures are changed by quantum size effect.

Optoelectronic properties of semiconductors can be described in terms of electron activities in semiconductors. These include (a) optical absorption by which free carriers are created, (b) electronic transport by which free carriers contribute to electrical conductivity of the material and (c) capture of free carriers, leading either to recombination or trapping (2). Major transitions in a homogeneous semiconductor are shown in Fig. 1.1.

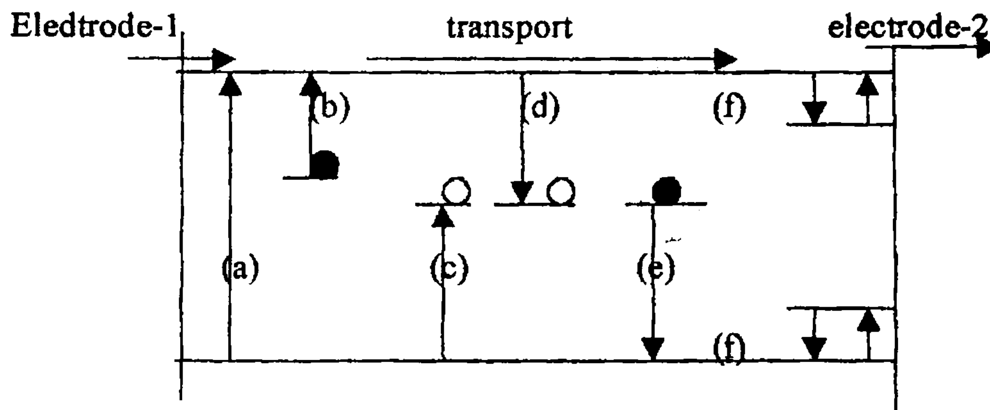

Fig. 1.1 Major transitions in homogeneous semiconductors. (a) intrinsic absorption, (b) and (c) extrinsic absorption, (d) and (e) capture and recombination, (f) trapping and detrapping.

1.1.1 Optical process

Optical process includes intrinsic optical absorption corresponding to raising of an electron from the valence band to the conduction band (a) and extrinsic optical absorption corresponding to the raising of an electron from an imperfection to the conduction band (b) or the raising of an electron from the valence band to an imperfection (c). Optical absorption is described quantitatively through the absorption constant α. If intensity of light incident on a material of thickness 'd' with absorption constant α is I_0, intensity of the transmitted light (I) is approximately (neglecting reflection and interference effects).

$$I = I_0 \exp(-\alpha d) \qquad (1.1)$$

(1) Intrinsic optical absorption

Intrinsic optical absorption corresponds to photo excitation of an electron from valence band to conduction band (Fig. 1.1(a)). It may be classified into two as direct and indirect optical transitions. If minimum of the conduction band is at the same point in '$\bar{k}$' space as maximum of the valence band, a transition occurs involving only absorption of a photon. Such a transition is called "direct optical transition". Minimum photon energy for absorption $h\nu_{min} = E_{Gd}$, where E_{Gd} is the direct band gap of the material and change in momentum on transition, $\Delta\bar{k} = 0$. If minimum of the conduction band is at a different point in '$\bar{k}$' space from maximum of the valence band, an optical transition from top of the valence band to bottom of the conduction band must involve absorption of a photon and a simultaneous absorption or emission of a phonon. In this case, $E_{Gi} = h\nu_{min} \pm E_{phonon}$, where E_{Gi} is the indirect band gap of the material and E_{phonon} is the energy of the phonon involved in the process. Compound semiconducting materials like CdS, GaAs and CdTe have direct band gap, whereas GaP has indirect band gap and Ge and Si have both direct and indirect band gap.

In a direct band gap material, optical absorption occurs near the surface of the material whereas for a material having indirect band gap, light penetrates much deeper into the material. Hence in the former case, the magnitude of the intrinsic photoconductivity (defined as increase in conductivity caused by intrinsic absorption) depends critically on the surface lifetime. In indirect band gap materials, the surface lifetime is much less important. If a direct band gap material is used in a p-n junction type device (where junction collection of photo excited carriers is important), a shorter diffusion length 'L' is required for carrier collection by the junction, where as in an indirect material a large L is necessary, if the entire photo excited carriers are to be collected.

Direct band gap materials have higher intrinsic luminescence efficiency, associated with recombination of electrons and holes resulting in the emission of photons, because of shorter value of radiative recombination lifetime. But indirect materials have a lower intrinsic luminescence efficiency since the longer lifetime for radiative recombination allows competing processes for non-radiative recombination to become important.

(2) Extrinsic optical absorption

Absorption involving imperfections is called extrinsic optical absorption. Here absorption coefficient is proportional to the density of absorbing centers (N_a).

$$\alpha = S_o N_a \qquad (1.2)$$

Here S_o is the proportionality constant called the "optical cross section" for the absorption process. If E_I is the depth of an impurity level below the conduction band and if energy of the incident radiation $h\nu > E_I$, continuous absorption will be caused due to excitation of electrons from the center to the conduction band (Fig 1.1(b)). If E_I is small (shallow impurities) its effect will be observed only at low temperatures when a considerable fraction of the impurity centers are not-ionized (Fig. 1.1(f)). Similarly, electrons may be excited into unionized acceptor centers near the valence band (Fig 1.1(c)). Impurity centers may be excited like group III and group V impurities in Si and Ge. Excitation from the ground state to the excited states of an impurity center would lead to a line absorption spectrum.

1.1.2 Carrier transport

Carrier transport phenomena arise from motion of electrons and holes in semiconductors under the influence of electric and magnetic fields. In a polycrystalline semiconductor thin film, factors like film defects, surface scattering and grain boundaries complicate identification of electrical properties. Grain boundaries in compound semiconductor films are different from those in elemental semiconductors. Boundaries for larger crystllite films differ from those for small-grained ones. The physical, structural, electrical and optical characteristics of grain boundary regions are drastically altered by exposure to impurities, diffusion and field effects (3). So care may be taken in applying a proper model for interpreting the analysis of electrical properties. Important parameters related to electrical properties are resistivity, carrier density, carrier mobility and surface recombination velocity.

1. Resistivity - In Petritz model (4) for measurement of resistivity, single grain and single boundary are considered initially. Then it is averaged over many grains. The total resitivity

$$\rho_g = \rho_1 + \rho_2 \qquad (1.3)$$

where the subscript (1) signifies the grain or crystallite and (2) signifies the boundary. Most of the semiconductors have resistivities in the range 10^{-3} to 10^{6} Ωcm at room temperature. The most important property of semiconducting material is the negative temperature coefficient of resistance. Addition of suitable impurities with low ionization energy can lead to variation of resistivity of the material. Commonly used measurement techniques are Four point probe and Van der Pauw method.

2. Carrier density – In intrinsic semiconductors charge carriers are thermally generated electron-hole pairs. Energy distribution of charge carriers can be obtained using Fermi-Dirac statistics.

When E_C-E_F >> kT

$$n = N_C \exp(-(E_C - E_F) / kT) \qquad (1.4)$$

and

$$p = N_V \exp(-(E_F - E_V) / kT) \qquad (1.5)$$

Where N_C and N_V are "effective density of states" in the conduction band and valance band respectively.

For intrinsic material, at absolute zero

$$n.p = N_C N_V \exp(-E_g / kT) \qquad (1.6)$$

Intrinsic carrier concentration varies with temperature and band gap. For semiconductors with large band gap there is practically negligible number of mobile charge carriers. In order to increase conductivity, impurities are added to the material, resulting in the formation of localized discrete energy levels within the forbidden band. Techniques to measure carrier density are Hall effect, Capacitance-voltage and Optical absorption measurement.

3. Mobility – Mobility is the velocity per unit field acquired by a charge carrier as a result of the application of an electric field. Mobility is intimately connected

with the nature of the energy band. In a non-ionic binding μ is proportional to $m^{*-5/2}$. Mobility is therefore characteristic of the material and the magnitude can be altered considerably by variations in temperature and purity of the material. In a material having increased ionic character, mobility is expected to decrease because of greater electrostatic interaction between the free charge carriers and the charged ions of the crystal. But a large increase in electron mobility is found as one goes from the period 5, group – IV element to III – V compound in the same period. Mobility maximum is associated with small effective masses found in the III – V compounds.

Mobility of charge carriers in materials with predominantly covalent bonding will usually be higher than that in materials with predominantly ionic bonding (5). In the case of compound semiconductors, the covalent nature decreases and ionic conductivity increases in the order IV-IV, III-V, II-VI and I-VII. Hence mobility decreases in the compound semiconductors in the same order.

Crystal vibrations and imperfections in the form of impurities, defects and dislocations interrupt motion of charge carriers in a crystal. Since effects of crystal vibrations can be expected to increase with increase of temperature, mobility should decrease with increasing temperature. At the imperfection, scattering changes the mobility of charge carriers. Scattering can be in two ways. In one type of scattering, Coulomb force is directly involved because of the attraction or repulsion between the charge carriers and charged ions of the crystal. The other type is the one in which scattering is the result of a deviation in the local potential experienced by a charge carrier. Hence the mobility of charge carriers will be greater for a given material, when it is pure and structurally perfect.

In a photoconducting material, contribution of photoexcited carriers to conductivity depends on free lifetime and mobility. Flow of current through polycrystalline material is limited by the presence of grain boundaries. Light absorbed in this region reduces resistance of the barrier and the current flow through the whole material will be much greater than it would be without radiation. The

effect of this barrier is described in terms of an effective mobility μ_g. According to Petritz model $\rho_1 << \rho_2$, the carrier concentration is not reduced but all carriers take part in the conduction process with reduced mobility (4).

$$\mu_g = \mu \exp(-e\phi_b/kT) \qquad (1.7)$$

If μ is the mobility of charge carriers inside the grain and free carrier density n, then to consider this material as a homogeneous one, μ is replaced by μ_g

$$\Delta\sigma = e\ (n\Delta\mu_{gn} + \Delta\mu_{gp}) \qquad (1.8)$$

Hence mobility variation with intensity can also change conductivity of the material. Svein Espevik et.al. (6) reported the effect of oxygen on mobility and hence photoconductivity in chemically deposited Lead sulfide thin film. C. Julien et al. (7) reported variation of mobility with temperature and the grain boundary effects. The effect of grain size on mobility and barrier height in In_2Se_3 was reported by G. Micocci et al. (8). Chen-ho Wu et al. (9) reported that photoconductivity of sprayed CdS thin film is caused primarily by an increase in electron mobility. Mobility variation with illumination intensity is also reported in this study.

4. Surface recombination velocity - One of the electrical properties due to minority carrier is surface recombination velocity. Electrons and holes recombine at the surface much greater than the body recombination rate. The net rate of holes (S_a) absorbed by the surface of an n-type material is

$$S_a = s\ \Delta p \qquad (1.9)$$

where 's' has the dimension of a velocity and is called the 'surface recombination velocity'. Surface recombination velocities in germanium is found to vary from 10^6 to 10^2 cm/S at 300 K. Large surface recombination velocities are found in ground or sand-blasted surfaces and low values for surfaces polished in a suitable etching solution. For many technological applications, special precautions are taken to ensure that surface recombination velocity is not high. If the surface recombination rate near a point contact is very high, it may adversely affect the

properties of the contact. In thin film photo conducting material, if surface recombination velocity is very high, decay process dominates and bulk lifetime will be reduced. If $s\tau << d$ (thickness of the film), surface recombination has little effect on the magnitude of the photocurrent. On the other hand, $s\tau >> d$ magnitude of the photocurrent is independent of τ and depends only on surface conditions.

1.1.3 Recombination and trapping

A free electron may be captured at an imperfection as in Fig. 1.1(d) or a free hole may be captured at an imperfection as in Fig. 1.1(e). Capture process is described through capture coefficient (β) such that the rate of capture (R) of a species with density 'n' by a species with density 'N' is given by

$$R = \beta n N \qquad (1.10)$$

β is often expressed as product of capture cross section (S) and average thermal velocity (v) of the free carrier.

$$\beta = \langle S(E)v(E)\rangle = Sv \qquad (1.11)$$

The averages are over electron energy. Lifetime of a free carrier (τ) is given by

$$\tau = 1/\beta N \qquad (1.12)$$

Comparing the above equation with Eq. (1.10) shows that rate of capture or rate of recombination is equal to n/τ. At steady state, rate of recombination is equal to rate of excitation G, we get

$$n = G\tau \qquad (1.13)$$

The above equation states that the average density of a species present at any time is given by the product of rate at which the species is being generated and the average lifetime of a member of the species. If more than one type of recombination process is present, the individual recombination rates are added to get total density of species.

A captured carrier at an imperfection may also be thermally reexcited to the nearest energy band before recombination occurs. In this case, the imperfection is referred to as a "trap", and the capture and release processes are called "trapping" and "detrapping" (Fig. 1.1(f)). If R_c is the capture rate of free carriers with density 'n' by imperfections with density 'N', such that $R_c = \beta nN$, and if R_d is the thermal detrapping rate given by $n_t \nu \exp(-\Delta E/kT)$, where '$n_t$' is the density of trapped carriers, 'υ' is a characteristic 'attempt to escape frequency', and 'ΔE' is the activation energy for detrapping, then the imperfection acts like a recombination center if $R_c > R_d$ but like a trap if $R_c < R_d$. Physical situation of electrical current flow under illumination involves the effect of the contacts and nature of the transport of free carriers. Electrical contacts must be ohmic, which is the ability to replenish carriers, to maintain charge neutrality in the material.

Presence of defects introduces more additional energy levels in the forbidden gap. Unlike the bands themselves, which extend throughout the crystal, the additional levels are localized at the crystal defect. General effects of defects on electronic properties are the following.

1. Due to donor or acceptor – A donor is a defect that is neutral when electron occupied or positive when unoccupied and an acceptor is a defect that is negative when electron occupied or neutral when unoccupied. This means that a donor defect has an extra electron that it can contribute to conduction band or an acceptor defect has a deficiency of an electron that can be filled from valence band in which it produces a hole. Presence of such defects affects the density of free carriers and hence electrical conductivity of the material. Important parameters of these defects are their density and ionization energy.

2. Due to trap – A defect can capture an electron or a hole with such a small release of energy that the trapped carrier is in general released to the nearest band before capture of a carrier of opposite type can occur. Presence of these defects can lead to carriers in localized states near the band edge. A typical effect of such trapping is to make photoconductivity decay time longer than the lifetime of free carriers (10). Important parameters of traps are their density and ionization energy for the trapped carrier.

3. Due to recombination center – A defect can capture an electron or a hole with large thermal ionization energy that the captured carrier has a high probability of recombining with a carrier of the opposite type before being thermally re-excited to the band. The presence of recombination centers usually reduces the lifetime of free carriers. Important parameters of recombination centers are their density and capture cross-sections for electrons and holes.

When capture or recombination occurs, excess energy of the captured/recombining carrier must be released. This occurs either by creation of a photon (radiative process-luminescence), or by the excitation of free carriers. Recombination centers can be classified according to their effects.

a. Sensitizing center – This center has large capture cross-section for minority carriers but much smaller capture cross-section for majority carriers so that lifetime of majority carriers and hence the magnitude of the photoconductivity is greatly increased (11).

b. Killer center – Killer centers have a large capture cross-section for majority carriers so that the number of free carriers and hence the magnitude of the photoconductivity are drastically decreased (12).

c. Poison centers – The centers have a large nonradiative capture cross-section for carriers, so that they compete with other defects with a radiative capture cross-section and reduce the luminescence efficiency.

d. Optical absorption center – An electron associated with a defect can be photo excited from the defect to conduction band, from the valence band to the defect, or between the ground state and excited states of the defect. In this way the defect makes a contribution to the extrinsic optical absorption of the semiconductor. Important parameters are the optical cross-section and the density of defects available for photo excitation.

e. Scattering center - These centers behave as scattering centers in determining the mobility of free carriers. Important parameters are the scattering

cross-section and the defect density. If the defects are charged they have large coulombic cross-section for scattering and make a major impact on the mobility. If the defects are neutral, their effect on the mobility is much smaller and important only at low temperature and for high density of neutral defects.

The same defect can play the role of donor, electron trap, recombination center for holes, optical absorption center or scattering center. It is also possible for the same defect to act as a trap under one set of temperature and photo excitation conditions and then as a recombination center under another set of conditions. Depending upon the nature of the defect in the material, relaxation process can be radiative or nonradiative. Imperfections incorporated in photoconductors can have three basic effects on photoconductivity. They may change photosensitivity, speed of response, and can extend spectral response of photoconductivity to long wavelength side of the absorption edge. Optoelectronic properties arising due to extrinsic optical absorption are luminescence, photoconductivity, negative or persistent photoconductivity, optical quenching etc: -

(1) Luminescence

In a transition, if the captured carrier has greater probability of recombining with carrier of opposite sign, the relaxation of electronic energy will be lost as photons and luminescence emission is observed. The possible transitions are depicted in Fig. 1.2

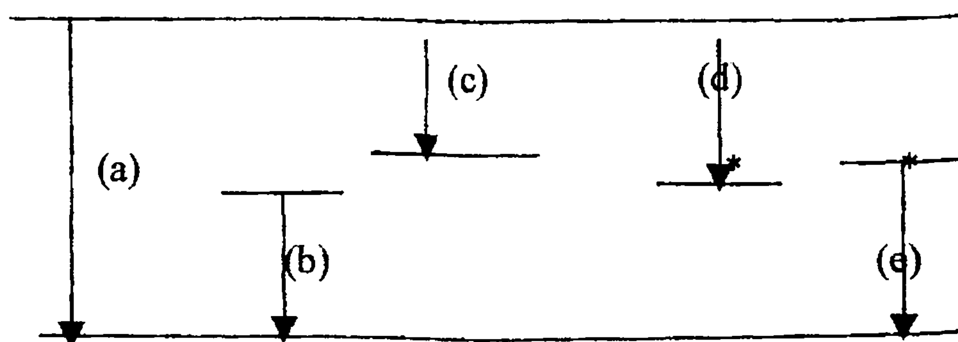

Fig. 1.2 Major radiative transitions in semiconductors

Free electron may recombine directly with free hole. But the probability of this transition is minimum. The lost energy in this case is emitted as photons with (approximately) the energy of the band gap (Fig. 1.2(a)). Such emission is called "edge emission". Another possible transition is either an electron being captured by an excited center containing a hole (Fig. 1.2(c)) or a hole being captured by an excited center containing an electron (Fig. 1.2(b)). Radiative transition is also possible when an electron is captured by an excited center containing a hole (Fig. 1.2(d)), or a hole being captured by an excited center containing an electron (Fig. 1.2(e)). The edge emission has its maximum at the absorption edge. But the band at the longer wavelength and lying near the edge is associated with recombination at an imperfection.

M. Balkanski et al. (13) reported two photoluminescence bands in α-In_2Se_3 semiconductor : one at 1.523 eV and the other at 1.326 eV. R. K. Ahrenkiel et al. (14) reported a strong band gap transition of CdTe that peaks at 1.47 eV. K. Topper et al. (15) studied the effects of post-deposition treatment on the PL spectra of $CuInSe_2$ absorber layers. It is reported that the intensity on the PL peak at 1.445 eV was drastically influenced by post-deposition treatments. G. A. Medvedkin et al. (16) identified the point defects in $CuInSe_2$ single crystals grown with the deviation from valence stoichiometry using photoluminescence and photoresponse studies.

(2) Photoconductivity

The basic principle involved in photoconductivity is that when photons of energy greater than that of the band gap of the semiconductors are incident on the material, electrons and holes are created resulting in the enhancement of electrical conductivity. This phenomenon is called intrinsic photoconductivity. It is also possible to observe photoconductivity when the energy of the incident photon is less than that of the band gap. When the energy of the photon matches the ionization energy of the impurity atoms, they are ionized, creating extra carriers and hence an increase in conductivity is observed. This phenomenon is called extrinsic photoconductivity.

In a homogeneous material, conductivity is expressed as

$$\sigma = e\,(n\mu_n + p\mu_p) \qquad (1.14)$$

where n and p are the densities of free electrons and holes, and μ_n/μ_p are the electron/ hole mobilities. In homogeneous material under equilibrium condition n and p are uniform throughout the material. Photoconductivity occures when the values of n and p are enhanced due to photon absorption.

$$\Delta\sigma = e\,(\Delta n\mu_n + \Delta p\mu_p) \qquad (1.15)$$

In insulators, values of Δn and Δp may be much larger than the corresponding free carrier densities in the dark. In semiconductors the effect of radiation can be considered as small perturbation on large dark carrier density. Consider the case of one carrier transport in a non-homogeneous material. Then on illumination

$$\sigma + \Delta\sigma = (n + \Delta n)\,e\,(\mu + \Delta\mu) \qquad (1.16)$$

$$\Delta\sigma = e\,\mu\,\Delta n + (n + \Delta n)\,e\Delta\mu \qquad (1.17)$$

But

$$\Delta n = G\tau_n \qquad (1.18)$$

Where G is the photo excitation rate and τ_n is the electron lifetime

$$\Delta\sigma = e\,\mu\,G\tau_n + n\,e\Delta\mu \qquad (1.19)$$

But in the above process τ_n may itself be a function of excitation rate $\tau_n(G)$. Therefore three types of effects may occur (17).

1. Increase in carrier density with constant lifetime τ_n, so that $\Delta\sigma = e\,\mu\,G\tau_n(G)$. The photoconductivity is proportional to G so that a log-log plot of $\Delta\sigma$ vs G has a slope of unity.

2. Increase in carrier density with lifetime (τ_n) as a function of photo excitation intensity so that $\Delta\sigma = e\,\mu\,G\tau_n(G)$. If τ_n varies as $G^{(\gamma-1)}$, then $\Delta\sigma$ varies as G^{γ}. If $\gamma<1$, the lifetime decreases with increasing excitation rate, the behavior is said to be "sub linear". If $\gamma>1$ the lifetime increases with increasing excitation rate, the behavior is said to be "supralinear".

3. Increase in carrier mobility, so that $\Delta\sigma = n\, e\Delta\mu$. The possible mechanisms arise due to the change in mobility are

   a. Scattering by charged impurities may change under photo excitation either through a change in density of such charged impurities or through a change in the scattering cross section of such impurities.

   b. If the material is polycrystalline and contains intergrain potential barriers, photo excitation can reduce the height of these barriers as well as the depletion width, giving rise to an increase in carrier mobility.

   c. Photo absorption may result in the excitation of carrier from a band characterized by a mobility to another band having a different mobility.

In the case of insulators at high photo excitation rates $\Delta n >> n$, $\Delta p >> p$ and

$$\Delta\sigma = Ge\,(\tau_n\mu_n + \tau_p\mu_p) \qquad (1.20)$$

Thus the lifetime – mobility product is a measure of the photoconductor's sensitivity to photo excitation.

Photoconductivity phenomenon is described on the basis of three quantities – photosensitivity, the spectral response and the speed of response.

1. Photosensitivity – It may be described as $\Delta\sigma$ or $\Delta\sigma/\sigma$. These two definitions may be complementary in some cases. In an optical process $\Delta\sigma$ and σ increases. If σ increases more rapidly than $\Delta\sigma$, then photosensitivity defined as $\Delta\sigma$ increases but the photosensitivity defined as $\Delta\sigma/\sigma$ decreases. So specific sensitivity is a measure of the materials' actual sensitivity in terms of $\tau\mu$ product. It is the photoconductance per unit excitation intensity, measured in units of m^2/Ω watt. Another measure of photosensitivity is the photoconductivity gain. It is the number of charges collected in the external circuit for each photon absorbed. Imperfections, which act as efficient recombination centers decrease photosensitivity by decreasing free carrier lifetime. On the other hand imperfection, which has large capture cross-section for one type of charge and small cross-section for another type may increase photosensitivity.

If an atom of group II or VI of a II-VI compound is substituted by an atom of group III or VII, respectively, then there will be an extra electron at the cation or at the anion site, ie, the impurity atom of these elements will act as a donor. Similarly, if they are replaced by atoms of group I and V, then there is a lack of electron and an acceptor state is created. The vacancies at anion sites are equivalent to donors since the electrons from cations are not used in the binding but they are free. Another method for increasing the sensitivity of a given material is by irradiating the sample with fast electrons (18). T. Yoshida et al. (19) reported the photoenhancement by irradiation in CdS. The mechanism of photoconductivity in polycrystalline cadmium sulphide layers, and the effect of doping on response time and mobility are discussed by J. W. Orton (20). Svein Espevik (6) reported the photoconductivity in chemically deposited lead sulfide thin film and the effect of oxygen on mobility and lifetime in this material. It is also reported that chemisorbed oxygen introduced donor-type imperfections in the PbS, which act as sensitizing centers for p-type photoconductivity in the material.

2. Spectral response of photoconductivity – There is a close correlation between the optical absorption spectrum and the photoconductivity spectral response. The general shape of absorption spectrum and spectral response of photoconductivity is pictured in Fig. 1.3

   In the high absorption region (I), photoconductivity is controlled by the surface lifetime. In the intermediate range of region (II), there is strong absorption and the photoconductivity is controlled by the bulk lifetime, with a maximum occurring when absorption constant is approximately equal to reciprocal of the sample thickness. In the low absorption region (III), the photoconductivity is also controlled by the bulk lifetime but decreases with increasing wavelength as the absorption decreases. Imperfections may extend the spectral response of photoconductivity to long-wavelength side of the absorption edge. It is also observed that the response goes down on the shorter-wavelength side also, even though the absorption coefficient is high in this spectral region. This is because the photons of these energies are absorbed at or near the surface of the semiconductor, where recombination velocity is higher than that in the bulk. The extension of spectral response to the high-energy side by

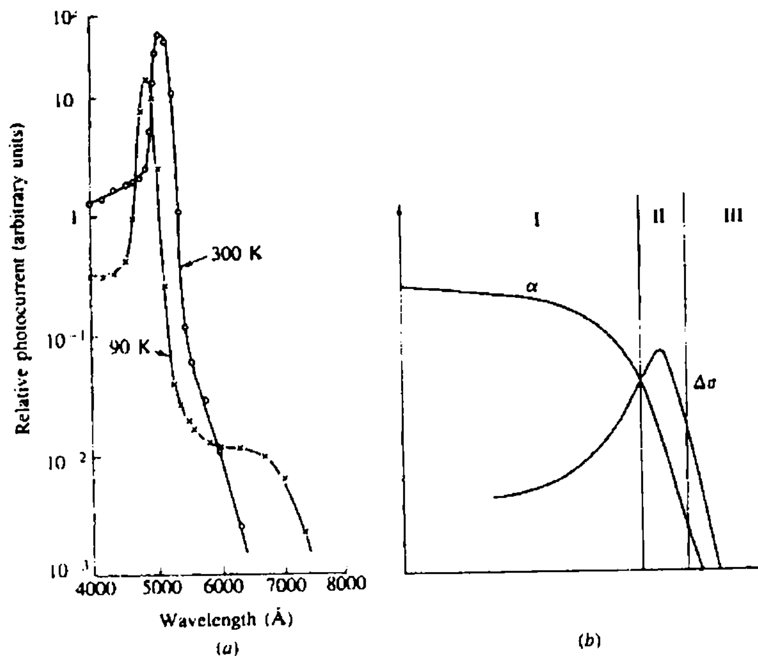

Fig.1.3 (a) Photocpnductivity spectral response curves for a photosensitive crystal of CdS at 90 and 300° C. (b) Comparison of the shape of the photoconductivity spectral response and the absorption contant of the material.

selecting a proper valence band structure of the photoconducting material is discussed by J. L. Shay et al. (21) and N. V. Joshi et al. (22). Again E. Bertran et al. (23) reported the shift of absorption edge in CdS due to doping of Indium and the influence of Indium concentration on the refractive index.

3. Speed of response – It is inversely proportional to the time constant associated with the increase of photoconductivity to its steady state value after turning on the photo excitation (the rise time), and the time constant associated with the decrease of photoconductivity to its dark value after turning off the photo excitation (the decay time). In the absence of traps in the material, free carrier lifetime determines the value of these time constants.

The simplest rate equation is

$$(dn/dt) = G - n/\tau \text{ (assuming } \Delta n = n \text{)} \qquad (1.21)$$

At steady state

$$n = G\tau \qquad (1.22)$$

The rise curve is described by

$$n(t) = G\tau\,[1-\exp(-t/\tau)] \tag{1.23}$$

and for the decay curve

$$n(t) = G\tau \exp(-t/\tau) \tag{1.24}$$

In the presence of traps, additional time-dependent processes are involved with "trap filling" during the rise and "trap emptying" during the decay. Therefore the measured response time τ_0 (usually taken to be the time required for the photoconductivity to decay to 1/e of $G\tau$ or steady state Fermi energy to drop by KT) will be larger than the free carrier lifetime τ.

(2a) Lifetime

Lifetime of photo-excited carriers is the key parameter in photoconductivity. The following are the different types of lifetimes involved in the study of photoconductivity.

1. Free lifetime – This is the time during which the charge carrier is free to contribute to conductivity. Or in other words it is the time that an excited electron spends in the conduction band or an excited hole spends in the valence band. Free lifetime of a charge carrier can be terminated by recombination. Again it can be interrupted if the carrier is trapped and is resumed when the carrier is freed from the trap. It is undisturbed if the carrier is extracted from the crystal by the field, at the same time an identical carrier is injected into the crystal from opposite electrode.

2. Excited lifetime - It is the total time the carrier is excited between the act of excitation and the act of recombination, or extraction without replenishment. The excited lifetime includes any time that the carrier may spend in traps, it is therefore usually longer than the free lifetime.

3. Pair lifetime - This is the free lifetime of an electron-hole pair. If either electron or hole is captured, or is excited without replenishment, the pair lifetime is terminated.

4. Minority-carrier lifetime - This is the free lifetime of the minority carrier – electrons in p-type materials and holes in n-type materials. Usually the pair lifetime is equal to the minority carrier lifetime.

5. Majority carrier lifetime - Majority carrier lifetime is the free lifetime of the majority carrier – electrons in n-type materials and holes in p-type materials. If the density of free carriers in a material is very much greater than the density of recombination centers, as in semiconductors, the majority carrier lifetime will be equal to the minority carrier lifetime. If the density of free carriers is much less than the density of recombination centers – as in insulators, the majority carrier lifetime can be much larger than the minority carrier lifetime. Photosensitivity is frequently obtained by incorporating centers, which capture minority carriers rapidly and have a much smaller probability of capturing majority carriers to bring about recombination (24).

J. W. Orton et al. (20) reported the mechanism of photoconductivity in polycrtystalline cadmium sulphide layers, and the effect of doping on response time and mobility. W. P. Lee et al. (25) reported the effect of ultra violet irradiation on the effective minority carrier recombination lifetime of silicon wafers. T. L. Chu et al. reported increase in lifetime of charge carriers in solution grown cadmium sulfide films due to doping of Boron (26).

(3) Negative photoconductivity

Negative photoconductivity occurs in a material when absorption of radiation causes decrease of conductivity lower than the dark conductivity of a material. This phenomenon is different from optical quenching of photoconductivity, in which the photoconductivity excited by a primary radiation is decreased by the absorption of a suitable secondary radiation.

If minority carriers are optically freed from centers, a negative photoconductivity will result because of the rapid recombination of these minority carriers with majority carriers. One of the models for negative photoconductivity is formulated by Stockmann (27). The two level model is outlined in the figure below (Fig.1.4).

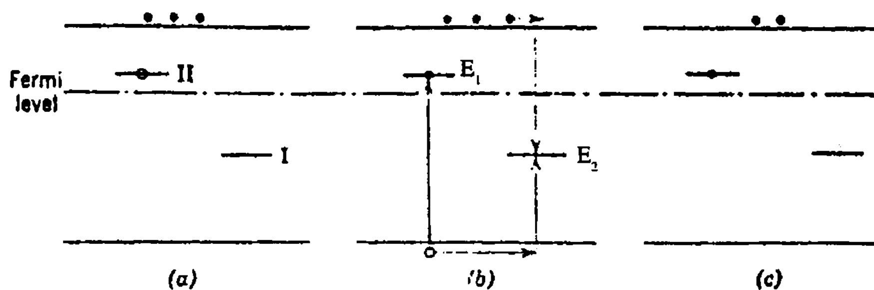

Fig.1.4 Energy-level representation of the steps involved in negative photoconductivity according to Stockmann

According to this model, occurrence of negative photoconductivity requires the following conditions :

1. Thermal ejection of electrons from level E_1 must be slower than the recombination of electron and hole at region I.
2. Holes must not recombine directly with electrons in level E_2.
3. Level E_1 must lie above the Fermi level.
4. Cross-section of centers E_1 for majority carriers must be much less than that of centers E_2.
5. Density of centers E_2 and their cross-section of minority carriers must not be too small.

In short, the function of these types of centers in the presence of radiation, is to create holes by accepting electrons from the valence band but at the same time not to increase the number of free electrons. The second type of centers have a high cross-section for electrons and holes and consequently they capture electrons from the conduction band and holes from the valence band, and recombine them. Thus the net number of mobile charge carriers is reduced due to incident radiation giving rise to negative photoconductivity. Its dependence on temperature, intensity of illumination and bias voltage have been studied in the ternary compound $TlGaSe_2$ by S. G. Abdullaev et al. (28) using this model.

Another model to explain the negative photoconductivity in p-type semiconductors has been reported by N. V. Joshi et al. (29). It is proposed that electrons ejected from the inner level can recombine with holes at the top of the valence band and bring about negative photoconductivity. This phenomenon has been demonstrated in $Cd_{1-x}Fe_xSe$, in the above reported study.

Fig. 1.5 shows the photoconductivity spectrum of $Cd_{1-x}Fe_xSe$ at 300 K. At 1.7 eV the reduction in the current was large in the presence of radiation, where the absorption continues to increase. In this model negative photoconductivity is explained on the basis of energy level scheme of iron in $Cd_{1-x}Fe_xSe$ (29). According to this model radiation of energy 1.72 eV excites electrons from the inner level of iron to the top of the valence band, where they recombine with the holes and the photoconductance attains a value lower than dark conductance. The two main features of this model are (1) it explains the reduction of current due to monochromatic radiation and (2) this model is applicable to low band gap materials where two or more types of localized levels are generally not observed. R. A. Hopfel (30) reported high negative photoconductivity in a p-type GaAs-AlGaAs quantum well structure at low temperature. In this material photoresponse is negative over the entire spectral range. In the

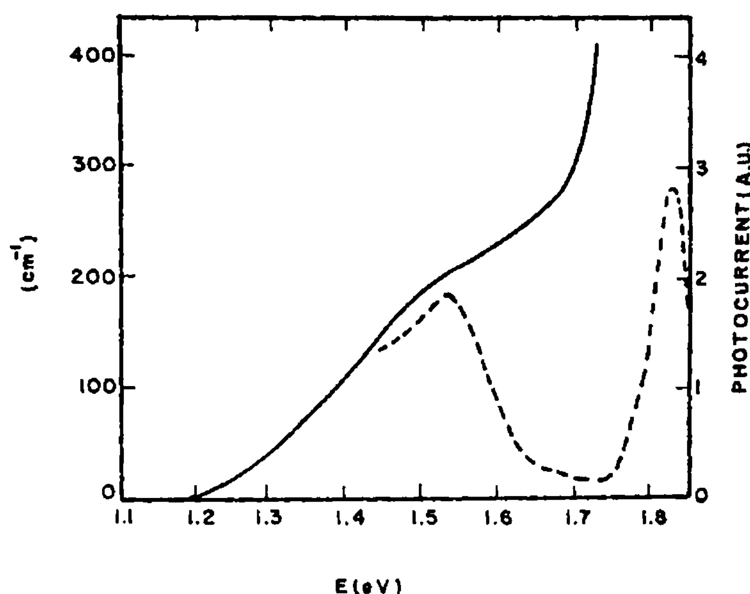

Fig.1.5 Photoconductivity and optical absorption spectrum of $Cd_{1-x}Fe_xSe$

earlier mentioned model reported by N. V. Joshi et al. (29), negative photoconductivity is observed only for a particular wavelength. This suggests that negative photoconductivity in quantum well structures has different types of origins and for the entire region of the spectrum it cannot be due to a single mechanism.

(4) Persistent Photoconductivity (PPC)

Photoconductivity that persists for a long time - minutes, hours or days after the cessation of the optical excitation is called persistent photoconductivity. The peculiar properties of semiconductors having persistent photoconductivity are :

1. Microscopic or macroscopic potential barriers separate charge carriers in real space and reduce the probability of recombination between them.

2. An energy state in the forbidden gap stores the charge carriers for a considerable amount of time before ejecting them to the conduction or to the valence band.

3. Photochemical reactions may create new trapping and recombination centers along with easily ionisable shallow donor levels.

4. The energy of the incident radiation is enough to deform the photosensitive material and perturb the localized energy states near the deformation sites.

Duration of time for which persistent photoconductivity is observed depends upon details of the origin of the potential barrier or types of traps or defect centers, their capture cross-section for electrons and holes and the probability of ejection of charge carriers to the conduction or valence band.

J. W. Farmer et al. (31) reported persistent photoconductivity in n-type GaAs epitaxial film on chromium doped semi-insulating GaAs substrate. A potential barrier similar to n-p junction is created due to relative difference between the Fermi-levels. Radiation reduces the height of the barrier and forward current cancels the reverse current originating from charge separation. When radiation is turned off, current will continue to flow until the barrier becomes sufficiently high to stop the flow. The time required for this, depends upon many

factors such as densities of charge carriers on both sides of the junction, width of the depletion layer and dielectric constant of the medium. D. V. Lang et al. (32) presented a model suitable for the CdS and CdTe type of materials based on the deformation of the lattice. According to this report, transition through the energy state caused by deformation of the defect can give rise to the observed persistent photoconductivity.

1.2 Lifetime measurements - different techniques

Techniques for lifetime determination are divided into two broad types, viz. those employing steady state measurements and those involving dynamic measurements. The measurement involves injection of carriers into the sample, together with some technique for monitoring the photocurrent or the time of decay. The appropriate technique is chosen depending upon the high or low injection levels, or carrier recombination via recombination center or deep trapping center.

1.2.1 Steady state methods

Steady state measurements include two methods: one depends on photoconductive (PC) and the other on photo electromagnetic effects (PEM). The same technique may be used to measure either lifetime or diffusion length. Both techniques do not measure time or length directly. Instead, lifetime or diffusion length is derived using a theoretical model to the measured photocurrent or photo voltage. Photoconductive methods are suitable only for measuring highly resistive material.

(a) Photoconductive measurements (PC)

A uniform semiconductor material is illuminated over its upper surface as shown in Fig. 1.6. Current flows between two ohmic contacts, c_1 and c_2 at each end. For PEM effect a magnetic induction B is applied normal to the direction of current flow and in the plane of the illuminated surface.

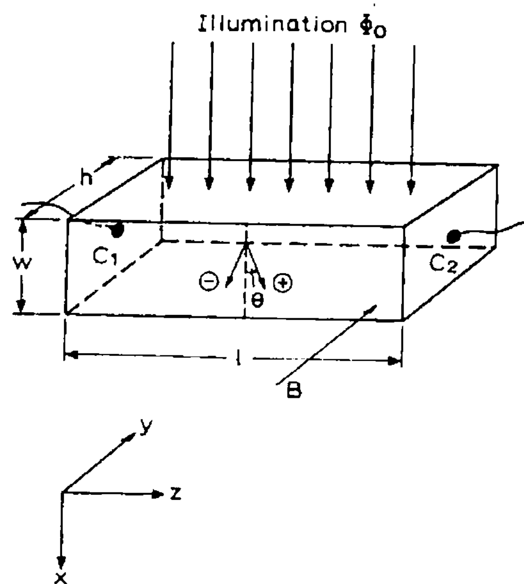

Fig.1.6 Sample geometry for measuring PC and PEM effects

The effect of photoconductivity is measured by applying an electric field E along the z direction. In the case of a thick sample and when the incident radiation is strongly absorbed ($h\nu > E_g$)

$$I_{pc} = Eh\,(1-R_0)e\Phi_0(\mu_n+\mu_p)\tau\,/1+s \tag{1.25}$$

Where R_0 is the reflection coefficient of the surface, Φ_0 is the number of photons incident on each square centimeter of the surface per second and 's' is the normalized surface recombination velocity. The above equation is derived on the assumption that the influence of deep states is negligible ($\Delta n = \Delta p$) and therefore $\tau_n = \tau_p = \tau$. Measurement of photocurrent under steady state conditions yields a value for τ provided the other parameters are known. Incident photon flux and carrier mobilities must be measured together with the recombination velocity on the illuminated surface. This experiment requires careful attention to get all other parameters to obtain reliable value for τ.

(b) Photo electromagnetic effect (PEM)

To study photo electromagnetic effect, a magnetic field is applied parallel to the y axis as shown in Fig. 1.6. It is assumed that incident radiation is absorbed close to the top surface. Both electrons and holes diffuse downwards into the bulk of the material. In the presence of

the magnetic field, the diffusing electrons and holes are deflected in opposite directions along the z axis, giving rise to a current I_{PEM}. The current is measured under short-circuit conditions by a low impedance meter connected across the end contacts. PEM effect is the Hall effect, measured on diffusing carriers rather than on carriers drifting in an applied electric field.

$$I_{PEM} = e\Phi_o (I-R_o)\ Bh\ (\mu_n+\mu_p)\ L_n/(1+s) \qquad (1.26)$$

This equation is valid when the thickness of the sample is greater than diffusion length. Steady state PEM effect may be used to measure the minority carrier diffusion length L_n provided μ_n and μ_p are known and both Φ_o and s can be measured. It is always better to have 's' very small and independent of L_n and τ. Similarity between I_{PC} and I_{PEM} suggests an alternative approach to measuring τ known as the ratio method.

$$I_{PEM}/I_{PC} = (B/E)(L_n/\tau) = (B/E)(D_n/\tau)^{1/2} \qquad (1.27)$$

$$(\ L_n = (\tau_n D_n)^{1/2}\ ) \qquad (1.28)$$

$$\tau = (I_{PC}/I_{PEM})^2\ (B/E)^2\ D_n \qquad (1.29)$$

Though equation (1.29) is independent of both light intensity and surface recombination velocity, it is still necessary to know the minority carrier mobility in order to determine diffusion coefficient D_n. If the sample has high conductivity it may be impossible to measure I_{PEM} under short circuit conditions because the measuring instrument has very high impedance. Under such conditions open circuit voltage V_{PEM} is measured instead of I_{PEM}.

1. 2.2 Transient methods of measuring lifetime

Variation of photoconductance as a function of time over a certain period for the photoresponse to reach its maximum or minimum value is called transient photoconductivity. Transient method of lifetime determination involves monitoring the decay of excess carrier density following an injecting pulse. The variety of these methods arises from the range of possible injection processes and means for sensing Δn or Δp.

Carriers may be generated by optical injection, electron beam injection, injection at a p-n junction or metal contact, or by impact ionization under the influence of an electric field (33). Detection may involve a measurement of conductivity, luminescence, transmission of an infrared beam, absorption of microwave power or the current collected by a local probe or p-n junction (34). Complications due to surface recombination can be minimized by suitable surface treatment to make $s << 1$ and by making sample dimensions very much greater than a diffusion length.

(a) Conventional experimental set up and its analysis

The simplest and most conventional experimental set up for photo conductance measurement is shown in Fig. 1.7

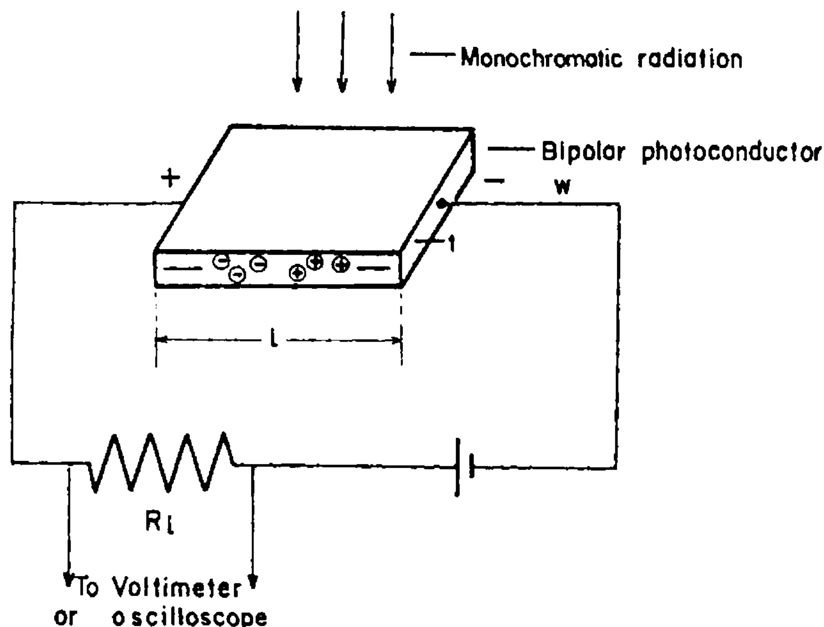

Fig. 1.7 A conventional experimental set up for photoconductance measurements

A constant DC source and a high resistance R_L are connected in series with the sample. Let R_d and R_{ill} be the resistance of the sample in the dark and under uniform illumination conditions. When there is no illumination photovoltage across the load resistance, R_L is

$$V_d = R_L V/R_L+R_d \quad (1.30)$$

Similarly, the voltage developed across illuminated sample is

$$V_{ill} = R_L V/R_L+R_{ill} \quad (1.31)$$

where V is the applied voltage. The difference between them is the signal response, which is given by

$$S(V) = R_L V[1/(R_L+R_{ill}) - 1/(R_d+R_L)] \quad (1.32)$$

$$= R_L V[\Delta R/(R_L+R_{ill})(R_d+R_{ill})] \quad (1.33)$$

$$\Delta R = R_D - R_{ill} \quad (1.34)$$

The difference in conductance caused by the radiation is

$$\Delta G = 1/R_{ill} - 1/R_d \quad (1.35)$$

$$\Delta R = (\Delta G)\ R_d R_{ill} \quad (1.36)$$

Signal response $S(V)= (V_R R_D R_{ill} \Delta G)/(R_L+R_d)(R_L+R_{ill})$ (1.37)

Two limiting cases which may be encountered in the laboratory are :

1. Variation in the resistance of the sample with and without radiation is very small compared to the dark resistance R_d, that is $R_d = R_{ill}$.

$$S(V) = VR_L R_D^2 \Delta G/(R_L+R_{ill})^2 \quad (1.38)$$

All the parameters in the above equation are characteristic of a given photoconductor except load resistance R_L. It is the only parameter that can be controlled to obtain the maximum photoresponse. The maximum response can be obtained by using $dS/dR_L = 0$. It is obtained when $R_L = R_d$. This is the reason for using load resistance equal to dark resistance of the sample when the photo signal is weak.

2. In the case of highly resistive material, dark current is low which makes it very easy to measure photo current or voltage without any need to optimize the load resistance.

(b) Contact configuration

Experimental set up, contact configuration, preparation of the sample, and sample thickness play crucial roles in the output and analysis of the results of photoconductivity measurements. Commonly used contact configurations are shown in the figure below.

In Fig. 1.8 (a) the contacts are on the lateral side of the sample and in Fig 1.8 (b) they are on the extreme ends. Here only a part of the sample is illuminated. In Fig. 1.8(c) the contacts are on the front and rear of the sample. Radiation passes through the transparent contact and is uniformly absorbed in the material. The amount of the absorbed radiation varies exponentially with the depth. Front surface recombination plays an important role in the first two cases, whereas the back surface recombination is also important for the last case.

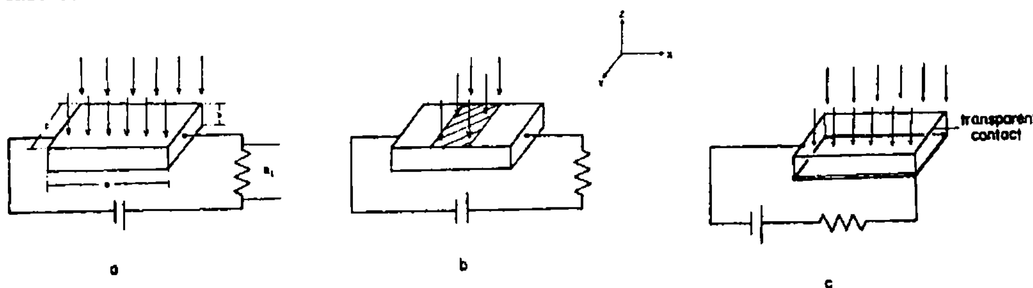

Fig. 1.8 Different types of contact configuration that affect the analysis of the results.

In photoconductivity measurements, the response depends not only on the number of photo-generated carriers but also on their transport to the electrodes. While the contacts are made between metals and semiconductors, depending upon the work function, there is a flow of carriers from the higher to the lower Fermi level to equalize the Fermi level at the contact. In this process, electrons transfer from the semiconductor to the metal resulting in a depletion region in the semiconductor. This gives rise to perturbation of the band at the metal-semiconductor interface. The flow of carriers is influenced by the length of the depletion region and the amount of perturbation at the interface. When the regions near the contacts are illuminated, quasi-Fermi levels for electrons and holes move relative to the Fermi level of the metal. If the illumination is intense, the movement of the Fermi level may be large enough to change its over all properties. Therefore a substantial change in the photoconducting properties is possible if the contact region is illuminated.

(c) Methods of measurement

Photoconducting properties of a given semiconductor depend on electrical and optical parameters. The semiconductor can have high or low resistance and the magnitude of variation in the resistance on illumination can be high or negligible. The response time can vary from pico seconds to a few minutes. The experimental technique must be different for each case.

Case 1. High resistivity and good photoresponse

These types of materials obviously have low dark current I_d, and photocurrent is much higher than I_d. In order to study photoconductivity response curves, photoresponse as a function of the wavelength is studied. Radiation source should be continuous in wavelength and the output is measured using a voltmeter as shown in the Fig. 1.7. If the relaxation curves are to be analysed, then the voltmeter should be replaced with an appropriate oscilloscope or digital multimeter. The most important aspect is that RC time constant of the measuring circuit should not be a limiting factor for the rise or decay curve. RC constant can vary from 10^{-6} to 10^{-1} sec. and this value sometimes coincides with the actual value of the response time. In a wide-band-gap semiconductor particularly group II-VI compounds, the response is slow and the above-mentioned situation may happen.

Case 2. Low resistivity and good photoresponse

This is common in narrow-band-gap materials ($E_g \leq 1eV$). Dark current is of the order of microamperes or even higher. In this case, modulation technique should be employed. The incident beam is chopped with a certain frequency by a mechanical or electro-optical chopper as shown in Fig. 1.9. This makes the photocurrent periodic with frequency equal to that of the chopper. The output is an ac photosignal on dc dark current. The ac signal, eventhough is very weak, can be separated by a lock in amplifier. This method has the additional advantage that it helps reduce the noise. N. V. Joshi et al. had used this technique in recording the photoconductivity spectrum of the ternary compound $AgInS_2$ (22).

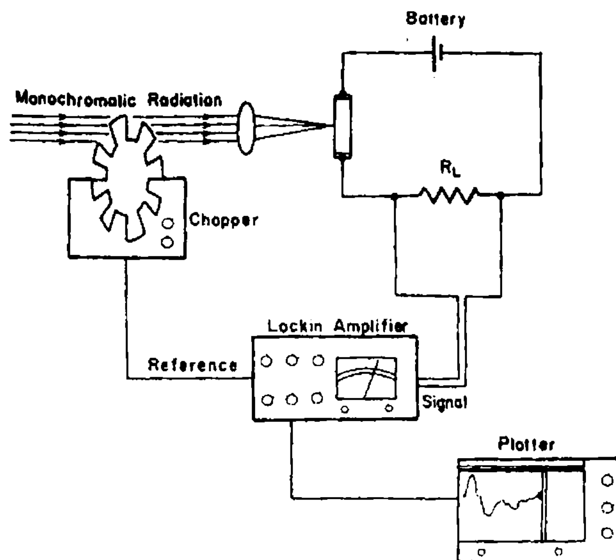

Fig. 1.9 Phase - Sensitive photocurrent measurement system.

Case 3. Low resistance and slow response

For such samples the value of the dark current is quite high and the chopping technique is not useful because of the slow response. In this case, dark current can be balanced by a wheatston's bridge and then an operational amplifier amplifies the potential difference originating from the variance of the resistance of the sample. This technique has been used to detect weak signal in the ternary compound $CuInTe_2$ by N. V. Joshi et al. (35)

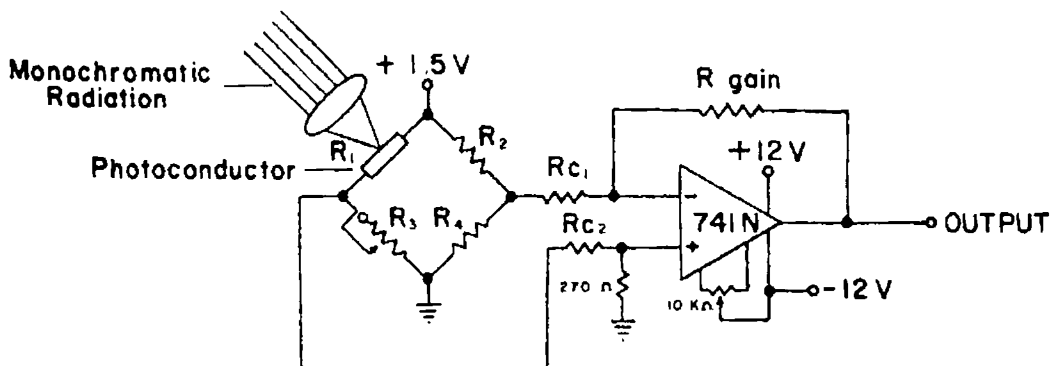

Fig. 1.10 Wheatstone bridge with a typical amplifying circuit used to detect a weak photosignal that has a slow response.

Case 4. High resistivity, slow response and very weak photosignal

This property is observed in organic semiconductors and also in some inorganic semiconductors. Examples are chromium-doped semi insulating GaAs or iron doped InP. Resistivity of such samples is high and response is slow. This is because impurity atom creates defect states, which may act as recombination centers. The recombination process reduces the lifetime of the carriers in conduction or valence band and therefore intensity of the response is reduced. In addition, traps retain electrons for a considerable time and hence the response becomes slow. In this case, measurement is taken for every wavelength giving sufficient time for each measurement for the photocurrent to reach its saturation value. Such a measurement is done in chromium doped GaAs for the study of structural details by P. Lenczewski and E. Fortin (36).

1. 2.2 (a) Modulation method

Measurement difficulties increase when lifetime decreases. Distortion free recording of a decay curve with a time constant of 10^{-8} sec. requires a receiver band width of 100 MHz and such band widths are not only difficult to achieve, but also carry much increased receiver noise. It is also difficult to provide the necessary short injection pulses. Signal voltages are usually small for low injection levels. A solution to this problem is to use ac modulation of the injection source and to measure the relative phase and amplitude of the resulting modulation in conductivity, photovoltage or luminescence (37). A large phase shift develops when $\omega\tau$ approaches unity, where ω is the angular modulation frequency = $2\pi f$.

Consider a spatially uniform generation rate of minority carriers through out the sample volume

$$G = G_0 + G_1 e^{i\omega t} \qquad (1.39)$$

Then component of conductivity at frequency ω is measured. As electrical conductivity, $\sigma \propto n$, the expression for $\Delta n(t)$, the excess electron density, as a function of time can be obtained by solving the continuity equation.

$$d\Delta n/dt = G - \Delta n/\tau_n \text{ (surface effects are neglected)} \qquad (1.40)$$

But the generation function may be nonuniform and the surface recombination rate will generally differ from that in the bulk. Diffusion equation describing spatial distribution of minority carriers within the sample having length and breadth much greater than thickness, in the direction of light propagation is

$$D_n [d^2(\Delta n)/dx^2] + G e^{-\Delta x} - \Delta n/\tau_n = d(\Delta n)/dt \qquad (1.41)$$

$$G = G_o + G_1 e^{i\omega t} = \alpha\phi = \alpha(\phi_o + \phi_1 e^{i\omega t}) \qquad (1.42)$$

ϕ = photon flux, ϕ_o – incident photon flux, ϕ_1 = amplitude of modulation in photon flux, $\phi = \phi_o + \phi_1 e^{i\omega}$, α being the absorption coefficient for the incident light, then

$$\Delta n = \Delta n_o + \Delta n_1 e^{i\omega t} \qquad (1.43)$$

where Δn_1 may be complex. Substituting the equation for Δn and G in the above equation

$$D_n d^2\Delta n_o/dx^2 + D_n d^2\Delta n/dx^2 e^{i\omega t} + G e^{-\Delta x} + G_1 e^{-\Delta x} e^{i\omega t} - \Delta n_o/\tau_n - \Delta n_1/\tau_n e^{i\omega t} = i\omega\Delta n_1 e^{i\omega t} \qquad (1.44)$$

Steady state component of Δn satisfies the relation

$$D_n d^2\Delta n_o/dx^2 + G_o e^{-\Delta x} - \Delta n_o/\tau_n = 0 \qquad (1.45)$$

Then equation for Δn_1 is

$$D_n d^2\Delta n_1/dx^2 + G_1 e^{-\Delta x} - \Delta n_1/\tau_n - i\omega\Delta n_1 = 0 \qquad (1.46)$$

Here electron lifetime τ_n is to be replaced by an effective recombination lifetime τ_n'

$$\tau_n' = \tau_n/(1+i\omega\tau_n) \qquad (1.47)$$

(a) Experimental set up

Kerr cell modulates an appropriate filtered light source and the beam is split to provide a reference signal from a photo multiplier. Modulated illumination produces a sinusoidal variation in sample conductance, which is converted to an ac voltage by passing a constant dc current through it. The amplitude and phase of this signal voltage may then be measured, as a function of modulation frequency, using the vector voltmeter. An oscilloscope can also be

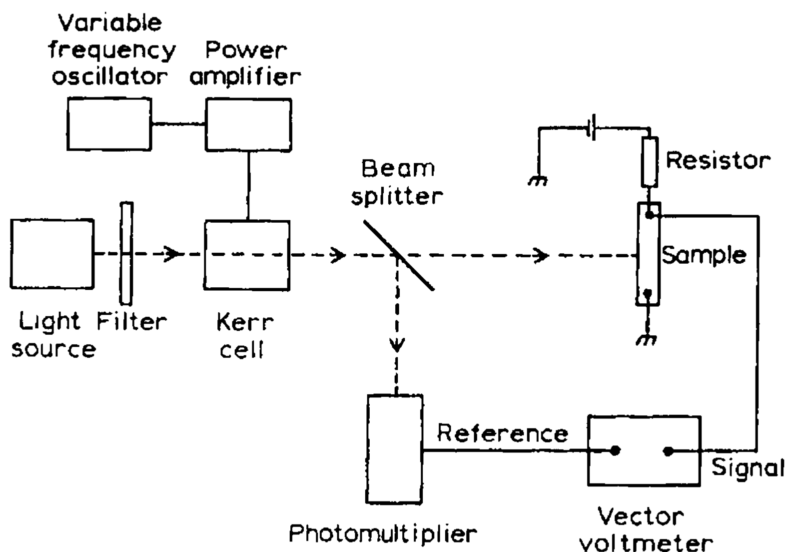

Fig. 1.11 Experimental set up to measure lifetime by way of modulated photoconductivity.

used as a detector, applying reference and signal voltages to the X and Y inputs, respectively, and resistance-capacitance time constant is adjusted until the two voltages are in phase. Then the photoconductive response time is given by τ_{eff} = RC. Choo et al. could measure lifetime in the order of sub-nanosecond using modulation frequencies from 1KHz to 40 MHz applied to GaAs light emitting diode (38)

Two complications may arise in interpretation, due to trapping and surface barrier effects. Effect of traps can be made inactive by shining an additional unmodulated white light source onto the sample to saturate the traps. Surface band bending occurs in most semiconductors and the incident light will modulate the amplitude of band bending. Carriers generated near the surface will exchange with those in surface states. This charge transfer represents a capacitive component of photocurrent, which is larger in heavily doped material. Its occurrence may be tested by observing whether tanϕ decreases with increasing light intensity.

1.2.2 (b) Stored charge method

In a forward biased p-n junction, the diode current is carried almost entirely by minority carriers on the low-doped side. Under steady state conditions, these holes are distributed over a region extending a few diffusion lengths into the n-type material, where they recom-

bine with majority electrons at a rate, which exactly balances the injection rate. If the forward bias is suddenly removed, the injected minority carrier distribution decays due to this recombination process and a measurement of the decay rate yields a value of the minority carrier lifetime τ_p (39).

There are two methods to measure τ. Both are initiated by forward biasing the diode and then switching it abruptly to either an open-circuit or reverse-biased condition. In the first case, the junction voltage is measured as a function of time and τ is derived from its decay rate. This method is known as open circuit voltage decay (OCVD). In the second case reverse current is monitored and τ obtained from its time dependence. In this case, the difference is that minority carriers are removed not only by recombination but also by being swept back across the junction by the reverse bias field. This reverse bias step-recovery method is referred to as the "stored-charge"method. In the case of asymmetric junction, one obtains a value of τ for the lightly doped (base) material. The most important aspect of this technique is that the material property (base) can be studied by making measurements on completed device.

In a forward biased abrupt p^+- n diode, current flows largely by injection of holes into the n-type base. Smaller density of minority electrons in p^+ side is neglected. The experimental arrangement is shown in the Fig. 1.12.

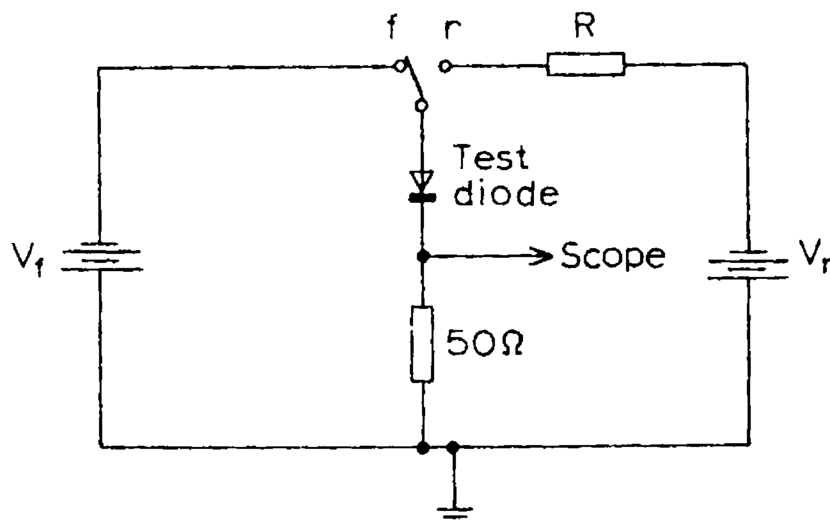

Fig.1.12 Experimental arrangement for measuring current in the stored charge method.

Initially the switch is in position f. Then the diode is forward biased and a forward current I_f flows. A steady state distribution of the injected holes is established in the base as indicated by curve-1 in Fig. 1.13. At time t = 0, the circuit is switched rapidly to position r, reverse biasing the diode with the voltage V_r in series with a current limiting resistor R. Initially because of the high density of holes in the junction region, the junction resistance remains low and the reverse current is given by $I_R = V_r/R$. This current represents the reverse flow of holes back into p^+ region and can be controlled by the choice of V_r and R. Hole density on the n side of the junction decreases as shown by curve-2 and after a time t_1, known as the storage time takes the form of curve-3. The time t_1 is defined as the time at which the hole density at the junction plane $\rho_n(0)$ has decayed to zero. For times $t > t_1$ the junction resistance is no longer negligible, the junction voltage rises and the reverse current falls to the steady state saturation value I_s appropriate to the reverse bias V_r. The hole distribution now appears as in curve-4 and the junction resistance is very much larger than R, therefore $I_s << I_r$ ($I_r = V_r/R$).

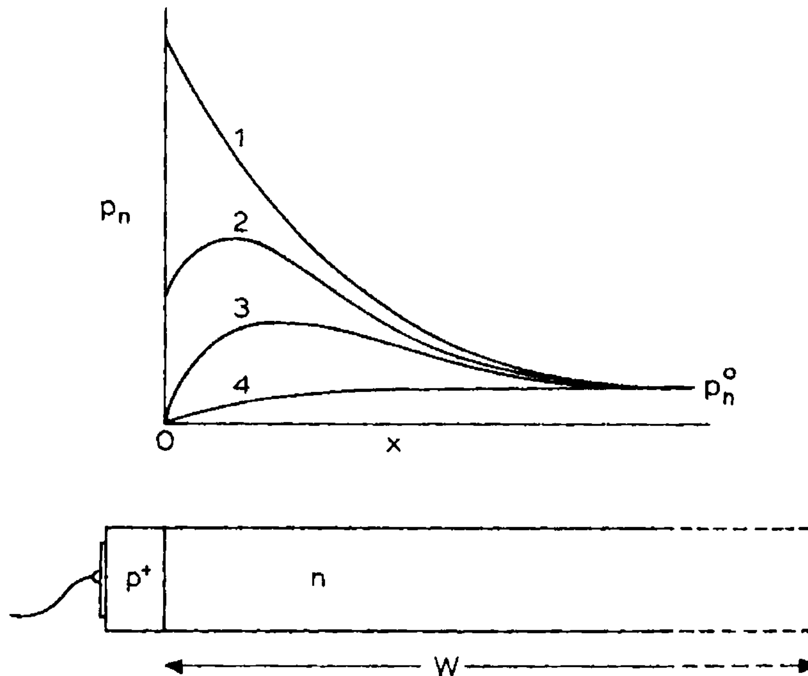

Fig. 1.13 The shape of the minority hole distribution on the n side of a p^+ - n diode during the recovery period.

Time dependence of the diode current is represented in Fig. 1.14. Storage time t_1 is characterized by the constant reverse current I_r after which the current decays to I_s. Recovery time (t_2) is usually defined as the time taken for the current to fall to a vlue of $I_r/10$. Recombination lifetime (τ_p) of the injected holes may be determined from this recovery behavior through any of the following three analyses (1) measurement of t_1 (2) measurement of t_2 (3) measurement of the integral under the reverse-current curve, which represents the total charge extracted from the n-side of the junction.

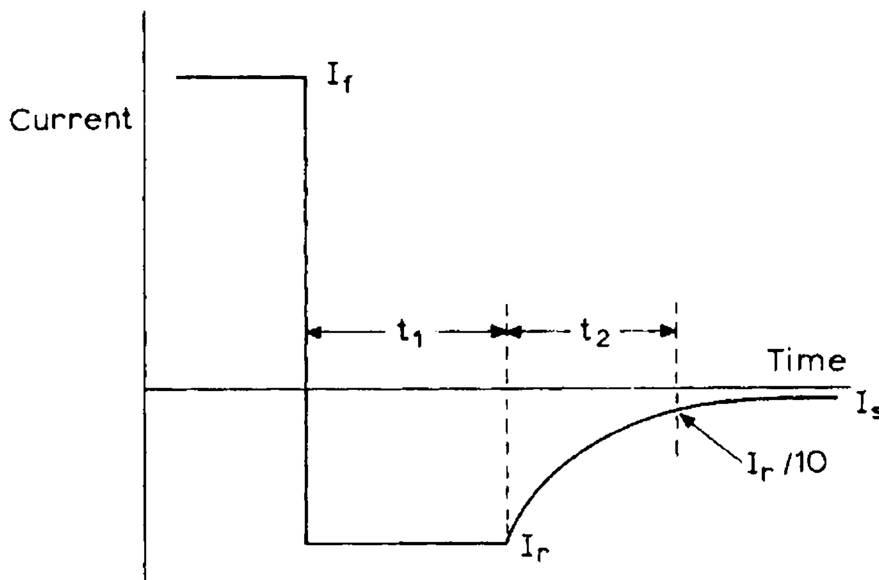

Fig. 1.14. The form of the reverse-current recovery curve for a p^+-n diode. The times t_1 and t_2 represent the charge-storage and charge-recovery periods. I_s is the steady-state reverse saturation current and $I_r = V_r/R$.

1.3 Effects of dopants and temperature on lifetime

Photoconductive decay curve deviates from simple exponential nature due to the presence of defect states and their distribution. Hence transient photo conductivity becomes one of the powerful techniques for studying optically active traps as the transient curves contain a wealth of information about kinetics of the charge carriers. But the parameters responsible for kinetics of the charge carriers vary from sample to sample and are very sensitive to the factors like temperature, level of radiation, effects of contacts and surface conditions.

1.3.1 Effect of dopants on carrier lifetime

A major effect of trapping is to make the experimentally observed decay time of the photocurrent, after the excitation has ceased, longer than the carrier lifetime. If no trapping centers are present, then observed photocurrent will decay in the same way as the density of free carriers do and the observed decay time will be equal to the carrier lifetime. If trapping centers are present, but the free carrier density is much greater than the density of trapped carriers, again the observed decay time of the photocurrent will be equal to the carrier lifetime. But if the density of free carriers is comparable to or less than the density of trapped carriers, then the trapping of carriers during the course of decay can prolong the decay so that the observed decay time is longer than the actual lifetime of a free carrier. If the density of trapped carriers is much greater than the density of free carriers, the entire decay of photocurrent is effectively dominated by the rate of trap emptying rather than by the rate of recombination.

In the absence of traps in the material, free carrier lifetime determines the value of the time constant. In the case of uniform generation of excess carriers throughout the sample and neglecting surface recombination, excess hole concentration in n-type material may be derived from the equation

$$d(\Delta p)/dt = G - \Delta p/\tau_p \qquad (1.48)$$

where G is the generation rate of electron hole pairs. After reaching a steady state condition, illumination is suddenly switched off. For values of Δp sufficiently small

$$\Delta p = \Delta p_0 \,(\exp(-t/\tau_p)) \qquad (1.49)$$

and the corresponding photocurrent is

$$i_p = i_{p0}(\exp(-t/\tau_p)) \qquad (1.50)$$

so that photoconductivity decays exponentially with time constant τ_p. When the illumination is switched on at $t = 0$, held constant from $t = 0$ to $t = t_0$ and switched off at $t = t_0$

Then

$$i_p = i_{p0}\,(1 - \exp(-t/\tau_p)) \qquad 0 \le t \le t_0 \qquad (1.51)$$

$$= i_{p0}\,(1 - \exp(-t_0/\tau_p))\, \exp\,(-(t-t_0)/\tau_p)) \quad t \ge t_0 \qquad (1.52)$$

The variation of I_p with time is shown in Fig. 1. 15

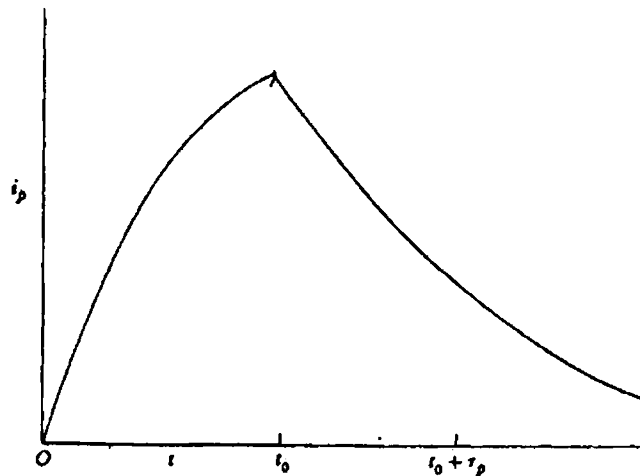

Fig 1.15. Photo-conductivity decay - no trapping

If only recombination centers are present the analysis will be unchanged. But if high density of traps ($\Delta n \neq \Delta p$) are present, transient decay will not correspond to an exponential with time constant τ_p. Consider a material having traps which can capture electrons but unlikely to capture holes. Such traps are called 'safe traps'. Let τ_p be the minority carrier lifetime of holes in n-type material and τ_1 the average lifetime of hole before it is caught in a safe trap (10). Let τ_2 represent the mean time a hole spends in a safe trap before being re-excited to the valence band. The equation satisfied by Δp is

$$d(\Delta p)/dt = G - \Delta p/\tau_p - \Delta p/\tau_1 + \Delta N_s/\tau_2 \qquad (1.53)$$

G – rate of generation of electron hole pairs and ΔN_s is the excess hole concentration in the safe traps

$$d(\Delta N_s)/dt = \Delta p/\tau_1 - \Delta N_s/\tau_2 \qquad (1.54)$$

so that in equilibrium

$$\Delta N_{so} = (\tau_2/\tau_1)\Delta p_o \qquad (1.55)$$

$$\Delta p_o = G\tau_p \qquad (1.56)$$

Presence of the safe traps does not therefore affect the number of minority carriers. From the condition of space charge neutrality

$$\Delta n = \Delta p + \Delta N_s \qquad (1.57)$$

In equilibrium

$$\Delta n_o = \Delta p_o + \Delta N_{so} = \Delta p_o(1 + \tau_2/\tau_1)) \qquad (1.58)$$

Total charge generation due to illumination is

$$e\mu_p\Delta p_o + e\mu_n\Delta_{no} = e\mu_p\Delta p_o + e\mu_n\Delta p_o(1+ \tau_2/\tau_1) \qquad (1.59)$$

$$e\Delta p_o\,(\mu_p + \mu_n + \mu_n\tau_2/\tau_1) \qquad (1.60)$$

But $\Delta p_o = G\tau_p$, Steady state conductivity due to illumination is

$$\Delta\sigma_o = eG\tau_p(\mu_p + \mu_n + \mu_n\tau_2/\tau_1) \qquad (1.61)$$

and steady state photocurrent is

$$i_{po} = eG\tau_pEd(\mu_p + \mu_n + \mu_n\tau_2/\tau_1) \qquad (1.62)$$

where 'd' is the thickness of the material and E is the applied potential between the electrodes. From the above equation, it is clear that if $\tau_2 >> \tau_1$ the traps will cause a considerable increase in photocurrent and when this condition holds, excess hole spends considerably longer time in a safe trap than in the conduction band.

Consider the case if $\tau_2 >> \tau_1$ and τ_p. If the illumination is suddenly cut off after the steady state has been established, the minority carrier concentration will drop rapidly with time constant τ_p since initially $\Delta p/\tau_1 = \Delta N_s/\tau_2$. After this initial drop

$$d(\Delta N_s/dt) = - \Delta N_s/\tau_2 \qquad (1.63)$$

so that ΔN_s decreases with time constant τ_2. The number of excess carriers (electrons) is now nearly equal to $\Delta N_{s,}$ so

$$\Delta n \cong \Delta N_s \qquad (1.64)$$

$$I_{po} = eG\tau_pEd\mu_n(\tau_2/\tau_1)\exp(-t/\tau_2) \qquad (1.65)$$

The trapped holes are slowly released and while they are trapped, they cause an excess of majority carriers equal to the number of trapped minority carriers. The form of variation of photocurrent is shown in Fig.1.16

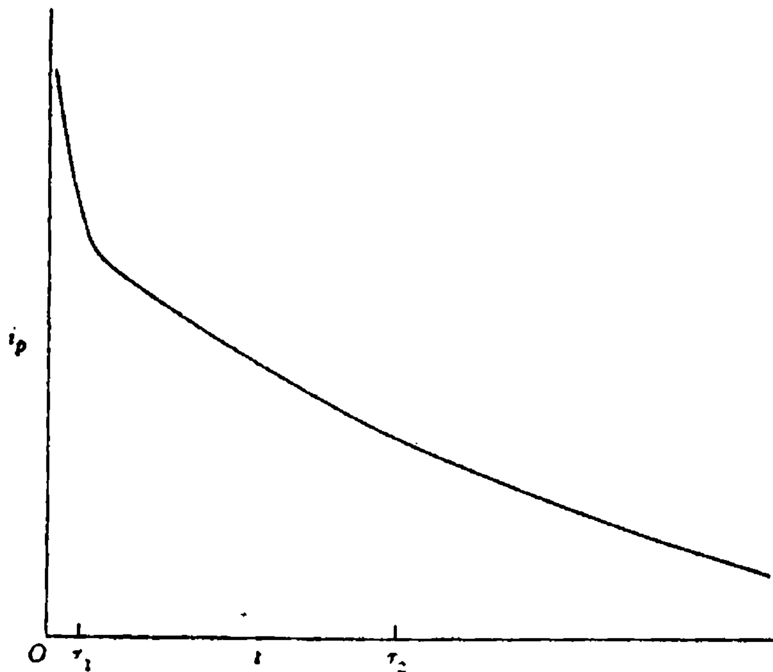

Fig.1.16. Photo-conductive decay - effect of trapping

Initial fractional drop in the photocurrent is small if $\tau_2 >> \tau_1$. The distribution of trapping centers in semiconductors is frequently much more complex than the above mentioned model. There may be several kinds of traps present, and each of them may not even correspond to a single energy level, but have a distribution of levels.

1.3.2 Effect of temperature on carrier lifetime

Recombination and capture processes are characterized by time constants that reflect capture cross-section and density of the imperfections involved. Thermally activated imperfection emptying or filling has a rate of change that depends upon the capture cross-section and ionization energy. These processes are functions of temperature also. At fixed temperature the rise or decay of photoconductivity, luminescence or photo capacitance is controlled by the value of the parameters like capture cross-section, density of imperfections involved and activation energy at that temperature. In thermally stimulated decay, the variables can be measured as a function of time but under conditions in which the temperature itself is varying with time (2).

The simplest decay process is one in which there is exponential decay.

$$i(t) = i_0 \exp(-t/\tau) \quad (1.66)$$

It is assumed that τ is independent of time. If the process involved is one in which trapped electrons are being thermally freed from traps to the conduction band, then

$$1/\tau = N_c\beta_n \exp(\Delta E/kT) \quad (1.67)$$

where N_c is the effective density of states in the conduction band, β_n is the capture coefficient of the traps for electrons and ΔE is the trap depth or ionization energy. If i(t) is measured at different temperatures, then a plot of ln i(t) vs t at each temperature is a straight line characterized by a time constant of $\tau(T)$. Then the plot of ln $\tau(T)$ vs 1/T (an Arrhenius plot) is a straight line with a slope equal to $-\Delta E/k$ and intercept depending on β_n.

1.3.3 Rate window technique

A decay sampling technique, particularly suited to computerized analysis, is known as the "rate window approach". Two times are chosen during the decay process, t_1 and t_2 ($t_2>t_1$) and the signal i(t) is measured at each of these times. Then $i(t_1) - i(t_2)$ is plotted as a function of temperature. The result is a curve exhibiting a maximum at a particular temperature, which can be suitably interpreted to obtain the trap parameters. Fig. 1.17 shows the rate window approach to measurement of DLTS. In the present study, decay time is calculated from the photoconductive decay (PCD) curve at different temperatures during a particular interval of time and plotted as a function of temperature. It is found that the decay time varies with trap parameters.

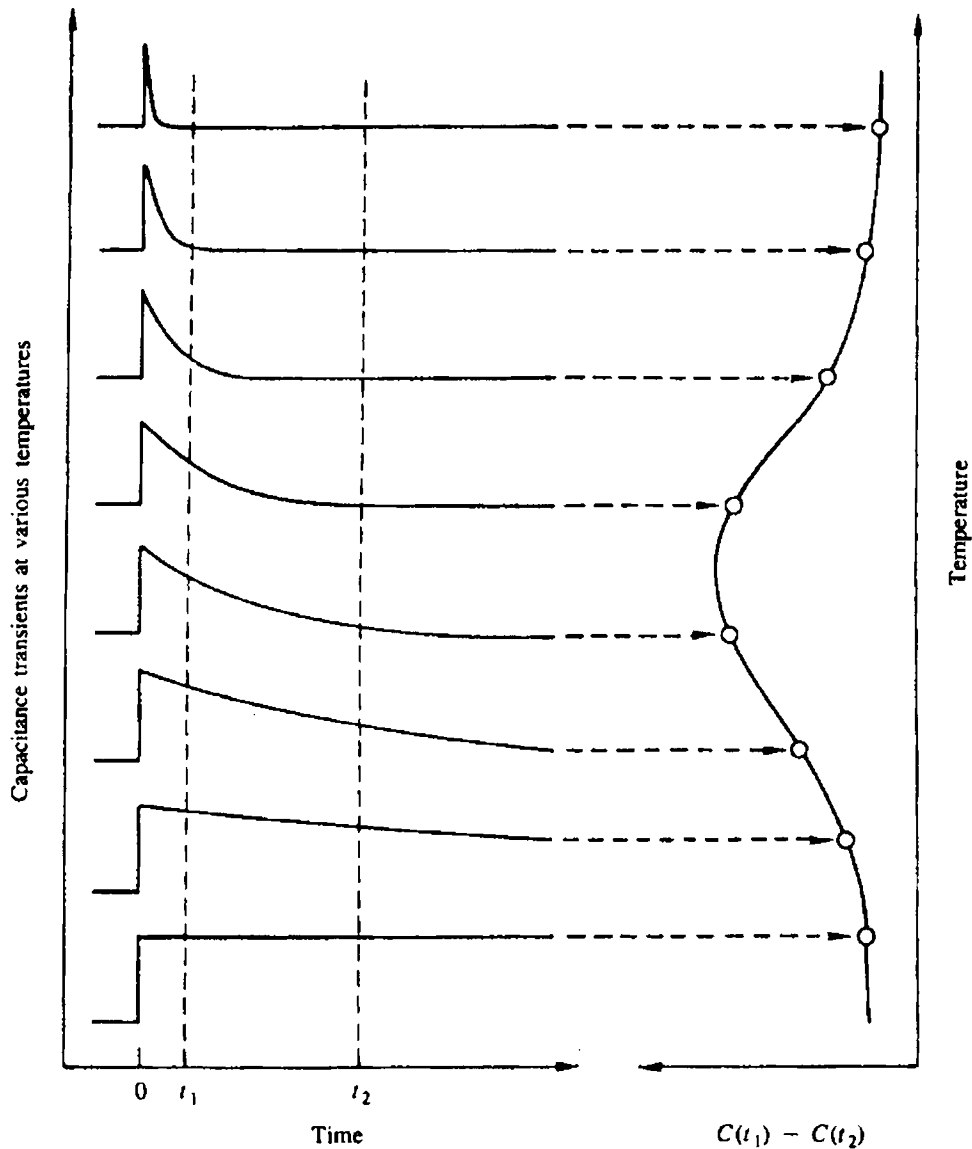

Fig. 1.17 Rate window approach for measurement of DLTS

1.4 Importance of lifetime measurements

The lifetime of charge carriers is one of the important parameters to characterize a material because it plays a critical role in determining the semiconductor device parameters. Room temperature minority carrier lifetime is expected to have a significant influence on the

conversion efficiency of solar cell since it is a direct measure of the efficiency of the various radiative and non radiative loss channels of the photoexcited carriers. B. Ohnesorge et al. reported the correlation between the carrier lifetime of the absorber layer at room temperature and short circuit current density (J_{sc}), the open circuit voltage (V_{oc}) and solar cell efficiency (η) in $Cu(In,Ga)Se_2$ solar cells (40). It is shown that a cell made of absorbing material with longer lifetime has a high open circuit voltage and hence high efficiency. However there was negligible increase in the short circuit current.

Lifetime measurement can be used to study the radiation effect on materials. W. P. Lee et al. reported the variation in lifetime due to ultraviolet irradiation on thermally oxidized silicon wafers (25). In this study, it has been established that UV photons modify the density of two interface traps and oxide charge density. These modifications directly affect the lifetime of charge carriers. K. L. Narayan reported the prolonging of photoconductive decay in ion implanted CBD CdS thin films (41).

The presence of traps and trap parameters can be studied from lifetime measurements. R. K. Arenkiel et al. reported the dominant transport and recombination mechanism in polycrystalline silicon and CdS thin films using temperature dependent lifetime measurements (14). R. H. Bube et al. used lifetime measurement as one of the techniques to determine trap parameters in CdS crystals (42). S. Mora et al. reported the measurement of minority carrier lifetime in $CuInS_2$ (43). They made an attempt to improve the efficiency of the homojunction $CuInS_2$ solar cells by improving the material property. M. Ichimura et al. reported the fast and slow decay components of the excess carrier concentration and measured the corresponding lifetimes. The origin of slow decay is discussed on the basis of the numerical simulation of the recombination process and the presence of traps with a very small electron capture cross-section (44).

References

1. J. W. Orton and P. Blood, The electrical characterization of semiconductors – Measurement of minority carrier properties, Academic Press Limited, (1990) 1

2. Richard H. Bube, Photoelectronic Properties of Semiconductors, Cambridge University Press, (1992) 1

3. Lawrence L. Kazmerski, Polycrystalline and amorphous thin films and devices, Academic press, U.K , (1980)

4. R. L. Petritz, Phys. Rev., 104 (1956) 1508

5. Richard H. Bube, Photoconductivity of Solids, Robert E. Krieger Publishing Co., New York (1960) 34

6. Svein Espevik, Chen-ho Wu and Richard H. Bube, J. Appl. Phys., 42 (9) (1971) 3513

7. C.Julien, M. Eddrief, K.Kambas and M. Balkanski, Thin Solid Films, 137 (1986) 27

8. G. Micocci, A. Tepore, R. Rella and P. Siciliano, Phys. Stat. Sol (a), 148 (1995) 431

9. Chen-ho Wu and Richard H. Bube, JAP, 45 (1974) 648

10. R. A. Smith, Semiconductors, Cambridge University Press, (1959) 348

11. Richard H. Bube, Photoconductivity of Solids, Robert E. Krieger Publishing Co., New York, (1960) 130

12. N. V. Joshi, Photoconductivity, MarcelDekker,INC. New York, (1990) 101

13. M. Balkanski, C. Julien, A. Chevy and K. Kambas, Solid State Communications, 59 (7) (1986) 423

14. R. K. Ahrenkiel and Steven Johston, Solar Energy Materials and Solar Cells, 55 (1998) 59

15. K. Topper, J. Kranser, J. Bruns, R. Scheer, A. Weidinger, D. Brauning, Solar Energy

Materials and Solar Cells, 49 (1997) 383

16. G. A. Medvedkin and M. A. Aagomedov, J. Appl. Phys., 82(8) (1997) 4013

17. Richard H. Bube, Photoelectronic Properties of Semiconductors, Cambridge University Press, (1992) 19

18. S. G. Patil, J. Phys. D5, (1972) 1692

19. T. Yoshida, T. Oka and M. Kitagawa, Appl. Phys. Lett., 21 (1972) 1

20. J. W. Orton, B. J Goldsmith, J. A. Chapman and M. J. Powel, JAP, 53 (3) (1982) 1602

21. J. L. Shay and J. H. Warnick, Ternary Chalcopyrite semiconductors: Growth, Electronic Properties and Applications, Pergamon, New York, 1975

22. N. V. Joshi, L. Martinez and T. Echeverria, J. Phys. Chem. Solids, 42 (1981) 281

23. E. Bertran, A. Lousa, M. Varela, M. V. Garcia-CUENCA and J. L. Morenza, Solar Energy Materials, 17 (1988) 55

24. Richard H. Bube, Photoconductivity of Solids, Robert E. Krieger Publishing Co., New York, (1960) 59

25. W. P. Lee, Y. L. Khong and W. S. Seow, JAP, 85(2) (1994) 994

26. T. L. Chu, Shirley. S. Chu, N. Schultz, C. Wang and C. Q. Wu, J. Elect. Chem. Soc., 139(9) (1992) 2443

27. Stockmann, Z. Physik, 143 (1955) 348

28. S. G. Abdullaev, V. A. Aliev, N. T. Mamedov and M. K. Sheinkman, Sov. Phys. Semicond., 17 (1983) 1141

29. N. V. Joshi, L. Mogollon, J. Sanchez and J. M. Martin, Solid State Communication, 65 (1988) 151

30. R. A. Hopfel, Appl. Phys. Lett., 52 (1988) 801

31. J. W. Farmer and D. R. Locker, J. Appl. Phys., 52 (1981) 401

32. D. V. Lang and R. A. Logan, Phys. Rev. Letter, 39 (1977) 635

33. J. W. Orton and P. Blood, The electrical characterization of semiconductors – Measurement of minority carrier properties, Academic Press Limited., (1990) 31

34. ibid 71

35. N. V. Joshi and H. Aguilar, J. Phys. Chem. Solids, 43 (1982) 797

36. P. Lenczewski and E. Fortin, Phys. Status Solidi (a) 3, (1970) K267

37. J. W. Orton and P. Blood, The electrical characterization of semiconductors – Measurement of minority carrier properties, Academic Press Limited., (1990) 125

38. Choo. S. C, Etchells. A. M and Watt. L. A. K, Phys. Rev. B, 4 (1971) 4499

39. J. W. Orton and P. Blood, The electrical characterization of semiconductors – Measurement of minority carrier properties, Academic Press Limited., (1990) 158

40. B. Ohnesorge, Appl. Phys. Lett., 73 (9) (1998) 1224

41. K. L. Narayan, Ph. D Thesis, CUSAT (1999)

42. R. H. Bube, Gustavo A. Dussel, Ching-Tao Ho and Lewis D. Miller, JAP, 37 (1) (1966) 21

43. S. Mora, N. Romeo and L. Tarricone, Solid State Communications, 29 (1979) 155

44. M. Ichimura, H. Tajiri, Y. Morita, N. Yamada and A. Usami, Appl. Phys. Lett., 70 (18) (1997) 1745

Chapter 2

Photoconductivity studies on CBD CdS thin films

2.1 Introduction

CdS is a well-studied II-VI semiconductor, which exists in two different structural modifications, namely stable wurtzite phase and metastable cubic sphalerite phase (1). CdS films prepared using Chemical Bath Deposition (CBD) technique is normally found to be either in the metastable phase or as a mixture of Cubic and hexagonal phase (2).

Thin film CdS is used as a window layer in most of the current thin film polycrystalline photovoltaic devices. CdS based thin film solar cells received considerable attention due to economic reasons and ease of fabrication of large-area thin film devices. T. L. Chu et al. reported that CdS is the best heterojunction partner for CdTe solar cells (3). K. W. Mitchell et al. reported that CdS is the most compatible window material for $CuInSe_2$ absorber material (4). CdS is also used as a buffer layer in solar cells. It is reported that a record efficiency of 18.8% is achieved with Cu(In, Ga)$(Se, S)_2$/ZnO cells containing such a buffer layer on a laboratory scale (5). A. N. Molin et al. reported the work done on CdS/Cu_2S heterojunction solar cell (6) and Siham A. Al Kuhaimi reported electron affinity differences in CdS/Si solar cell (7). Device performance has been linked to the deposition technique and post treatment of the CdS layer. CdS thin films were grown by a variety of techniques such as thermal evaporation (8), sputtering (9), spray pyrolysis (10), flash evaporation (11) and CBD technique (12). Among these, CBD is a low cost process and is suitable for preparing large area

thin films. It is possible to obtain uniform films with good adherence and reproducibility using this technique. Intensive studies were reported earlier on CdS thin films prepared using CBD technique (13-18).

Growth of CdS film is columnar and perpendicular to the substrate surface (19). Hence grain boundaries parallel to the junction that impede the flow of photogenerated carriers are few. More over CdS is a direct band gap material having a band gap of 2.4 eV. As prepared CdS is n-type and its electrical property is mainly determined by the quantity of excess Cd^{++} and S^{--} vacancies present in it. K. P. Varkey et al. reported conversion of n-type CdS, prepared using spray pyrolisis technique into p-type by the diffusion of Cu and fabrication of CdS homojunction solar cell (20). J. M. Dona and J. Herrero reported that deposition temperature plays an important role on electrical characteristics of CBD CdS thin film (21). They found that conductivity of the film increased on increasing the deposition temperature due to the increase in Sulphur uncompensated vacancies and the corresponding free carrier density. One of the factors affecting efficiency of the solar cell is minority carrier density and lifetime, which in turn depends mainly on the presence of different trap levels existing in the band gap of the material.

Photoconductivity (PC) processes may be the most suitable technique for obtaining information about the states in the gap. At a fixed temperature, rise or decay of photoconductivity of a semi conducting material is influenced by parameters such as activation energy, capture cross-section and density of imperfections present in the material (22). In the presence of traps, additional time-dependent processes are involved with trap filling (during the rise) and trap emptying (during the decay). The measured response time (τ) is very much greater than the free carrier lifetime in the absence of traps. R. H. Bube reported that the decay time for pure cadmium sulphide crystals may be as small as a fraction of a milli second, whereas the decay time for conducting crystals containing halide may be as large as a hundred milliseconds (23). K. L. Narayan reported decay time in CBD CdS in the order of seconds and after ion implantation decay time increased to hours (24). R. K. Ahrenkiel et al. used radio frequency photoconductive decay (RFPCD) technique to measure the photoconductive lifetime of CdS prepared using CBD and laser deposition technique (25). Room temperature minority-carrier lifetime has a significant influence on the conversion efficiency of the solar cells (26,27). A. Carbon et al. reported the lifetime dependence on temperature, light intensity and wavelength in Ag doped CdS film using steady state and transient photoconductivity (28).

In the present study, photoconductivity measurements were done on CBD CdS thin films of three different thicknesses at room temperature in air and vacuum. The dependence of photoconductivity on film thickness and diffusion of oxygen into the film was also studied. XPS analysis was done to supplement this result. Decay time of charge carriers in these samples was measured using Photoconductive Decay (PCD) method, which is one of the simple methods used for lifetime measurements in semiconductor materials. Decay time variation study with temperature in the range 100 – 300 K depicted the contribution of carriers from different defects present in the material. Activation energy of these defects was found out using Thermally Stimulated Current (TSC) measurement technique.

2.2 Preparation of CBD CdS thin films

CBD technique is the controlled precipitation of a compound from a solution on to a suitable substrate. In this process, precipitation of the solid phase occurs due to the super saturation of the reaction bath. At a particular temperature, when ionic product of reactants exceeds the solubility product, precipitation occurs. CdS is deposited on to the glass substrate by the reaction of Cd^{++} and S^{--} ions released in the aqueous alkaline bath. A complexing agent is added to control the hydrolysis of the metal ion. The process depends on slow release of sulphur ions into the alkaline solution. Release of ions depends on temperature and pH of the reaction bath. Increase in temperature of the bath increases the release of ions and speed up the precipitation where as increase in pH slows down the release of ions and hence the precipitation. Mondal et al. reported the TEA method for complexing Cadmium ions and producing CdS thin films based on the following reactions (29).

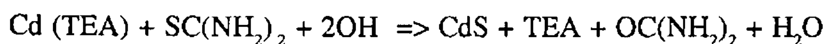

$$Cd\,(TEA) + SC(NH_2)_2 + 2OH \Rightarrow CdS + TEA + OC(NH_2)_2 + H_2O$$

In the present work CdS was prepared from a reaction mixture containing aqueous solution of 10 ml (1M) $CdCl_2$, 10 ml (1M) Thiourea ($SC(NH_2)_2$) 3ml TEA and Ammonia. $CdCl_2$ solution was first mixed with TEA. A white precipitate was formed. Excess Ammonia was added and stirred well till the precipitate was completely dissolved. Thiourea was then added to the mixture. Solution was stirred well and taken in a 50 ml beaker. Glass slides were placed in the beaker containing the solution, leaning against the walls of the beaker. The beaker was placed in a water bath kept at a temperature of 80 °C. Glass slides were taken

out of the reaction bath after 30 minutes and washed in distilled water. Thickness of the film was increased by dipping this film repeatedly in a fresh solution of the same composition for 30 minutes each to obtain two dip and three dip films. The film on the glass slide facing the beaker was taken for photoconductivity studies. The film on the other side was more powdery, due to the settling of particulate CdS by gravity. This film was removed using cotton swabs dipped in dilute HCl. These samples were then dried at 100 ° C for one hour in electric oven. Thickness was measured by gravimetric method and found to be 1, 1.3 and 2 μm for single, double and triple dip films. These samples are named sample ‘a’, ‘b’ and ‘c’ respectively. Sheet resistance of these samples was above 2000 MΩ/cm^2.

2.3 Photoconductive decay measurements

2.3.1 Experimental set up

Film was loaded on the cold finger of a liquid Helium Cryostat (CTI-Cryogenics-Helix Technology Corporation) and temperature was controlled using Lakeshore Auto tuning Temperature Controller (Model-321). Experimental set up is shown in Fig. 2.1. Pressure in the cryostat was 10^{-5} mbar for measurements in vacuum.

Electrodes were painted on the top surface with a separation of 1.2 mm using silver paste. An opaque, non-conducting mask with a slit of area 1x7 sq.mm was placed over the sample to illuminate only the required area. Contacts from the electrodes were taken through two holes on the mask on both sides of the slit and care was taken not to allow light to fall on the electrodes. White light of intensity 20 mW/cm^2 was used to illuminate the sample. Duration of illumination was chosen to be 5 minutes in all cases. Heat radiation from the light source was avoided by passing the light beam through water filter.

For photoconductivity measurements, a constant dc source (0-30 V) and a high resistance R_L (10 MΩ) were connected in series with the sample. Decay of the voltage across the high resistance after switching off the illumination was measured using Kiethely 2000 multimeter.

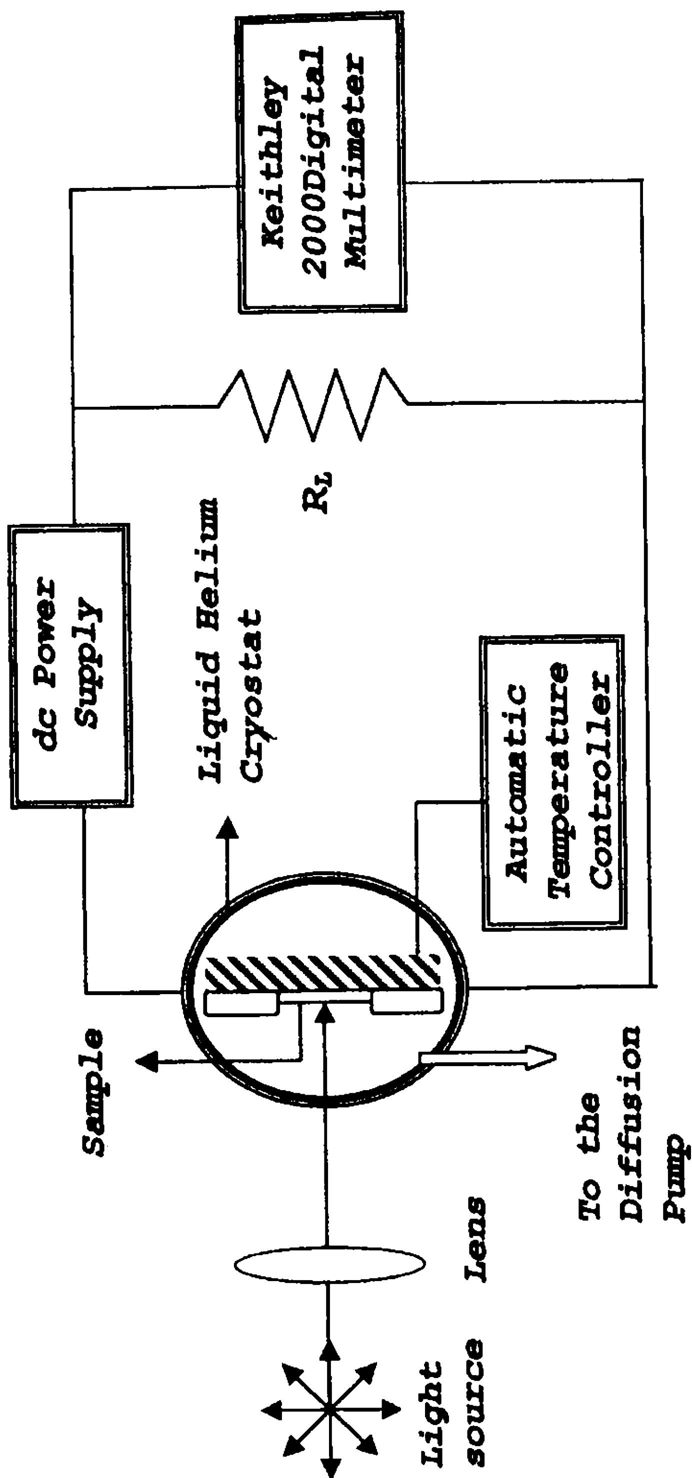

Fig.2.1. Experimental set up for photoconductivity measurements

Care was taken to get steady value for dark conductivity before illuminating the sample for each measurement.

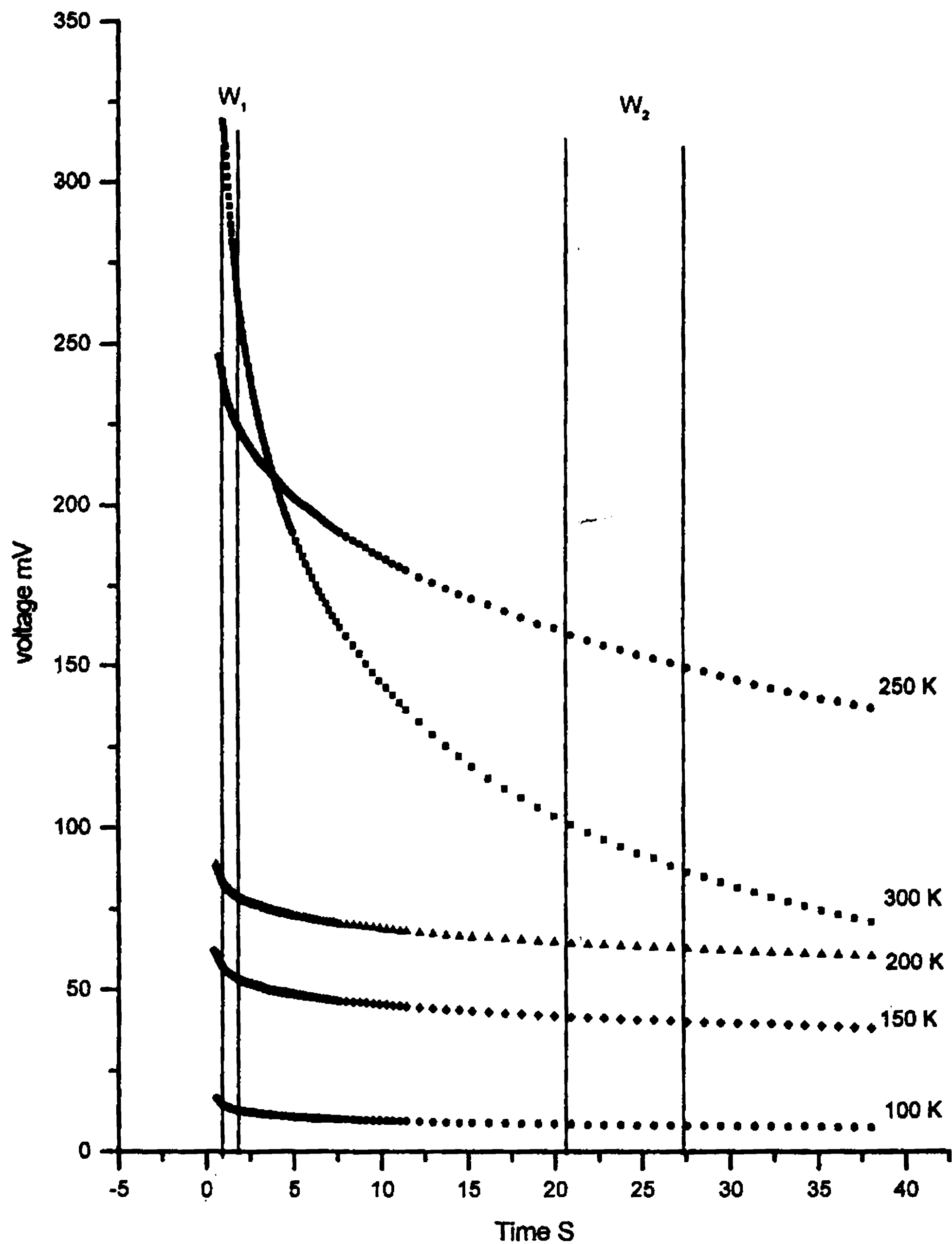

Fig. 2.2. PCD curves at different temperatures and windows chosen at fast and slow decay regions

PCD measurements were taken in the temperature range 100 – 300 K in an interval of 10 K. Photoconductive decay method was chosen to measure the decay time of charge carriers. Decay time variation study with temperature was done using "rate window technique". Since PCD curves had two well-defined regions, two windows were chosen, one at fast decay region and the other at slow decay region as shown in Fig. 2.2. These curves were exponentially fitted using Microsoft Excel 2000 programme. The equation for the curve and R^2 value on fitting are as shown in Fig. 2.3.

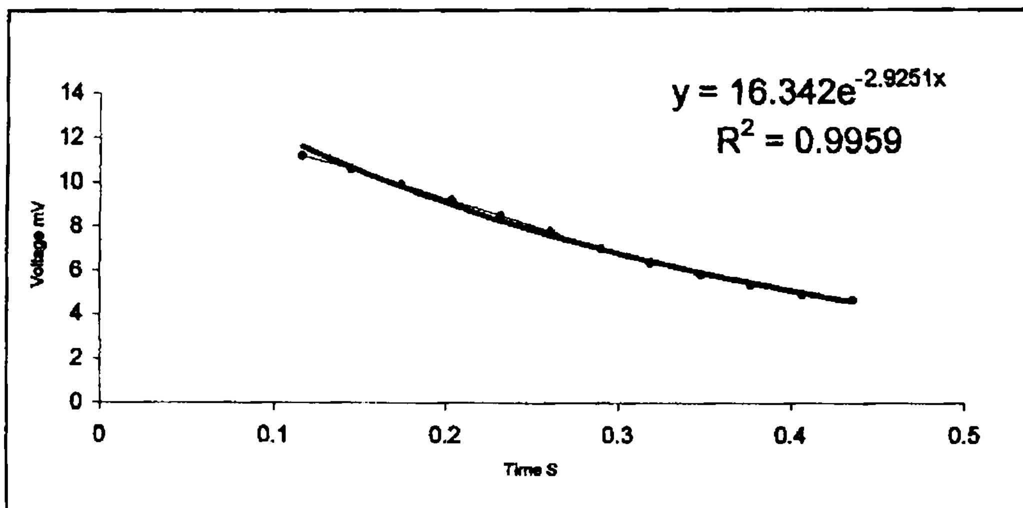

Fig. 2.3. Exponentially fitted curve using Microsoft Excel 2000 programme.

From the fitting, the equation matching the experimental curve is obtained as

$$Y = 16.342\, e^{-2.9251x}$$

which is of the form

$$I = I_0\, e^{-t/\tau}$$

and the percentage of fitting corresponding to $R^2 = 0.9959$ is 99.59. From this, τ was calculated to be 0.341 S. Decay time calculated in the fast decay region is termed as τ_f and that at the slow decay region as τ_s. The relation between measured decay time (τ) and lifetime (τ_0 – decay time when there is no defects in the material) is (22)

$$\tau = \tau_0(1 + n_t/n)$$

where 'n_t' is defined to be the density of traps that must empty in order for the steady state Fermi energy to drop by KT and 'n' is the number of photo excited charge carriers. If $n >> n_t$, for low trap densities and/or high photo excitation rates, $\tau \approx \tau_0$, whereas if $n << n_t$, for high trap densities and/or low photo excitation rates, $\tau = \tau_0(n_t/n)$. In the present work intensity of illumination is kept constant and low. Then the variation in decay time is considered to be due to variation in trap density.

2.3.2 Photoconductivity decay time measurements at room temperature in air and vacuum

Carrier decay time in CBD CdS thin films kept in air at 295 K was measured using photoconductive decay technique. The experiment was repeated for three different thicknesses, three different bias voltages and three different illumination conditions. PCD curves obtained for samples 'a', 'b' and 'c' for a biasing voltage of 20V and illumination 25 mW/cm^2 are shown in Fig. 2.4.

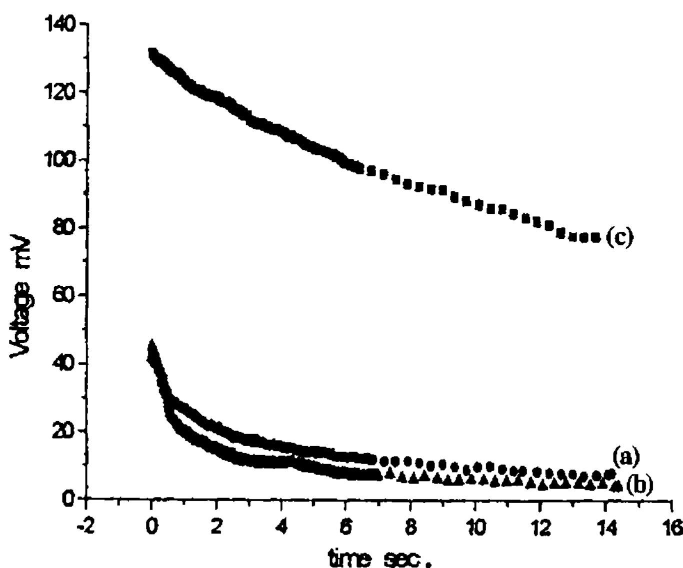

Fig. 2.4 PCD Curves for sample 'a', 'b' and 'c' for a bias 20 V and illumination 25 mW/cm^2

The PCD curves showed two well-defined regions-fast decay and slow decay regions for samples 'a' and 'b'. Fast decay may be due to the defects present at the surface of the sample, which are mainly recombination in nature (30). The decay time corresponding to the initial fast decay region (τ_f) were found to be ~2 sec. for sample 'a' and ~1 sec. for sample 'b'. The decay time corresponding to the slow decay region (τ_s) for sample 'a' and sample 'b' were around ~4.2 sec. and ~3.2 sec., respectively. However for sample 'c' there was only one decay region within the decay time of 14 sec. and the decay time was found to be 20.5 sec. It was about five times the value of τ_s for sample 'a' and sample 'b'. The experiment was repeated for three different illumination conditions and three different biasing voltages. Decay times were calculated for two different regions of PCD curves in each case and tabulated in Table. 1.

Table 1.

CdS – 1dip				CdS – 2dip				CdS – 3 dip		
Bias V	Illum. mW/cm²	τ_f sec.	τ_s sec.	Bias V	Illum. mW/cm²	τ_f sec.	τ_s sec.	Bias V	Illum. mW/cm²	τ_s sec.
10	25	2.1	4.0	10	25	1.1	4.0	10	25	22.9
10	45	1.8	4.3	10	45	1.3	3.8	10	45	25.9
10	58	1.7	3.6	10	58	1.3	3.5	10	58	20.1
15	25	2.0	4.7	15	25	1.1	3.4	15	25	17.2
15	45	1.9	4.1	15	45	1.1	4.1	15	45	18.6
15	58	1.9	4.1	15	58	1.1	3.4	15	58	20.2
20	25	2.0	4.2	20	25	1.1	3.2	20	25	20.5
20	45	1.8	4.1	20	45	1.1	3.4	20	45	17.5
20	58	1.7	4.0	20	58	1.6	3.2	20	58	18.4

In all cases it is observed that variation of biasing voltage and illumination in this range did not affect the decay time. But R. H. Bube already reported the variation of photoconductivity with light intensity and biasing voltage (31, 32). According to the studies, a high electric field reduced the probability of retrapping, rather than to empty trap directly by a field ionization effect and increased the rate of decay of photoconductivity. Since the samples under study were highly resistive, variation of electric field in this range did not

affect the decay time. It was also observed that in sample 'a' and sample 'b', surface recombination was more. That is, more charge carriers are lost at the surface and hence the charge carriers reaching the bulk is less and photoconductivity is reduced, where as in sample 'c', the surface recombination was less and less number of charge carriers were lost at the surface. Hence charge carriers reaching the bulk is increased and decay time increased. It is also observed that photoconductivity increased as the film thickness increased (33).

Knowledge of the effect of ambient conditions on photoconductivity and carrier lifetime in semi conducting material is important for surface pacification, which is necessary in many devices. In this study, PCD measurements were taken in air and vacuum on samples 'a' and 'b' at 300 K. PCD curves of these samples are shown in Fig. 2.5. Here it is evident that fast decay time (τ_f) has a strong dependence on sample thickness and ambient conditions (like air or vacuum) in which the PCD is taking place. In air both samples exhibited equal values for τ_f. Photoconductivity was also very low when the samples were in air. When the measurements were taken in vacuum, τ_f was 9 sec. for sample 'a' and 12 sec. for sample 'b'. Photoconductivity also increased considerably for both samples when kept in vacuum. Another observation was that values of τ_s (35 sec.) did not depend upon sample thickness or ambient conditions. The dependence of photoconductivity and fast decay time on ambient conditions may be due to the diffusion of oxygen into the film. Muzeyyan et al. had reported earlier that the initial fast decay is dominated by surface recombination of the carriers when the source of excitation is turned off (30). Again J. Woods had reported that photosensitivity of CdS crystals decreased considerably when exposed to oxygen due to the diffusion of oxygen into sulphur vacancies (34). Another observation on CdS crystal by Peter Mark was that as the partial pressure of oxygen was lowered the photoconductivity gains and decay time increased (35). R. H. Bube reported that physically adsorbed oxygen could take an electron from the material to form a chemically adsorbed surface state, leaving behind a depletion region near the surface of the material (32). These earlier studies very well support our conclusion that diffusion of oxygen can be one of the reasons for the decrease in fast decay time on exposure to air.

Fig. 2.6 gives the XPS depth profile of sample 'b'. It gives variation of concentration of different elements from the surface to the substrate-film interface. This is done by removing the sample, layer by layer by sputtering off (represented as cycles in Fig. 2.6) each layer. Here it is clearly seen that oxygen is present at the top surface and correspondingly there is

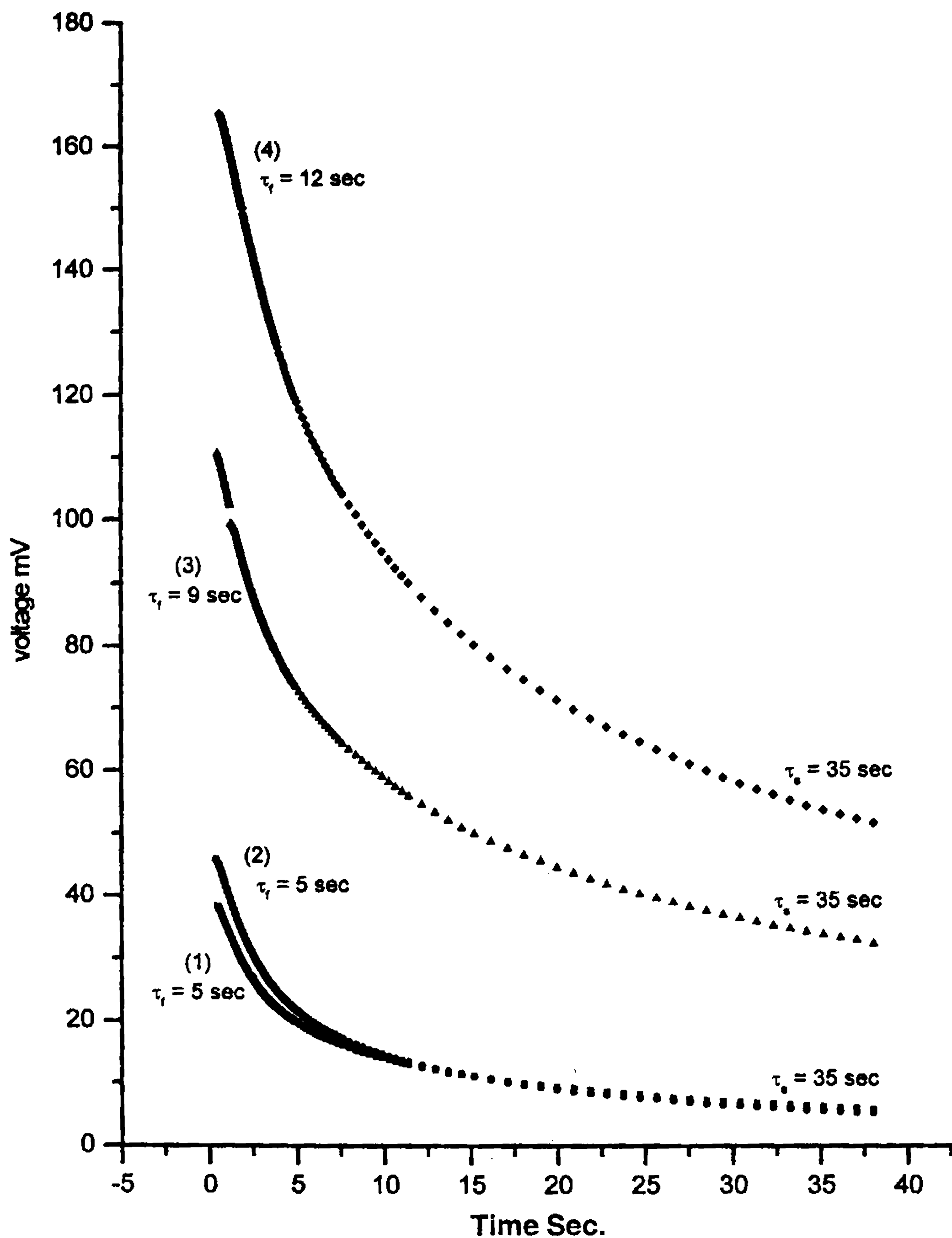

Fig. 2.5 PCD curves for sample 'a' in air (1) and vacuum (2), for sample 'b' in air (3) and vacuum (4)

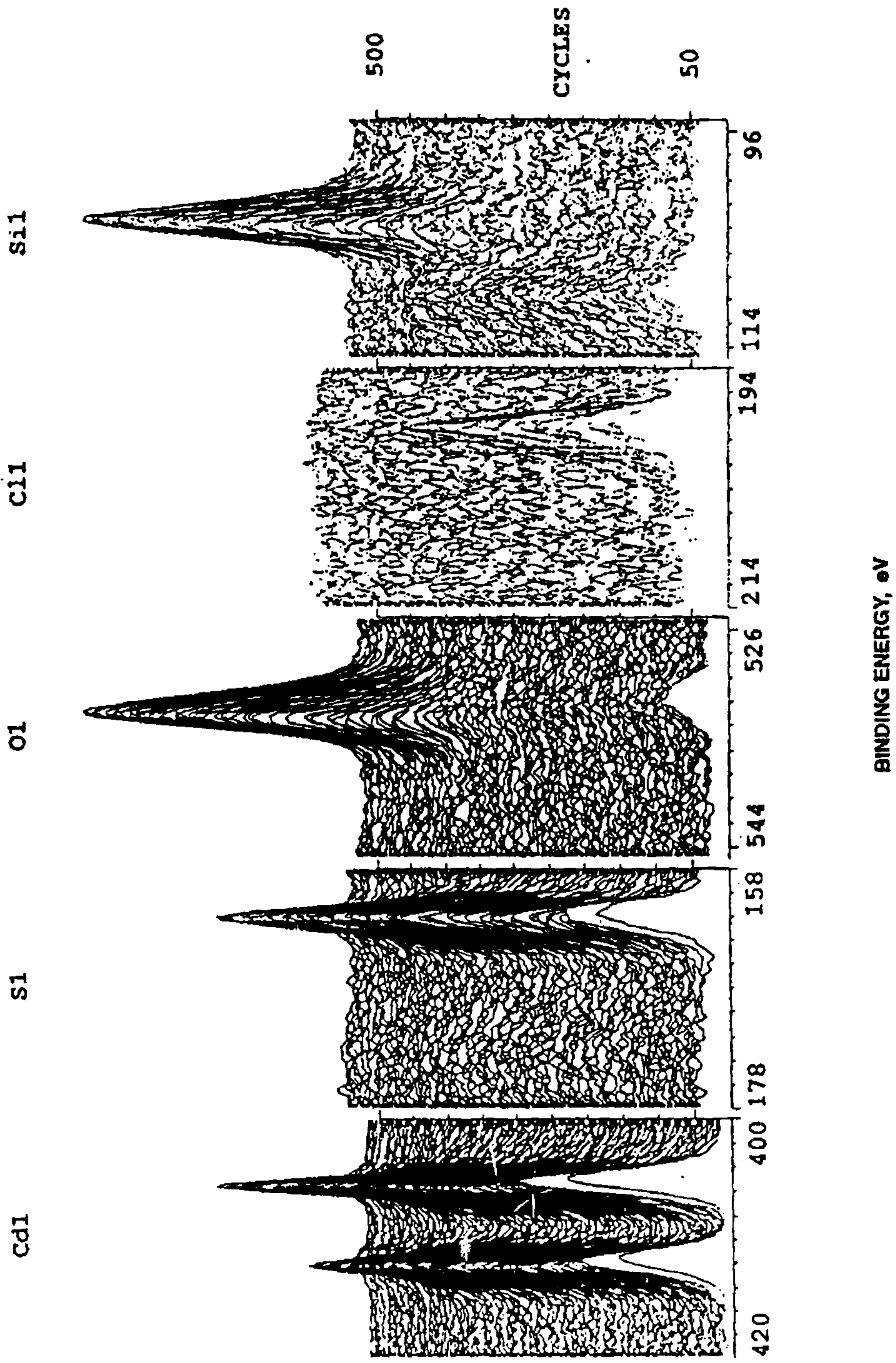

Fig. 2.6 XPS depth profile of sample 'b'.

a decrease in Sulphur concentration. (The strong peak of Oxygen (533 eV) present at the back is from SiO_2 of glass). Binding energy of the Oxygen at the surface of CdS is 531 eV, which corresponds to CdO and this oxygen is present only for a few hundred Angstroms thickness. The presence of Chlorine (199 eV) arises from $CdCl_2$ used in the CBD solution as the supplier of Cd ion. This analysis proves the presence of Oxygen at the sample surface and hence the difference in the value of τ_f for samples kept in vacuum and air.

2.3.3 Decay time variation with temperature

In order to understand the effect of trap levels on carrier decay time, τ_f and τ_s were measured in the temperature range 100 – 300 K for two different thicknesses of the film. Curves (1) and (2) in Fig. 2.7 show variation of fast decay time τ_f with temperature for samples 'a' and 'b', respectively. In Fig. 2.8 curves (1) and (2) show variation of τ_s with temperature for these samples. Curve (1) of Fig. 2.7 has three well defined peaks at 190 K, 250 K and around 275 K with a shoulder around 295 K. Here the maximum height is for the peak at 273 K indicating that this defect is probably the most prominent one. But in curve (1) of Fig. 2.8, it is found that all these peaks are present, with the one at 250 K being the most prominent. Curves (2) of Fig. 2.7 and Fig.2.8 also show the presence of these peaks with the one at 250 K to be the most prominent. This increase in decay time is a clear indication of the release of carriers by different types of traps/defects, having activation energies corresponding to these temperatures. In thick film and bulk of the thin film, the defect having activation energy at 250 K is most prominent.

Fig. 2.9 and Fig. 2.10 are the TSC spectra for samples 'a' and 'b', respectively. Gaussian fitting of the TSC curve of sample 'a' shows two peaks with maximum at 195K and 247 K with a kink at 295 K. Corresponding activation energies are 0.07 eV and 0.15 eV with capture cross-section of the order of 10^{-28} and 10^{-27} /cm^2, respectively. An important

observation here is that the TSC spectra is found to be in close agreement with the decay time vs. temperature curves except for the peak at 273 K. Gaussian fitting of the TSC spectra for the sample 'b' (Fig. 2.10) has maximum around 192 K and 248 K with an additional peak around 297 K instead of the kink seen in Fig. 2.9. These three peaks correspond to three different trap levels, whose trap depths are identified as 0.07 eV, 0.14 eV and 0.19 eV, and capture cross sections are 4.7×10^{-28}, 9.2×10^{-27} and 1.9×10^{-26}, respectively. These values of the activation energies of the traps in the band gap can be seen to be in reasonable agreement with the previously determined values of the traps in CdS thin film (36) and single crystals (37, 38). Similar trap levels were also detected in the thermo luminescence study of CdS single crystals by Choon-Ho Lee et al. (39).

By comparing with earlier reports, detected trap level corresponding to 0.07 eV (190 K, 4.7×10^{-28}), has been attributed to grain boundary defects (40). The defect level of 0.14 eV (248 K, 9.2×10^{-27}) is observed in both the TSC glow curves. This is a shallow trap level found in all Cadmium excess CdS thin film and single crystals. It is a level arising due to the Chlorine impurity at an individual Sulphur vacancy (36,41). A similar electron trap was observed by the DLTS study in CdS thin films prepared by chemical vapour transport (42). In our case, the XPS analysis also showed (Fig. 2.6) the presence of Chlorine throughout the sample.

The peak at 297 K corresponding to 0.19 eV with a capture cross section of $\approx 10^{-26}/cm^2$ is seen only in sample 'b'. This level is reported by Ho B. Im (37) in single crystal CdS. Though this defect is observed in sample 'b', in sample 'a' this could cause only a kink and could not be fitted accurately. The 0.19 eV peak (297 K, 1.9×10^{-26}) exists only in the thicker samples near room temperature and it is due to a complex of Sulphur vacancies (41). This complex is found in all Cadmium excess CdS crystals.

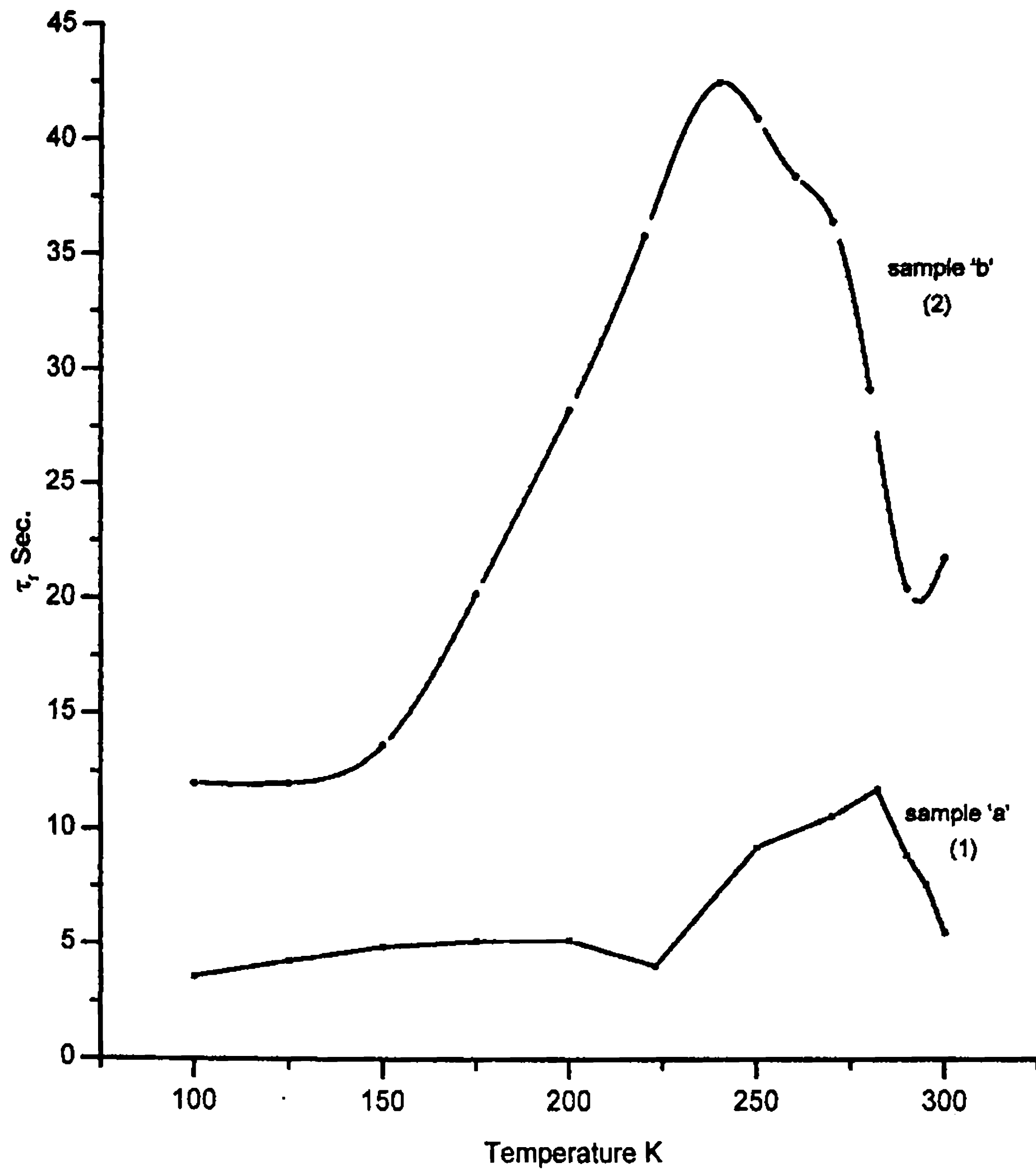

Fig. 2.7 Variation of τ_f with temparature for samples 'a' (1) and 'b' (2)

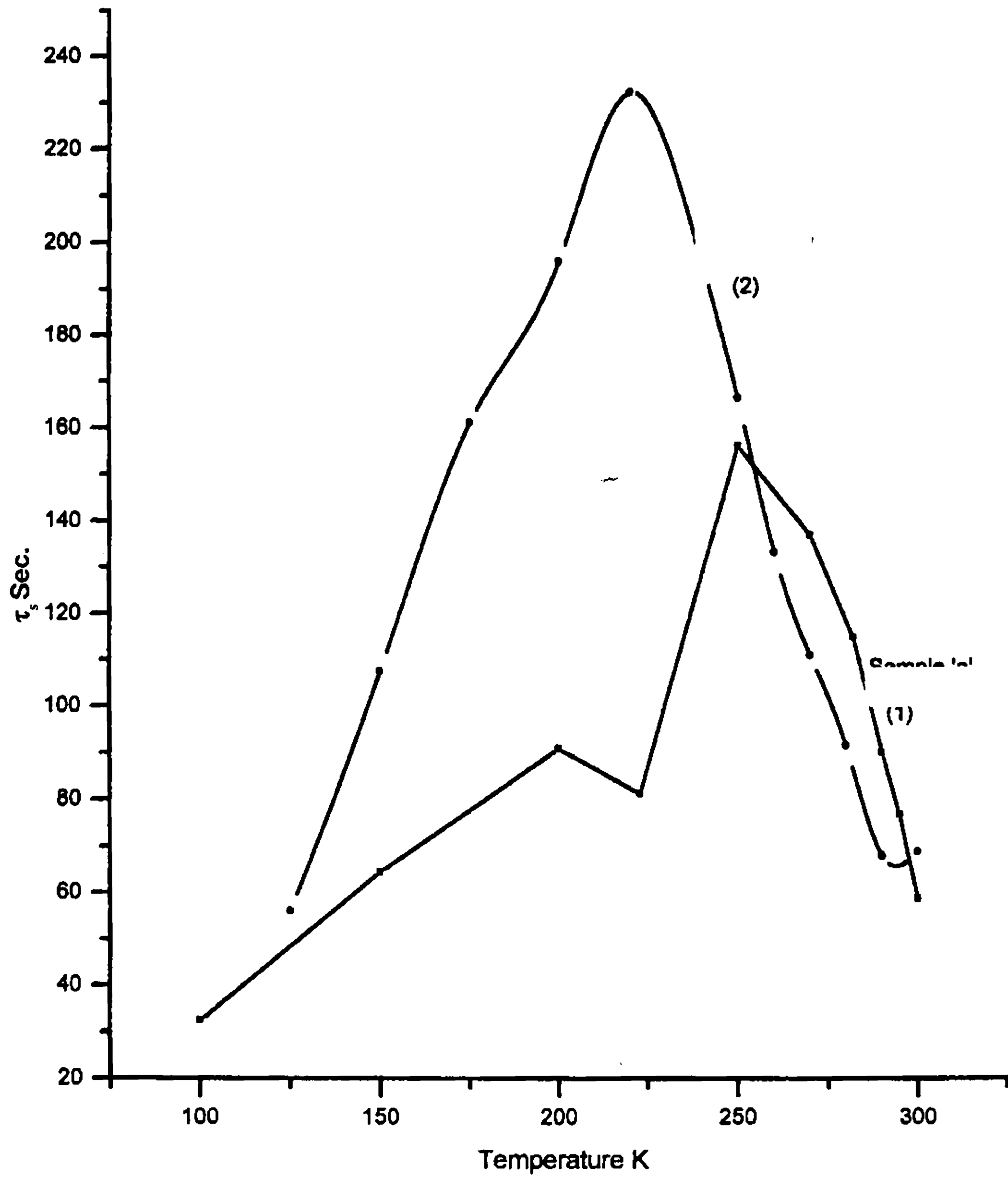

Fig.2.8 Variation of τ_s with sample temperature for samples 'a' (1) and 'b' (2).

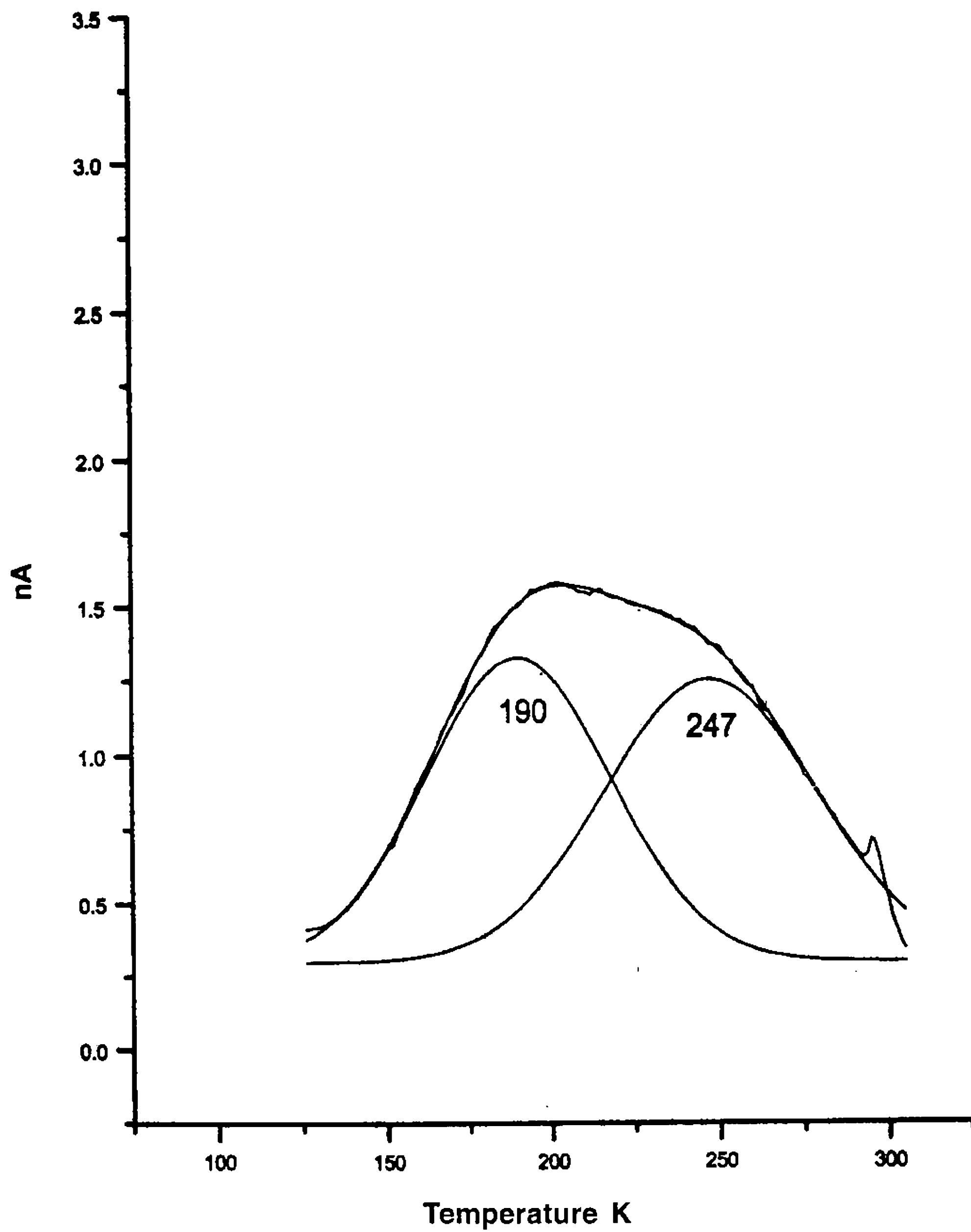

Fig.2.9 TSC curve for sample 'a', optical excitation - 10 min., rate of heating 3K/min

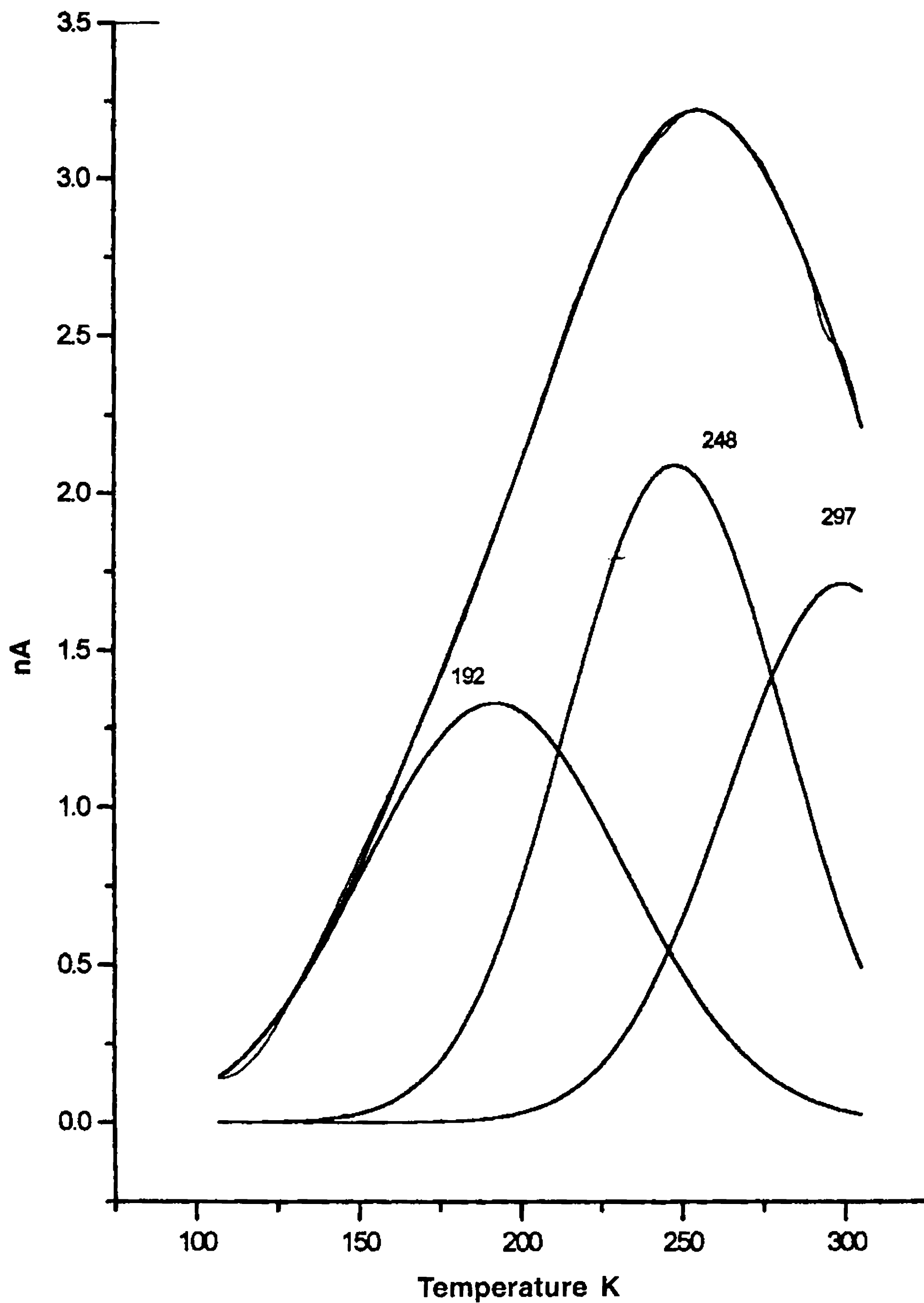

Fig.2.10 TSC curve for sample 'b', optical excitation - 10 min., rate of heating 3K/min

Comparing the variations of decay time with TSC curves, in the case of sample 'a', τ_f is more in the temperature range 270 – 290 K (curve (1) of Fig. 2.7) while τ_s is more in the range 225 - 270 K (curve 1 of Fig. 2.8). Temperature dependence of τ_f due to oxygen could not be found because it could be identified only at higher temperature (~400 K) (43). That was not possible in our cryogenic system. For sample 'b', τ_f and τ_s have maximum value in the range 200 – 250 K. From this study it is clear that the relative density of defects responsible for the different peaks varies from surface to bulk and from one sample to other though they are prepared at the same temperature and from the same solution.

2.3.4 The effect of thickness

The effect of thickness can also be studied from Fig. 2.7 and 2.8. The peak around 190 K in curve (1) of Fig. 2.7 is prominent, whereas that prominence is lost in curve (2). The slow decay time variation study (Fig. 2.8) also shows a similar variation with thickness. That is, the effect of grain boundary on decay time decreased as the film thickness increased. It is due to the fact that as the film thickness increases, the grain size increases and the number of grain boundaries per unit area decreases. E. Bertran et al. reported a detailed study on the increase in grain size with film thickness of CdS thin film (40). Similarly the peak around 250 K in curve (2) is more prominent than that of curve (1) in Fig. 2.7 and Fig. 2.8. Comparing the present TSC studies with earlier reports, the trap level at this temperature is identified as Chlorine impurity at an individual Sulphur vacancy (36, 41). So it may be assumed that as the film thickness increased more Chlorine impurities might have entered the film.

2.4 Conclusion

Decay time of minority carriers was calculated using photoconductive decay technique. PCD measurements showed that the decay curve had two well-defined regions - the initial fast decay region followed by a slow decay region. For single and double dip films, surface recombination was more, whereas it was less for triple dip film. Photoconductivity also increased as the film thickness increased. From the photoconductivity study at 300 K in air and vacuum, it is found that fast decay time was reduced (probably due to diffusion of Oxygen) when exposed to air. XPS analysis was done on this sample and was found that Oxygen was present only on the surface of the film. Fast decay time and photoconductivity

increased when PCD measurements were done in vacuum. Again in vacuum measurements, both these parameters increased as the thickness increased, whereas thickness dependence is lost when the measurements were done in air.

Decay time variation with temperature was studied in a temperature range 100 – 300 K using the rate window technique. Variation of τ_f and τ_s with temperature showed three well-defined peaks at 190 K, 250 K and 273 K with a shoulder around 295 K. The increase in decay time is due to the release of charge carriers from different traps having activation energy corresponding to that temperature. Activation energies of these defects were calculated using TSC technique. Comparing with earlier reports, these defects were identified to be due to charge release from grain boundary defects, Chlorine atom in sulphide ion vacancy and Cadmium Sulphur vacancy complex. The significance of decay time variation study is that the prominence of defects at the surface and bulk can be understood. In most of the earlier reports, the initial fast decay region was neglected for the calculation of decay time stating that it was merely due to surface recombination (30). But our study revealed that this region gives information not only about surface recombination but also about other traps at the surface. The variation of the prominence of traps from surface to bulk and with thickness of the film is also reported in this study.

References

1. R. L. Call, N. K. Jaber, K. Seshan and J. R. White, J. of Solar Energy Materials, 2(1980) 27
2. A. Mondal, T. K. Chaudhari and P. Pramanik, Sol. Energy Mater., 7(1983) 431
3. T. L. Chu, S. S. Chu, C. Ferekides, C. Q. Wu, J. Britt and C. Wang, J. Appl. Phys., 70 (1991) 7608
4. K. W. Mitchell, C. Eberspacher, J. Ermer and D. Pier, Conference Record of the 20th IEEE Photovoltaic Specialists Conference, Las Vegas, NV, (1988) 1384
5. M. A. Green, K. Emery, D. L. King, S. Igari and W. Warta, Solar Cell Efficiency tables (Version 17), Prog. Photovoltaics, 9 (2001) 49
6. A. N. Molin and A. I. Dikusar, Thin Solid Films, 237 (1994) 72

7. Siham A. Al Kuhaimi, Jpn. J. Appl. Phys., 37 (1998) 4850

8. N. Romeo, G. Sberveglieri and L. Tarricone, Thin Solid Films, 43(1977) L15

9. I. Martil, N. de Diego, C. Hidalgo, Phys. Stat. Sol. A, 94(1986) 587

10. K. P. Varkey, Fabrication and characterization of spray pyrolysed Cadmium sulphide homojunction solar cell, Ph.D Thesis, Cochin University of Science and Technology, (1990)

11. V. Canevari, N. Romeo, G. Sberveglieri, S. Azzi, A. Tosi, M. Curti and L. Zanotti, J. Vac. Sci. Technol. A, 2(1984) 9

12. R. Jayakrishnan, J. P. Nair, B. A. Kuruvilla, S. K. Kulkarni and R. K. Pandey, J. of Mat. Sci. Materials in Electronics, 7 (1996) 193

13. K. L. Narayanan, K. P. Vijayakumar, K. G. M. Nair and G. V. N. Rao, Bull. Mater.Sci., 20(1997) 287

14. P. J. Sebastian, J. Campos and P. K. Nair, Thin Solid Films, 227 (1993) 190

15. P. K Nair, J. Campos and M. T. S. Nair, Semiconducting Science and Technology, 3(1988) 134

16. P. K. Nair, M. T. S. Nair, J. Campos and L. E. Sansores, Solar Cells, 22(1987) 211

17. P. K. Nair and M. T. S. Nair Solar Energy Materials, 15(1987) 597

18. G. Sasikala, P. Thilakan and C. Subramanian, Solar Energy Materials and Solar Cells, 62(2000) 275

19. T.J. Coutts, Thin Solid Films, 90(1982) 451

20. K. P. Varkey, K. P. Vijayakumar, T. Yoshida and Y. Kashiwaba, Renewable Energy, 18 (1999) 465

21. J. M. Dona and J. Herrero, J. Electrochem. Soc., 144 (11) (1997) 4091

22. R. H. Bube, Photoelectronic properties of semiconductors, Cambridge University Press, (1992).

23. R. H. Bube and S. Milton Thomsen, J. of Chem. Phys., 23 (1) (1955) 15

24. K. L. Narayan, Ph. D. Thesis, Cochin University of Science and Technology, (1998)

25. R. K. Ahrenkiel, D. H. Levi, S. Johnston, W. Song, D. Mao and A. Fischer, 26th IEEE Photovoltaic Specialist Conference, Anaheim, California, (1997)

26. B. Ohnesorge, R. Weigand, G. Bacher and A. Rorchel, Appl. Phys. Letters, 73 (1998) 1224

27. R. Menner and H. W. Schock, Proceedings of the 12th EC Photovoltaic Solar Energy Conference (Stephons, Bedford, 1994), p.834

28. A. Carbon and P. Mazetti, Physical Review B, 51 (1995) 13261

29. A. Mondal, T. K. Chaudhuri and P. Pramanik, Solar Energy Materials, 7 (1983) 431

30. Muzeyyan Sarithas, Harry D. McKell, J. Appl. Phys., 63(9), (1988) 4561

31. R. H. Bube, Photo conductivity conference, Wiley, New York, (1956) 575

32. R. H. Bube, Photoconductivity of solids, Wiley, New York, (1960) 292

33. S. B. Syamala. K. P. Vijayakumar and C. Sudha Kartha, 43rd DAE – Solid State Physics Symposium, 2000

34. J. Woods, J. Electronics and Control, 5 (1958) 417

35. Peter Mark, J. Phys. Chem. Solids, 25 (1964) 911

36. O. Vigil, O. Zelaya-Angel, Y. Rodriguez and A. Morales-Acevedo, Phys. Stat. Sol.(a), 167 (1998) 143

37. Ho B. Im, Herman E Mathews and R. H. Bube, J.Appl.Phys.,41 (1970) 2581

38. Akihiko Kobayashi, J. Appl. Phys., 49 (1978) 934

39. Choon-Ho Lee, Seuny-Ken Kim, Ha-Yung Du and Gyoung-Nam Jeen, J.Phys. D, Appl. Phys., 24 (1991) 422

40. E. Bertran, J. L. Morenza and J. Esteve, Thin Solid Films, 123 (1985). 297

41. J. Woods and K. H. Nicholas, Brit.J.Appl.Phys.,15 (1964) 1361

42. Paul Besomi and Bruce Wessels, J. Appl. Phys., 51 (1980) 4305

43. N. A. Zeenath, Ph. D Thesis, Cochin University of Science and Technology, (1999)

Chapter 3

Photoconductivity studies on γ-In_2Se_3 thin films

3.1 Introduction

Indium Selenide is a compound semiconductor with a general formula A_2B_3 belonging to the group III-VI having hexagonal structure (1). It has a layer structure with low density of dangling bonds on the surface because of the almost complete chemical bonds within the layer (2). Each layer consists of five atomic sheets with atomic structure Se-In-Se-In-Se. These sheets are bound together by strong covalent forces. Interaction between adjacent layers is much weaker and to be of Vander Walls type (3).

Indium Selenide exhibits a complicated phase diagram and hence there is a probability of forming multiphase like InSe, In_4Se_3, In_2Se_3 and In_6Se_4 during the growth process (4). Since each phase has specific chemical and physical properties, multiphase thin films can induce problems in potential applications such as photovoltaic devices (5). Structural, electrical and optical properties of the material and thus the corresponding device performance are highly dependent on the growth conditions as well as post deposition/preparation heat treatment (6). D. Manno et al. reported investigations of structural, electrical and optical properties of as-deposited and thermally annealed polycrystalline In_2Se_3 thin films, and the thermal annealing effects on structure and morphology of the films (7). G. Micocci et al. reported that higher mobility values are obtained at higher annealing temperature corresponding to larger grain sizes in polycrystalline In_2Se_3 thin films (8). M. Yudasaka et al. reported that on increasing the substrate temperature, electrical conductivity of Indium Selenide thin film decreased (9).

Among the different phases, In_2Se_3 phase exists in at least three different modifications - α, β and γ (10). M. Balkanski et al. investigated presence of α and γ phases in In_2Se_3 film using Photo luminescence studies (11). Herrero et al. reported the influence of annealing temperature on the structure and optical properties of β- In_2Se_3 (12). C. Julien et al. investigated optical properties of different phases of In_2Se_3 crystals (13). They also studied variation of fundamental absorption edge of γ- In_2Se_3 film as a function of temperature. C. De. Groot et al. reported a new κ phase of In_2Se_3 (14). J. Jasinski et al. investigated structural properties of single-phase films of κ- In_2Se_3 and γ- In_2Se_3 (15).

In_2Se_3 of γ-type has a distorted "wurtzite" like structure, in which a third of the metal sites are vacant (9,16). Semiconductors with such a structure have the merit of being able to trap ions or molecules selectively at vacant sites. Because of this property they are suitable as sensors of small particles. As there are no dangling bonds on the layer surfaces, it is a potential material for heterojunction devices. S. Marsillac et al. reported fabrication of γ-In_2Se_3/TCO(SnO_2/ZnO) thin films rectifying heterojunction (17). γ-In_2Se_3 is a photovoltaic semiconductor with a high absorption coefficient ($\alpha > 10^3$ cm^{-1}) (18). Its energy gap varies in the range 1.84 – 2.41 eV at room temperature depending upon the preparation temperature of the sample (19). γ- In_2Se_3 film prepared at temperatures below 423 K is n-type (19). M. Emziane et al. performed photoconductivity studies on γ- In_2Se_3 thin films to study the effect of crystalline quality on the photoconductive behavior of the film. It is also reported that photocurrent is higher in films with good texture and large grain size (20). C. De. Blasi et al. reported photoconductivity studies carried out on Indium Selenide crystals as a function of wavelength, excitation intensity and temperature (21). N. K. Banerjee et al. reported phenomena of photoconductivity and long-term photo relaxation in Indium Selenide thin films (22). It is also reported that the process involved during photo relaxation is structure sensitive. J. Martinez- Pastor et al. reported conditions for efficiency improvement and optimization in Indium Tin Oxide/p-Indium Selenide solar cells (23).

γ- In_2Se_3 thin film can be prepared using different techniques vs. double source evaporation (9), solid state reaction (5), molecular beam epitaxy (21), electro deposition (12), electron beam evaporation (8) and elemental evaporation (25). In our laboratory, γ- In_2Se_3 thin films could be prepared by annealing In-Se bilayer (19). Here the Selenium film is deposited

using Chemical Bath Deposition (CBD) technique. This method of preparation of γ- In_2Se_3 is simple and useful as it avoids the conventional and hazardous selenization process using Selenium vapour/H_2Se gas. More over in this technique, the unreacted Selenium remaining in the solution, used for the preparation of Selenium film can be reused avoiding wastage of material (26).

In this chapter, room temperature photoconductivity studies done on γ- In_2Se_3 thin films prepared at different temperatures are reported. Decay time of charge carriers in these samples was measured using Photoconductive Decay (PCD) method, which is one of the simple methods used for lifetime measurements in semiconductor materials. PCD measurements were also done in the low temperature range (50-300K) in vacuum (10^{-5} m bar) for each sample and decay time variation with sample temperature was studied to get an idea of traps/defects releasing charges. The results of Dark Conductivity (DC) and Thermally Stimulated Current (TSC) measurements done on these samples are included to supplement the PCD studies. In order to understand the effect of variation of Indium concentration in the film on photoconductive decay time, the variation of decay time with sample temperature is studied on three samples having different Indium concentration, keeping preparation temperature constant.

3.2 Preparation of γ- In_2Se_3 thin films

γ-In_2Se_3 thin films were prepared using Stacked Elemental Layer (SEL) technique. SEL structure was grown using chemical bath deposited a-Se film and vacuum evaporated Indium thin films. In this method, film preparation of γ-In_2Se_3 involves two steps. The first step is the preparation of Se-In stack layers and the second stage is the process of annealing the stack layers. These are described in detail elsewhere (19) and hence only a brief description of the process is included in the following paragraph.

Preparation of In-Se stack layer consisted of two steps. In the first step, amorphous selenium film was deposited on a glass substrate from an aqueous solution of sodium seleno

sulphite using Chemical Bath Deposition (CBD) technique. The temperature, pH and molarity of the reaction bath and time of deposition were optimized at 300 K, 4.5, 0.006 M and 3 h respectively (26). Orange-red films were obtained after 3 h of deposition. For the preparation of Indium Selenide films, triple dipped selenium films of thickness ~ 0.5 μm, having an area of 5.5 cm^2 were chosen. After deposition, amorphous Selenium film was dried in open air at room temperature. In the second stage, this film was loaded in the vacuum chamber (Box coater-BK350) to deposit Indium layer on it. A layer of Indium of thickness 350 Å (5 N purity) was deposited by evaporating (at a pressure – 10^{-5}m bar) 40 mg of Indium to get the atomic ratio between Indium and Selenium to be approximately 2:3. In the last stage, Indium Selenide film was prepared by annealing In-Se bilayer for one hour in an annealing chamber in high vacuum (10^{-5} m bar). The rate of heating and cooling were fixed at 2.5 K/minutes. A set of films was prepared by annealing the bilayer at different temperatures viz. 373 K, 403 K, 423 K, 473 K, 573 K, 673 K and 773 K keeping the heating/cooling rate and annealing time to be the same for all the samples. These samples were named 'is373', 'is403', 'is423', 'is473', 'is573', 'is673' and 'is773' respectively. Another set of films was also prepared by evaporating 40mg, 30mg and 20mg of Indium on Selenium film and annealing at 373 K, keeping heating and cooling rate at 2.5 K/minutes. These samples were named 'is40', 'is30' and 'is20' respectively.

Structural analysis of the films, prepared at different temperatures are shown in Fig.3.1. XRD pattern of as-deposited Se-In stack layers shows only a single peak corresponding to Indium layer, as the Se film is amorphous (Fig 3.1(a)). For the sample prepared at 373 K, there is one prominent peak at $2\theta = 23.3^{\circ}$, corresponding to (101) plane and another one at $2\theta = 29.6^{\circ}$ corresponding to (204) plane, which are characteristics of γ-In_2Se_3. As the preparation temperature increased, γ-In_2Se_3 became amorphous. On increasing the preparation temperature, it became crystalline again with characteristic peaks of γ-In_2Se_3.

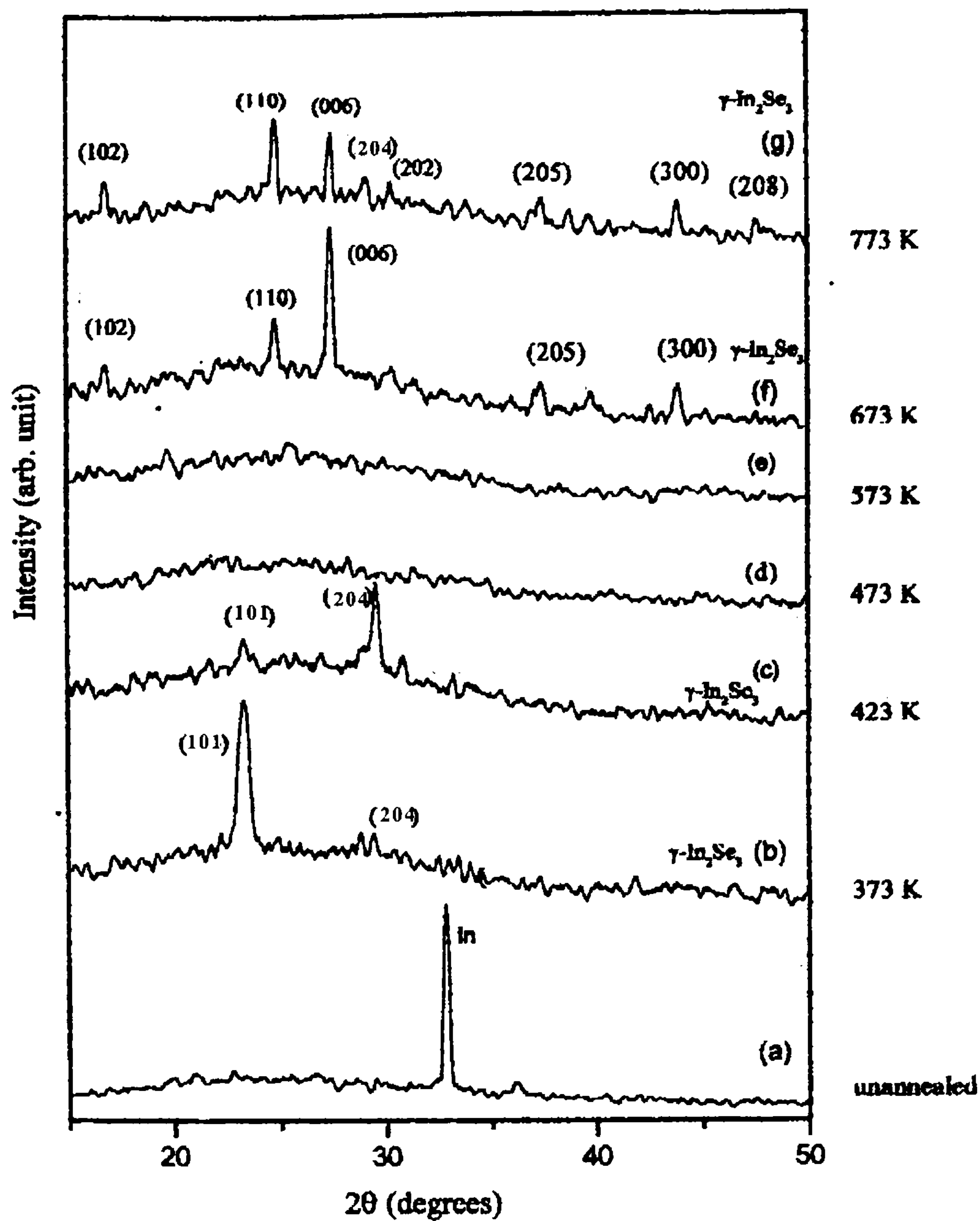

Fig.3.1 XRD pattern of (a) un-anneded Se-In stack layers (b) 'is 373', (c) 'is 423', (d) 'is 473' (e) 'is 573' (f) 'is 673' (g) 'is 773'

3.3 Steady state photoconductivity studies at room temperature

For photoconductivity measurements, a film was loaded on the cold finger of a liquid Helium Cryostat (CTI- cryogenics- Helix Technology Corporation) and temperature was controlled using Lakeshore Auto tuning Temperature Controller (Model-321). The pressure in the cryostat was 10^{-5} m bar. White light of intensity 25 mW/cm^2 was used to illuminate an area of 1x7 mm^2 of the sample. The duration of illumination was 1 minute for all samples. Heat radiation from the light source was avoided by passing the light beam through a water filter. A high resistance and a constant dc source of 40 V (Keithely Source Measurement Unit) were connected in series with the sample. Details of experimental set up is shown in chapter 2. Steady state photocurrent was measured using Keithely SMU.

Steady state photocurrent at room temperature (373 K) was measured for samples prepared at different temperatures in the range 373 K – 773K and the dependence of photocurrent with sample preparation temperature is plotted in Fig. 3.2. It shows that photoconductivity is maximum for 'is373' and it decreased as sample preparation temperature increased. Samples 'is573', 'is673' and 'is773' were highly resistive at room temperature and photoconductivity could not be measured.

3.4 Variation of decay time at room temperature for samples prepared at different temperatures

Decay time of carriers is calculated using Photoconductivity Decay (PCD) technique. Decay of the voltage across the high resistance (Fig. 2.1) after switching off the illumination was measured using Keithely 2000 multimeter. Measurements were taken in an interval of 0.029 sec. Irradiation on sample surface was cut off using a mechanical shutter with shutting time less than the minimum decay time measured. Care was taken to get steady value for dark conductivity before illuminating the sample for each measurement.

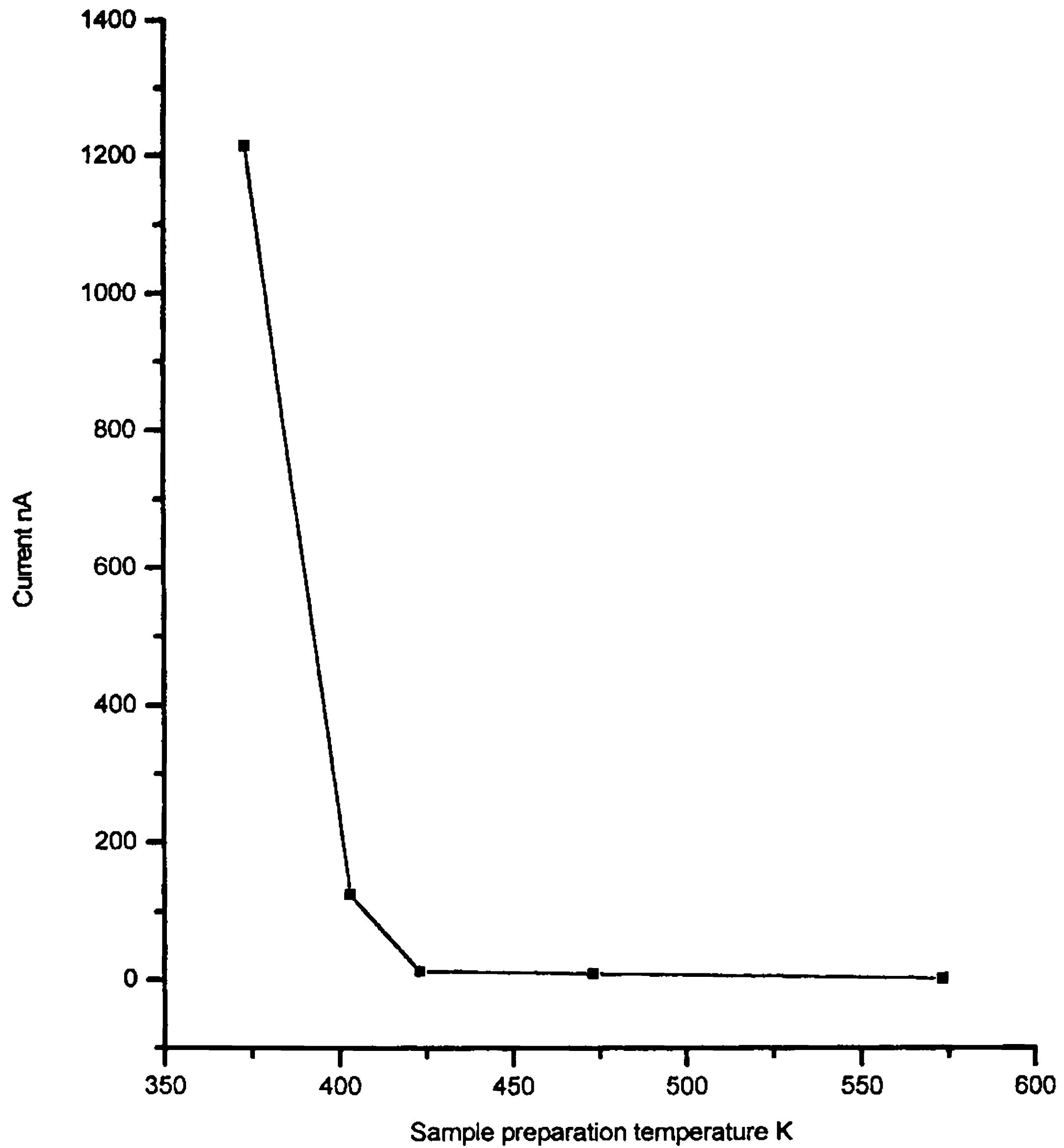

Fig. 3.2. Variation of steady state photocurrent with sample preparation temperature

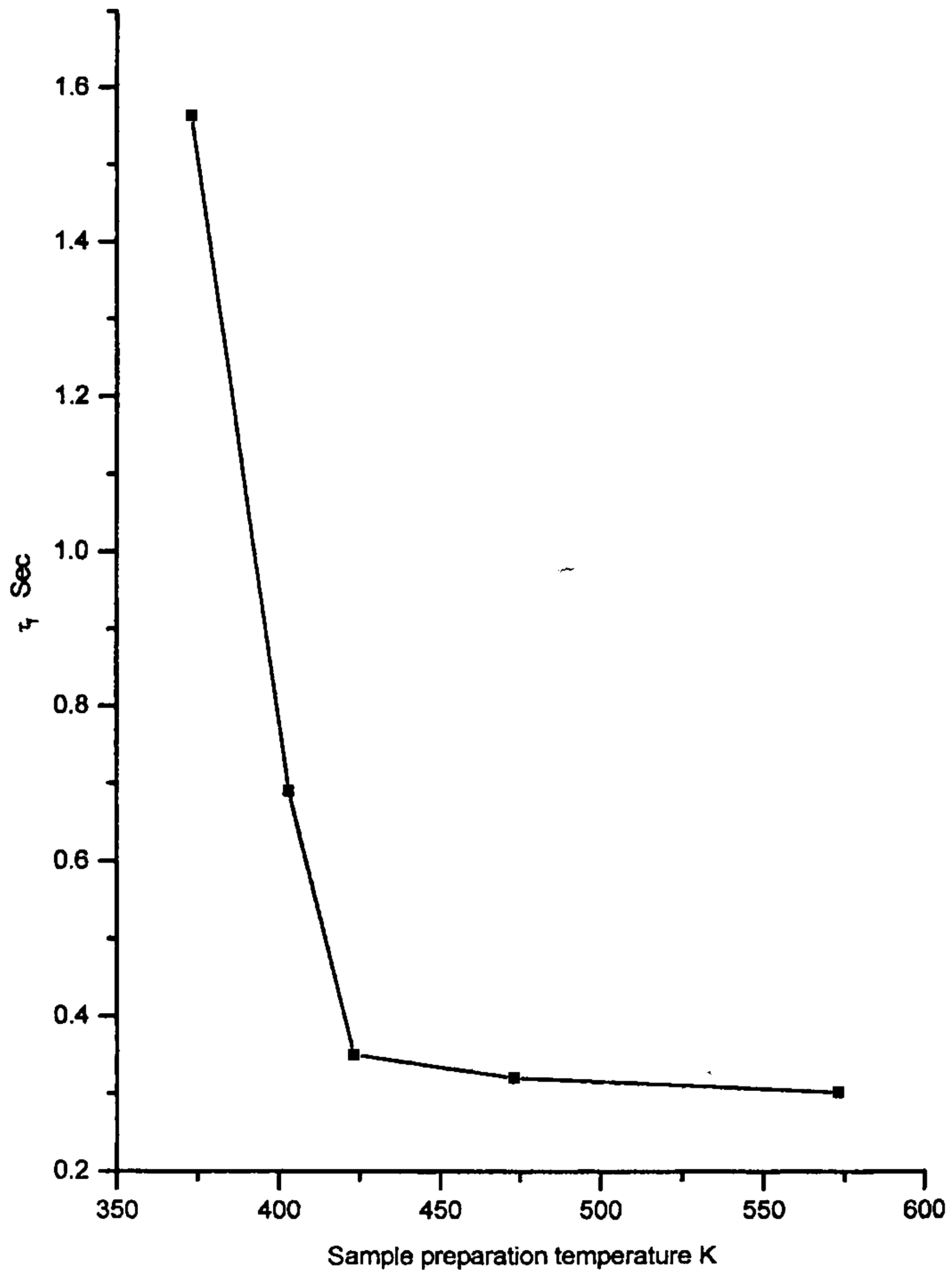

Fig.3.3 Variation of τ_r with sample preparation temperature

Room temperature photoconductivity decay (PCD) measurements were done on samples prepared at different temperatures in the range 373 K-773 K. PCD curves had two regions - fast decay and slow decay region. For all decay curves, a window was chosen at the fast decay region (rate window technique explained in chapter 2) and τ_f was calculated for the portions of the curve in the particular window using Excel 2000 programme. τ_s could not be calculated for samples prepared above 473 K, as the slow decay region was in the noise level. Variation of τ_f with sample preparation temperature was shown in Fig. 3.3. Decay time for 'is373' was in the order of 1.58 sec. As the preparation temperature increased decay time decreased and for sample 'is573' it was 0.3 sec. Variation in decay time is considered to be due to the variation in trap density when the intensity of illumination is kept constant. Decrease in decay time with sample preparation temperature may be due to the decrease in trap density. Samples prepared at a temperature greater than 573 K might have lost Selenium and excess Indium leading to carrier loss. These samples were highly resistive. At room temperature photoconductivity was negligibly small and decay time could not be calculated for these samples (27).

3.5 Variation of decay time with sample temperature

PCD measurements are done on a particular sample at different temperatures in the range 50 – 300 K. The decay curves had two well-defined regions viz. fast decay and slow decay regions (Fig. 3.4). For the set of curves two windows were chosen at these two regions. Decay time corresponding to the portions of the curves in a particular window are calculated using Excel 2000 programme. Fig 3.5 shows the variation of decay time-τ_f (calculated for the curves in a window chosen at the fast decay region) with temperature. Similarly the experiment is repeated for other samples prepared at different temperatures and included in Fig 3.5. This measurement could not be taken for samples prepared above 473 K, as the photoconductivity was very small for these samples. Fig 3.6 shows the variation of the decay time -τ_s with temperature. Here the graphs could not be plotted for samples prepared above 403 K, as the slow decay region was in the dark level and noise was very high. Variation of τ_f and τ_s are similar in nature but τ_f is in the order of milliseconds, while τ_s is in the order of seconds. Lower value of τ_f may be due to the defects present at the surface of the sample, which are generally recombination in nature (28, 29). Both set of curves for τ_f

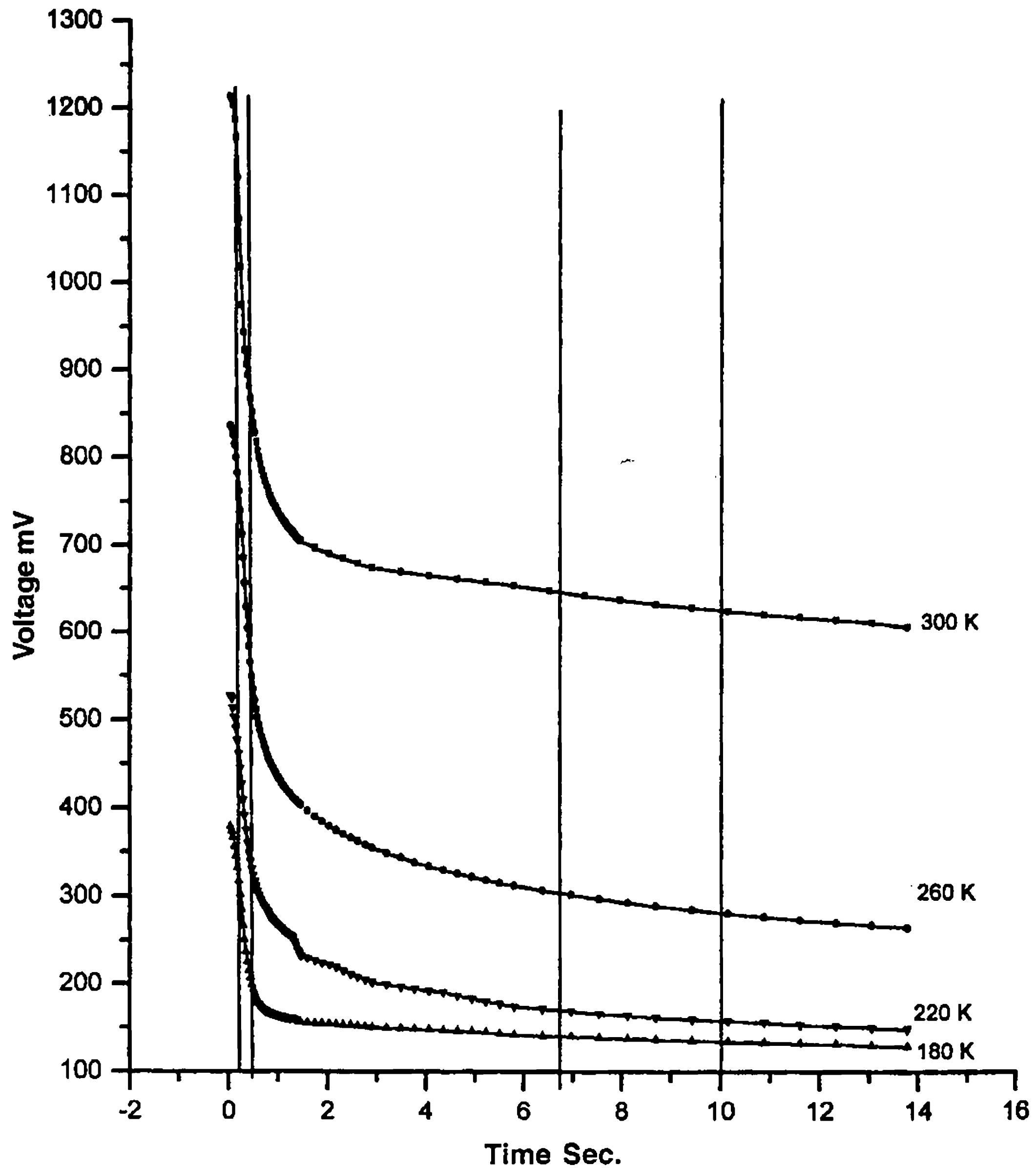

Fig.3.4 PCD curves at different sample temperatures and two windows closen at fast and slow deeay regions for 'is 373'

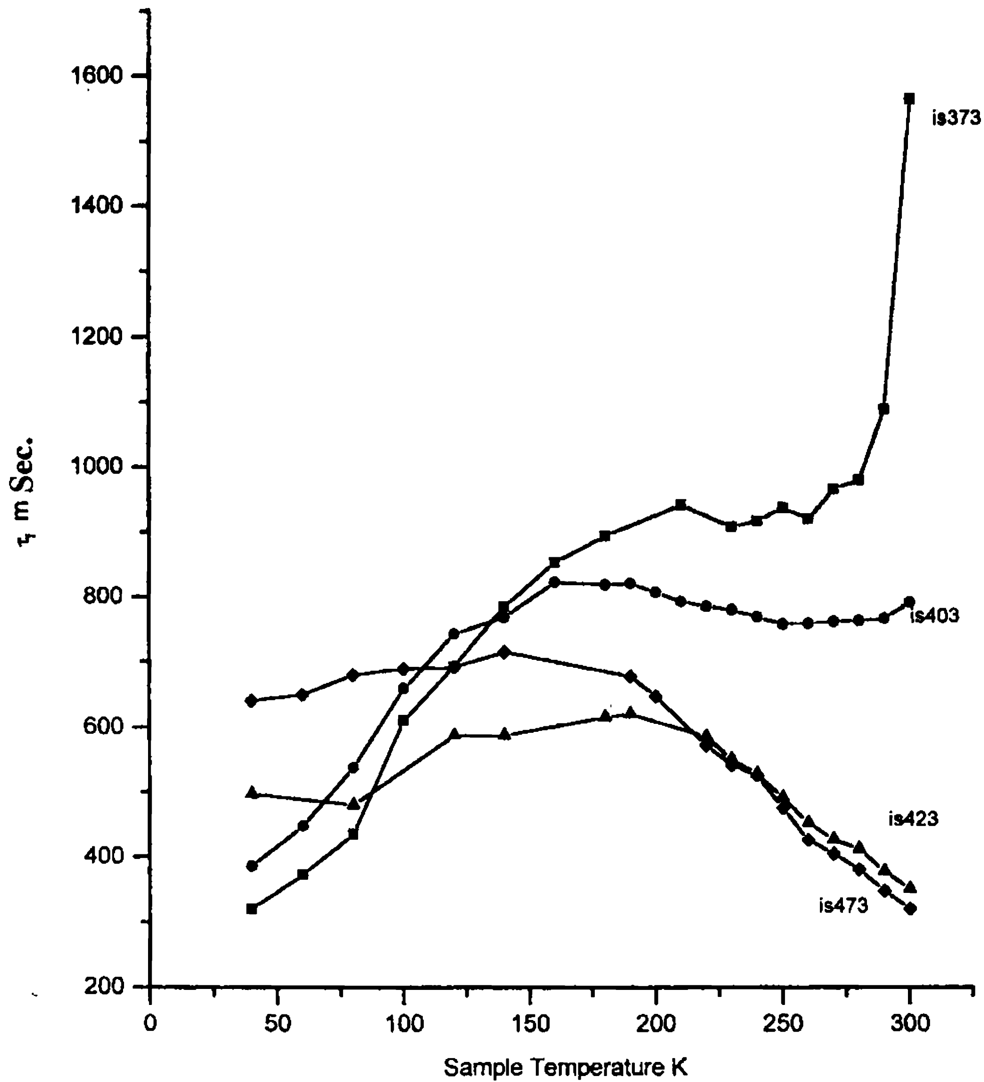

Fig.3.5 Variation of τ_r with sample temperature for 'is 373', 'is403', 'is423' and 'is 473'

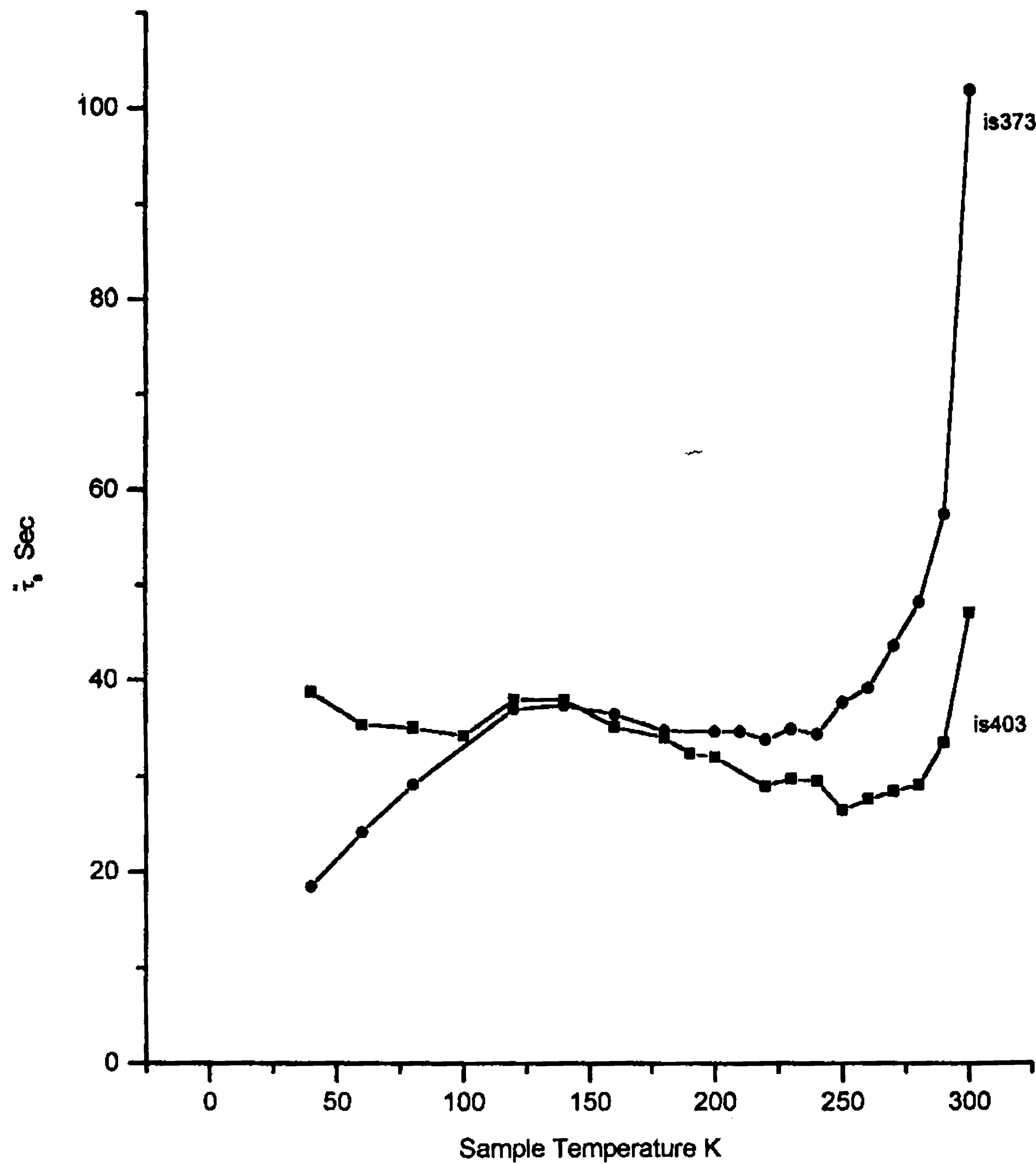

Fig.3.6 Variation of τ_s with sample temperature for 'is 373', 'is403'

and τ_s showed a sharp increase around 300 K for 'is373', whereas for samples prepared at higher temperatures, τ_f was found to decrease around 300 K. It is to be noted that photoconductivity and decay time measured at room temperature decreased as the sample preparation temperature increased (Figs. 3.2 and 3.3). An increase in decay time with increase in sample temperature indicates the release of excess carriers. This will happen only if some traps/defects release excess carriers, which mean that the traps/defects have activation energy corresponding to this temperature at which maximum of decay time occurs. Another peak around 150 K existed in all samples and that also decreased as the sample preparation temperature increased. It is observed from this study that photoconductivity decay time increased at two temperatures, 150 K and 300 K. So it is to be concluded that carriers are released from two different traps/defects around these temperatures. But in the case of samples prepared at temperature higher than 373 K the increase in lifetime at 300 K does not take place, indicating that this defect is not there in those samples.

3.6 Effect of Indium concentration on decay time

In order to understand the effect of variation of Indium concentration on photoconductive decay time, measurements were done on three samples viz. 'is40', 'is30' and 'is20' having different Indium concentration. PCD measurements were done on each sample at different sample temperatures in the range 50 – 300 K and τ_f and τ_s were calculated. Variation of τ_f and τ_s with sample temperature showed similar nature and variation of τ_s with sample temperature is shown in Fig. 3.7. These curves also showed two peaks, one around 150 K and the other around 300 K. An increase in decay time around 300 K could be observed in three cases and it increased with increase in Indium in the film. This indicates that the density of traps/defects is enhanced when Indium concentration is increased in the film. Hence it may be possibly the excess Indium, which is acting as the defect causing increase of τ_f at 300 K. In the case of samples 'is403' to 'is473' (Fig. 3.5), this peak at 300 K does not occur. It is quite natural that excess Indium may not be there in these samples prepared at higher temperatures. For the other peak observed around 150 K, it is found that the peak height decreased with increase in Indium concentration. Hence most probably it should be Indium vacancy, which is causing increase of decay time at 150 K. But for samples 'is 403' to 'is473' (Fig. 3.5) also, this peak height is decreasing. This may be due to the fact that more Selenium is lost and hence the increase in Indium vacany is not predominant.

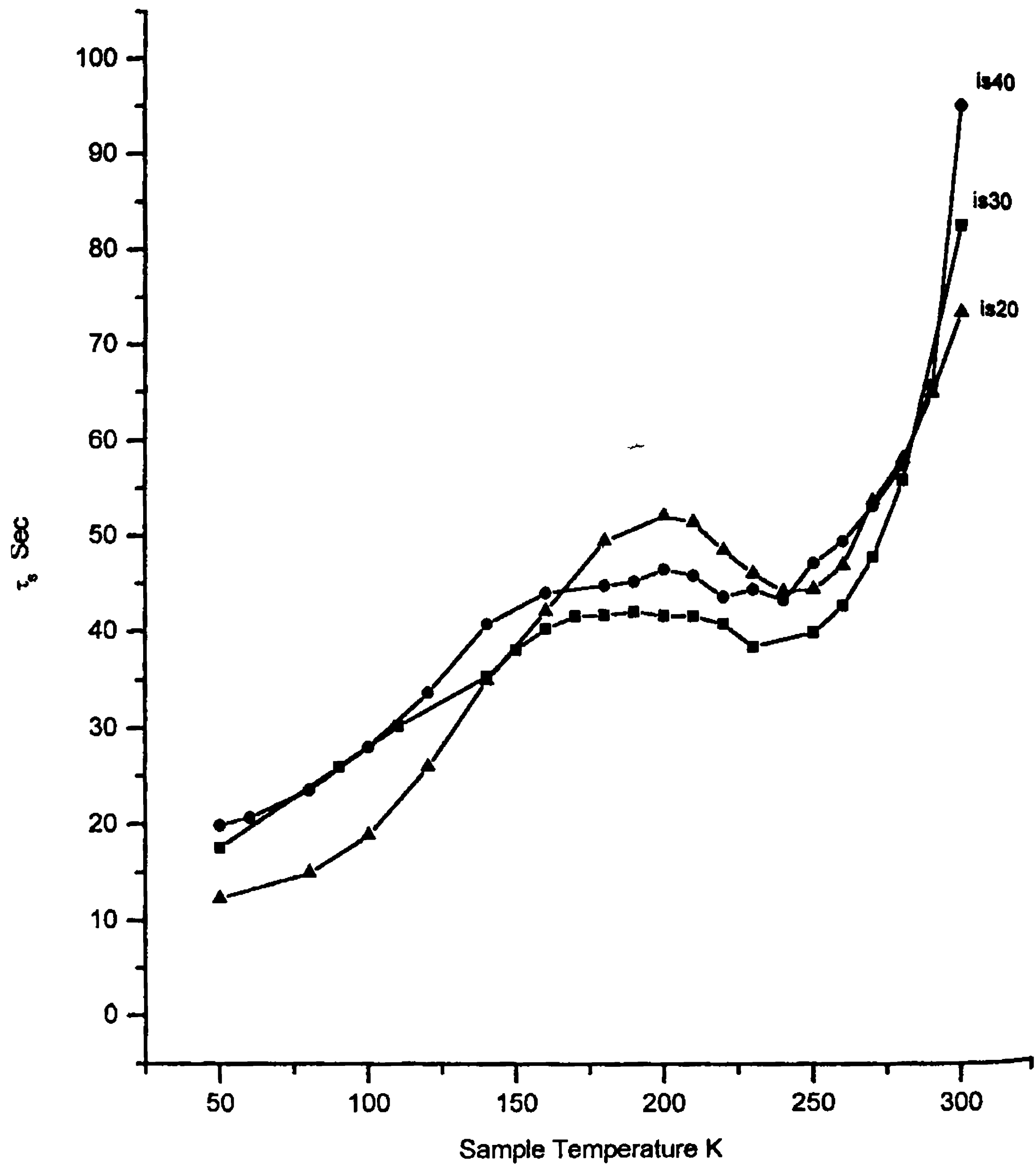

Fig.3.7 Variation of τ_s with 'is40', 'is30' and 'is20'

3.7 Dark conductivity measurements

Dark conductivity measurements were done on selected samples in the range 50 – 300 K and a representative curve for 'is373' is shown in Fig 3.8. The rate of heating was 4 K/minute. Dark current increased with sample temperature around 300 K. An Arrhenius plot was drawn for this region and activation energy of 0.34 eV was obtained. C. De. Blasi et al. reported 0.34 eV as a donor level, giving rise to an electron-trapping center at room temperature (30). M. Yudasaka et al. reported that n-type conductivity of γ-In_2Se_3 film increased on decreasing substrate temperatures (9). It is also reported that n-type conduction should be attributed to excess Indium atoms. From Fig. 3.7, it is evident that decay time increased with amount of Indium in the film indicating that the defect density increased with Indium concentration. So it may be concluded that excess Indium in the film may be responsible for increase in photoconductivity and decay time at room temperature. When sample preparation temperature is increased, naturally the chance to have excess Indium in these samples is low and hence the increase in decay time at 300 K is not observed. The other expected peak around 150 K could not be analysed using dark conductivity measurements, which may be due to shallow defect level.

3.8 Thermally stimulated current measurements (TSC)

TSC measurements were done on samples 'is40', 'is30' and 'is20' in the range 50 – 200 K and the expected peak around 150 K could be analysed using this technique. The experimental technique is described elsewhere (31). The rate of heating was fixed to 3 K/minute and duration of optical excitation was 5 minute. Current measurements were carried out under a dc biasing of 20 V. Activation energy of the defect responsible for this peak was found to be 0.04 eV with a capture cross-section of 6.3×10^{-26} cm^2.

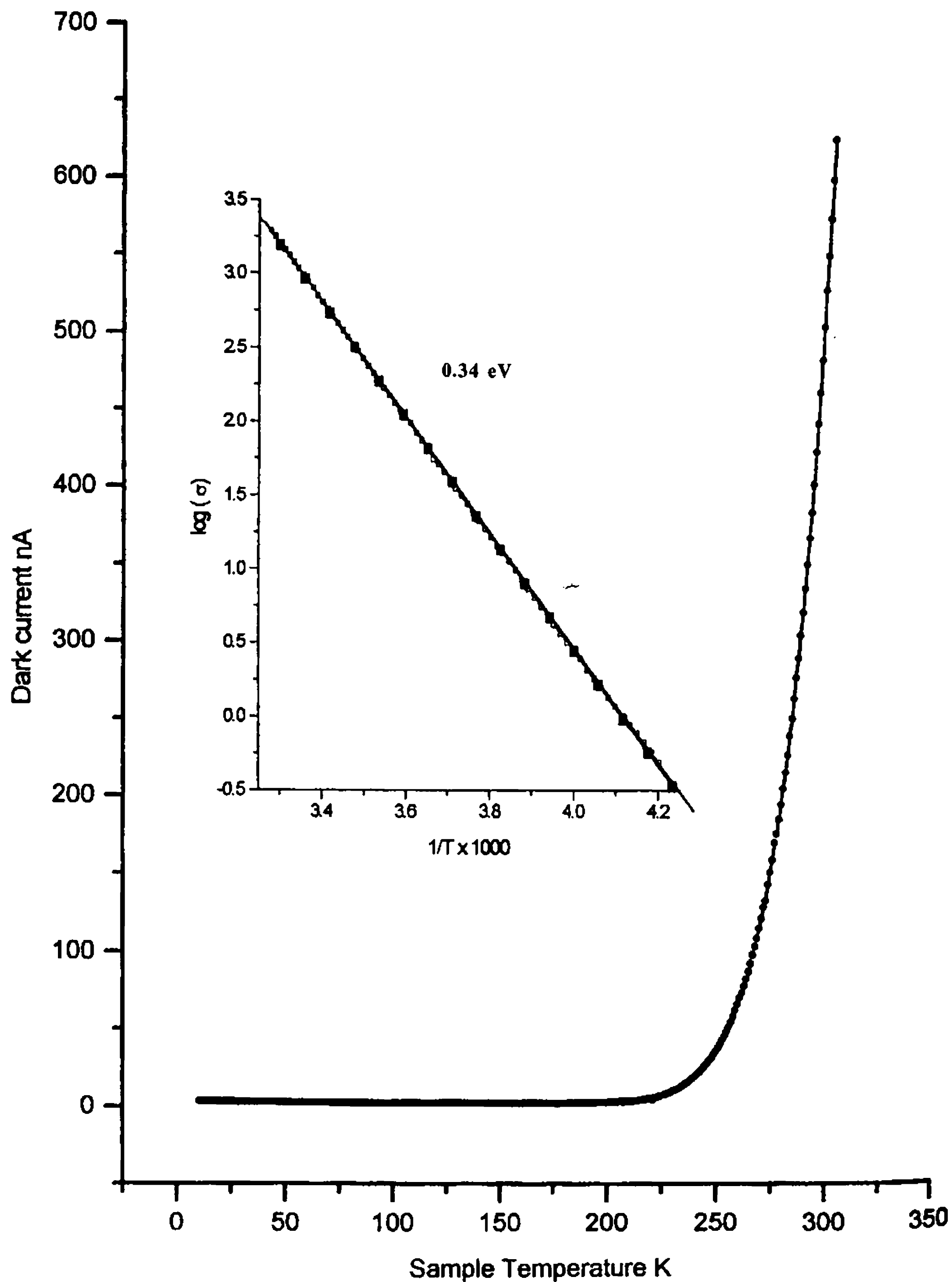

Fig.3.8 Dark current vs sample temperature for 'is 373', and the Arrhenius plot

3.9 Conclusion

γ-In_2Se_3 films were prepared by annealing In/Se bilayer at different temperatures. The present study revealed that 'is373' is most photo conducting. Steady state photocurrent and photoconductivity decay time at 300 K decreased as the sample preparation temperature increased. Decay time measurement on these samples indicated that there are two decay times τ_f and τ_s. Decay time variation with temperature showed that charge carriers are released from two defects having activation energy corresponding to temperatures around 150 K and 300 K. The density of defects, releasing charge carrier at 300 K was found to decrease on increasing sample preparation temperature. It is also observed that the release of charge carriers at 300 K increased with the increase of Indium concentration in the film. Dark conductivity measurements showed a sharp increase only at 300 K and activation energy of this defect is found to be 0.34 eV, while that of the defect, releasing charge carrier around 150 K, is found to be 0.04 eV using TSC technique.

γ-In_2Se_3 film is a promising window material for solar cells. Its photoconductivity, decay time of charge carriers and resistance can be properly chosen by varying the sample preparation temperature and through this study we found that the sample prepared at 373 K is most photoconducting. Also the preparation technique is very simple and non hazardous as selenium film is deposited using CBD technique. In this technique even the unreacted Selenium remaining in the solution, used for the preparation of Selenium film can be reused.

References

1. M. Parlak, C. Ercelebi, I. Gunal, Z. Salaeva and K. Allkhverdiev, Thin Solid Films, 258 (1995) 86
2. M. Yudasaka and K. Nakanishi, Thin Solid Films, 156 (1988) 145
3. C. Julien and M. Eddrief, Materials Science and Engineering B, 13 (1992) 247B
4. Thomas and T. R. N. Kutti, Phy. Stat. Sol (a), 119 (1990) 127
5. S. Marsillac, A. M. Combot-Marie, J. C. Bernede and A. Conan, Thin Solid Films, 288 (1996) 14
6. M. Emziane and R. Le Ny, Phys. D. Appl. Phys., 30 (1999) 1319

7. D. Manno, G. Micocci, R. Rella, P. Siciliano and A. Tepore, Vacuum, 46 (8) (1995) 997

8. G. Micocci, A. Tepore, R. Rella and P. Siciliana, Phys. Stat. Sol.(a), 148 (1995) 431

9. M. Yudasaka, T. Matsuoka and K. Nakanishi, Thin Solid Films, 146 (1987) 65

10. J. Van Landuyt, G. Van Tendeloo and S. Amelinckx, Phys. Stat. Sol.(a), 30 (1975) 299

11. M. Balkanski, C. Julien, A. Chevy and K. Kambas, Solid State Communications, 59 (7) (1986) 423

12. J. Herrero and J. Ortega, Solar Energy Materials, 16 (1987) 477

13. C. Julien, A. Chevy and D. Siapkas, Phys. Stat. Sol (a), 118 (1990) 553

14. C de Groot and J. S. Moodera, J. Appl. Phys., 89 (2001) 4336

15. J. Jasinski, W. Swider, J. Washburn, Z. Lillental-Weber, A. Chaiken, A. Nanka, G. A. Gibson and C. C. Yang, Appl. Phys. Lett., 81 (2002) 23

16. Tomohiko Ohtsuka, Kazuyuki Nakanishi, Tamotsu Okamoto, Akira Yamada, Makoto Kongagai and Uwe Jahn, Jpn. J. Appl. Phys., 40 (2001) 509

17. S. Marsillac and J. C. Bernade, Thin Solid Films, 315 (1998) 5

18. S. Marsillac and J. C. Bernade, R. Le. Ny, A. Conan, Vacuum, 46 (11) (1995) 1315

19. K. Bindu, C. Sudha Kartha, K. P. Vijayakumar, Y. Kashiwaba and T. Abe, Appl. Surf. Sci., 191 (2002) 138

20. M. Emziane and R. Le. Ny, Thin Solid Films, 366 (2000) 191

21. C. De. Blasi, G. Micocci, A. Rizzo and A. Tepore, Phys. Stat. Sol.(a), 74 (1982) 291

22. N. K. Banerjee, A. K. Chaudhuri and B. K. Samantaray, J. Phys. D. Appl. Phys., 26 (1993) 1714

23. J. Martinez-Pastor, A. Segura, J. L. Valdes and A. Chevy, J. Appl. Phys., 62 (4) (1987) 1477

24. L. Brahim-Otsmane, Y. Y. Emery and M. Eddriel, Thin Solid Films, 237 (1994) 291

25. B. Thomas, Appl. Phys. A, 54 (1992) 293

26. K. Bindu, M. Lakshmi, S. Bini, C. Sudha Kartha, K. P. Vijayakumar, Y. Kashiwaba and T. Abe, Semicon. Sci. and Techn., 17 (2002) 270

27. S. B. Syamala, K. Bindu, K. P. Vijayakumar and C. Sudha Kartha, M-25, 13th AGM – MRSI & Theme symposium on 'Perspectives in Materials Characterisation', Hyderabad, 2002.

28. Richard H. Bube, Photoelectronic Properties of Semiconductors, Cambridge University Press, (1992)

29. Muzzeyan Saritas, Harry D. McKell, J. Appl. Phys., 63 (1988) 4561

30. C. De Blasi, G. Micocci, A. Rizzo and A. Tepore, Physical Review B, 27 (4) (1983) 2429

31. N. A. Zeenath, P. K. V. Pillai, K. Bindu, M. Lakshmi and K. P. Vijayakumar, J. Mater. Sci., 35 (2000) 1

Chapter 4

Photoconductivity studies in $CuInSe_2$

4.1 Introduction

$CuInSe_2$ (CIS) belongs to I-III-VI chalcopyrite compounds. Depending upon the nature of deviation of its composition from the ideal formula $Cu_aIn_bSe_c$ (a = 1, b=1 and c=2), the compound can be Cu rich, In rich, Selenium excess or Selenium deficient. By making deviation from stoichiometric composition within a fraction of atomic percent, n-type or p-type material can be prepared (1). Hence homojunction devices are possible with this material. R. J. Matson et al. reported the formation of $CuInSe_2$ homojunction on deposition of CdS onto single-crystal p- $CuInSe_2$ (2). The chemical origin of possible defects was identified and the experimental evidence for this type of conversion was also presented in their report. Electron affinity and lattice parameters of this material are comparable with binary semiconductors such as CdS, with which heterojunctions are made. This material has a direct band gap of 1.04 eV. The highest absorption coefficient (10^5/cm) of the material makes it a prominent candidate for thin film photovoltaic device. Y. Horikoshi et al. reported an efficiency of 17.7 % for CIS based thin film Solar Cells (3). Recently, efficiency as high as 18.8 % is reported for single junction CIS solar cells (4). Shalini Menezes reported the construction of n-$CuInSe_2$ thin film absorber and the electrochemical conversion of $CuIn_2Se_2$ surface to a semi-insulating, lattice-matched $CuIn_xSe_yI_z$ transition layer and a semiconducting p-$CuISe_3$ window (5). The $CuISe_3$ layer was anodically formed on n-type/p-type $CuInSe_2$ and it formed rectifying p-n junction with n-$CuInSe_2$ and an ohmic contact with p-$CuInSe_2$.

The electrical and optical properties of this material depend on the presence of intrinsic point defects (vacancies, interstitials and antisite defects) (6, 7). These defects are related to the stoichiometry and the thermal history of the specimen (8-10). Hence identification of dominant defects would enhance understanding of the properties and allows one to have a better control over electrical properties of the film (11). Rincon et al. reported detailed studies on theoretical approach of electrical activity and activation energy of various possible intrinsic defects in the material and compared with experimental data (12). Electrical activity of the defects determines the type of conductivity. p–type conductivity is achieved either by cation vacancies or anion interstitials and n-type conductivity is due to either anion vacancies or by cation interstitials (13). In general, Cu/ (In+Se) ratio is the criteria, which determines the type of conductivity. If the Selenium pressure is kept constant during formation of $CuInSe_2$ film, then Cu/In ratio is the main parameter, which controls the conductivity of the films. Cu-rich films are generally p-type and In-rich films are n-type. L. Essaleh et al. reported effect of impurity band conduction on the electrical characteristics of n-type $CuInSe_2$ single crystals (14). M. Igalson reported steady state and decay of photoconductivity in p-type $CuInSe_2$ thin films and single crystals, in the temperature range 130 to 300 K (15). K. Puech et al. reported measurements of carrier lifetimes in polycrystalline $CuInSe_2$ thin films, using time-resolved photoluminescence measurements (16). B. Ohnesorge reported that long lifetime of charge carriers in absorber material correlated with high open circuit voltages and conversion efficiencies, while no significant influence on the short circuit current (17). Knowledge of this parameter is therefore essential to understand limitations and capabilities of photovoltaic devices.

CIS films can be prepared by different techniques – co-evaporation of three sources (18), spray pyrolysis (19), dc-sputtering (20), rf-sputtering (21), electro deposition (22), CBD (23), MBE (24) and SEL (25). For the present study CIS is prepared using Stacked Elemental Layer (SEL) technique. Chemical Bath Deposited (CBD) amorphous Selenium thin film is used for the preparation of $CuInSe_2$ films, which avoids the usage of highly toxic Selenium vapor or H_2Se gas (26). Both p-type and n-type CIS films are prepared by varying amount of Cu in the film. T. L. Chu et al. reported selenisation of vacuum evaporated Cu-In pre cursor in H_2Se atmosphere (27).

In this chapter, variation of nature of photoconductivity with Cu concentration in the film is studied. Room temperature photoconductivity and decay time of charge carriers in each sample are measured. Variation of decay time with sample temperature is measured in p-type samples.

4.2 Preparation of $CuInSe_2$ thin films

The process of film preparation involves three steps. In the first step Selenium films of thickness about 5000 Å were deposited using CBD technique (as explained in Chapter- 3). Thickness of the Selenium layer was chosen such that CIS film formed will be nearly stoichiometric with Cu:In:Se ratio 1:1:2. In the second stage, Indium and Copper layers were vacuum evaporated sequentially on the Selenium layer. In order to analyse compositional dependence on photoconductivity, films were prepared by varying Cu/In ratio in the stack layers. This was done by changing the thickness of Cu layer keeping thickness of Indium layer same at 350 Å. 30 mg of Indium was taken in a Mo boat and evaporated to get an Indium layer of thickness 350 Å. The ratio was calculated knowing the values of density and atomic weight of Cu (8.9 g/cc and 63.54 respectively) and In (7.3 g/cc and 114.8 respectively), and distance from the source to substrate is 15 cm. Thus an elemental stack layer of Se/In/Cu with Selenium forming the lower layer on glass was obtained. To study the variation of photoconductivity with Cu concentration in the film, different weights of Cu were taken to prepare Se/In/Cu stack layer. The calculated Cu/In ratio for different weights of Cu was 0.45 (10 mg), 0.9 (20 mg), 1.22 (27 mg) and 1.3 (30 mg). In the final stage, the stack layers were annealed in vacuum (10^{-5}m bar) at 673 K for one hour, keeping rate of heating 3 K/min. These samples were named 'CIS 0.45', 'CIS 0.9', 'CIS 1.22' and 'CIS 1.3' respectively. In this 'CIS 0.45' was n-type and all other samples were p-type (26). XRD pattern of CIS films formed at 673 K having different Cu/In ratio is shown in Fig. 4.1. As Cu/In ratio increased, the crystallinity of the film also increased and conductivity changed from n to p-type.

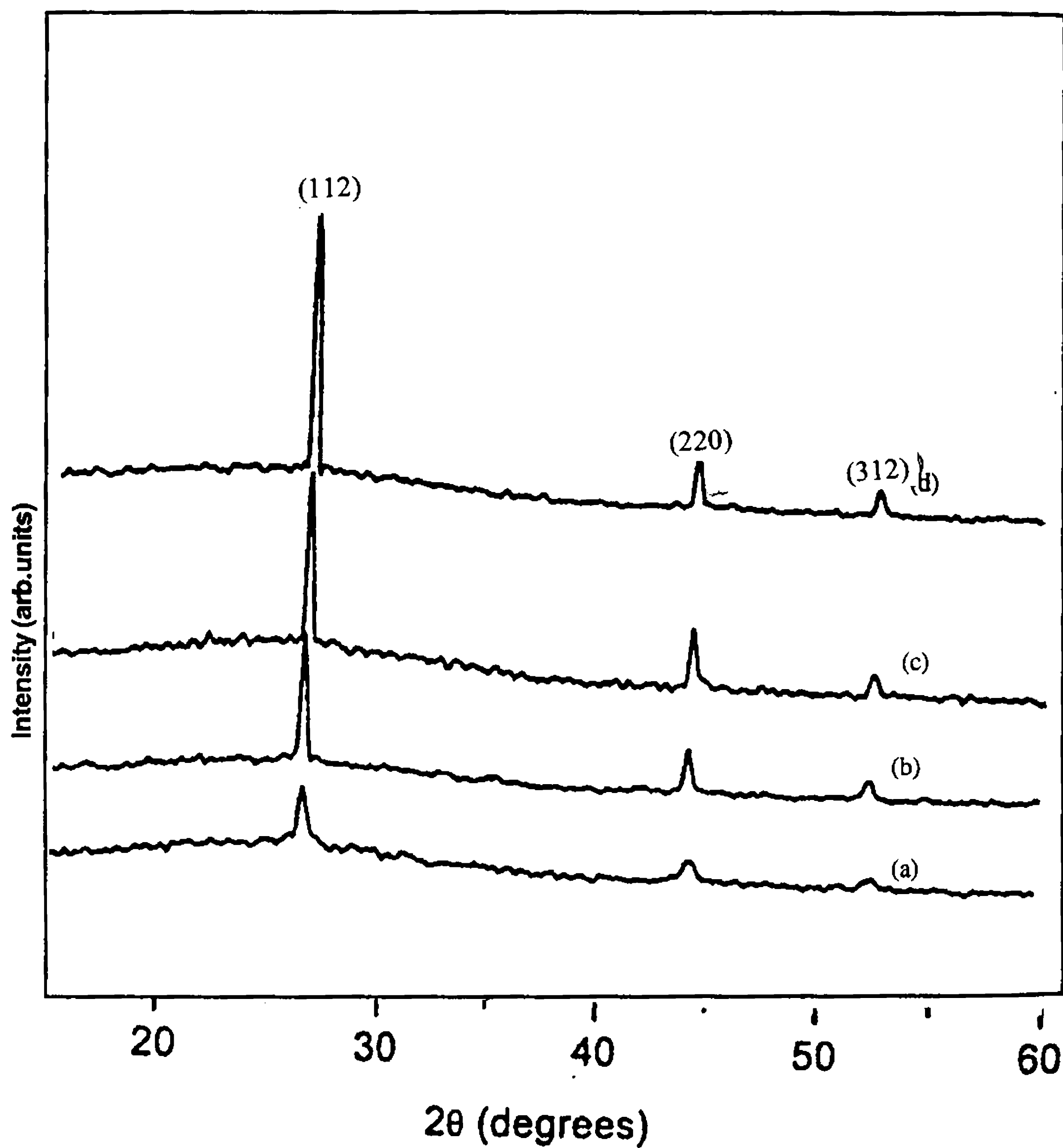

Fig.4.1 XRD pattern of CIS films formed at 673 K having different Cu/In ratio (a) 'CIS 0.45' (b) 'CIS 0.9' (C) 'CIS 1.22' and (d) 'CIS 1.3'

4.3 Experimental set up

Experimental set up was explained in detail in chapter 2. For photoconductivity measurements of $CuInSe_2$, a constant dc voltage of 0.1 V and a resistance R_L (10 MΩ) were connected in series with the sample. Duration of illumination was 5 minutes. Care was taken to get steady value for dark conductivity before illuminating the sample for each measurement. For positive photoconductivity measurements ('CIS 0.45' and 'CIS 0.9') decay of the voltage across the resistance after switching off the illumination was measured using Kiethely 2000 multimeter. For negative photoconductivity measurements ('CIS 1.22' and 'CIS 1.33') the current in the circuit was directly measured using Source Measurement Unit.

4.4 Variation of nature of photoconductivity with Cu concentration in the film

PCD measurements were done on different samples viz. 'CIS 1.3', 'CIS 1.22', 'CIS 0.9' and 'CIS 0.45'. Among the above samples 'CIS 1.3' and 'CIS 1.22' showed negative photoconductivity and, 'CIS 0.9' and 'CIS 0.45' showed positive photoconductivity.

Negative photoconductivity

Fig. 4.1 shows the negative photoconductivity of the sample 'CIS 1.3'. On illuminating the sample, current decreased to 2.9 μA, and on removing the illumination, it increased to the dark value. For sample 'CIS 1.22' negative photoconductivity is decreased and the change in current was only 0.15 μA (Fig. 4.2).

Negative photoconductivity occurs in a material when the absorption of radiation decreases the dark conductivity of the material. According to N. V. Joshi et al., negative photoconductivity in p-type semiconductors occurs when electrons ejected from the inner level recombine with holes at the top of the valence band (27). Rincon et al. reported various possible intrinsic defects in $CuInSe_2$ (12). In Cu rich films, the antisitic defect – Cu_{In} (Cu in place of Indium) and Indium vacancy (V_{In}) act as acceptor levels contributing holes for p-type conductivity. In Indium rich films In_{Cu} (Indium in place of Copper) is the major defect

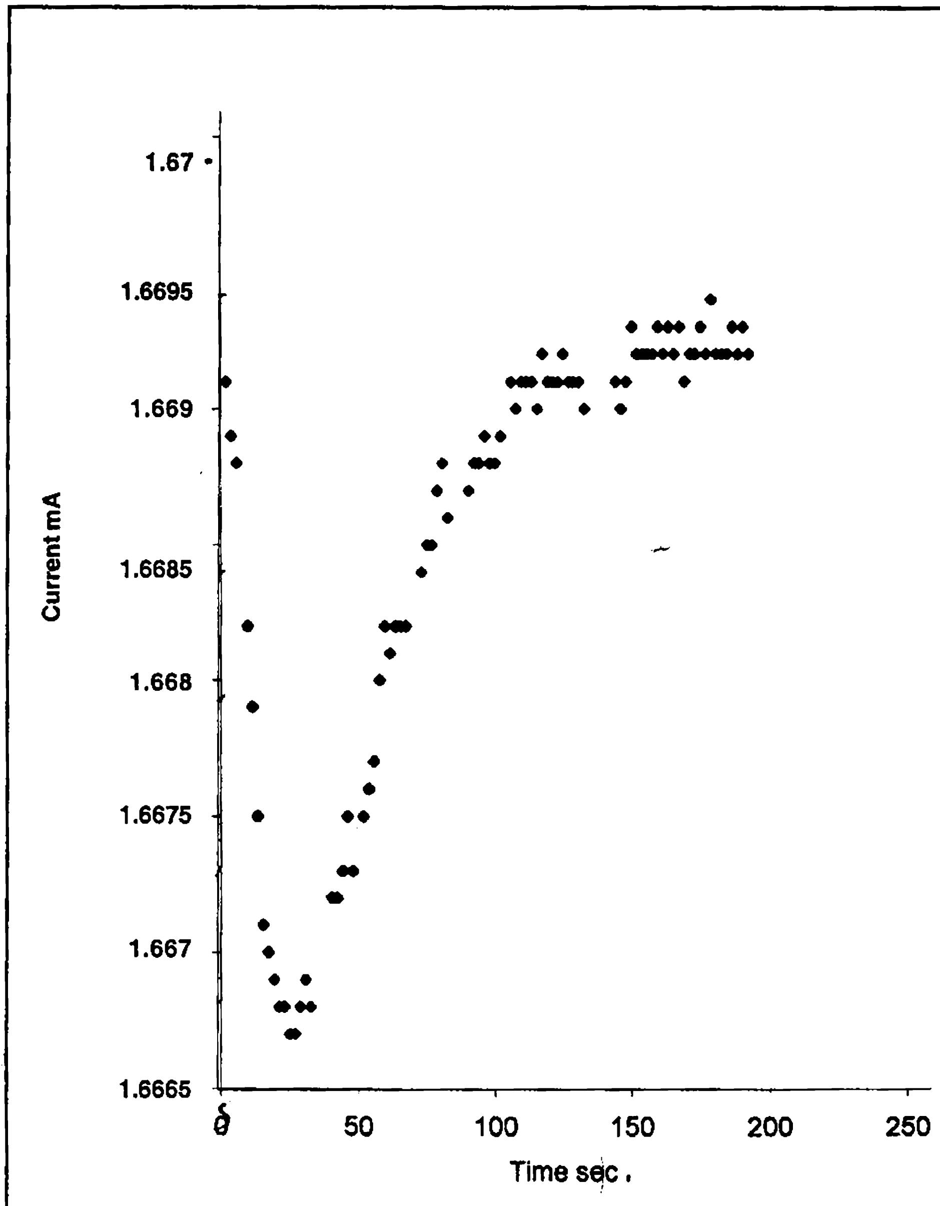

Fig.4.2 Negative photocpnductivity of the sample 'CIS 1.3'

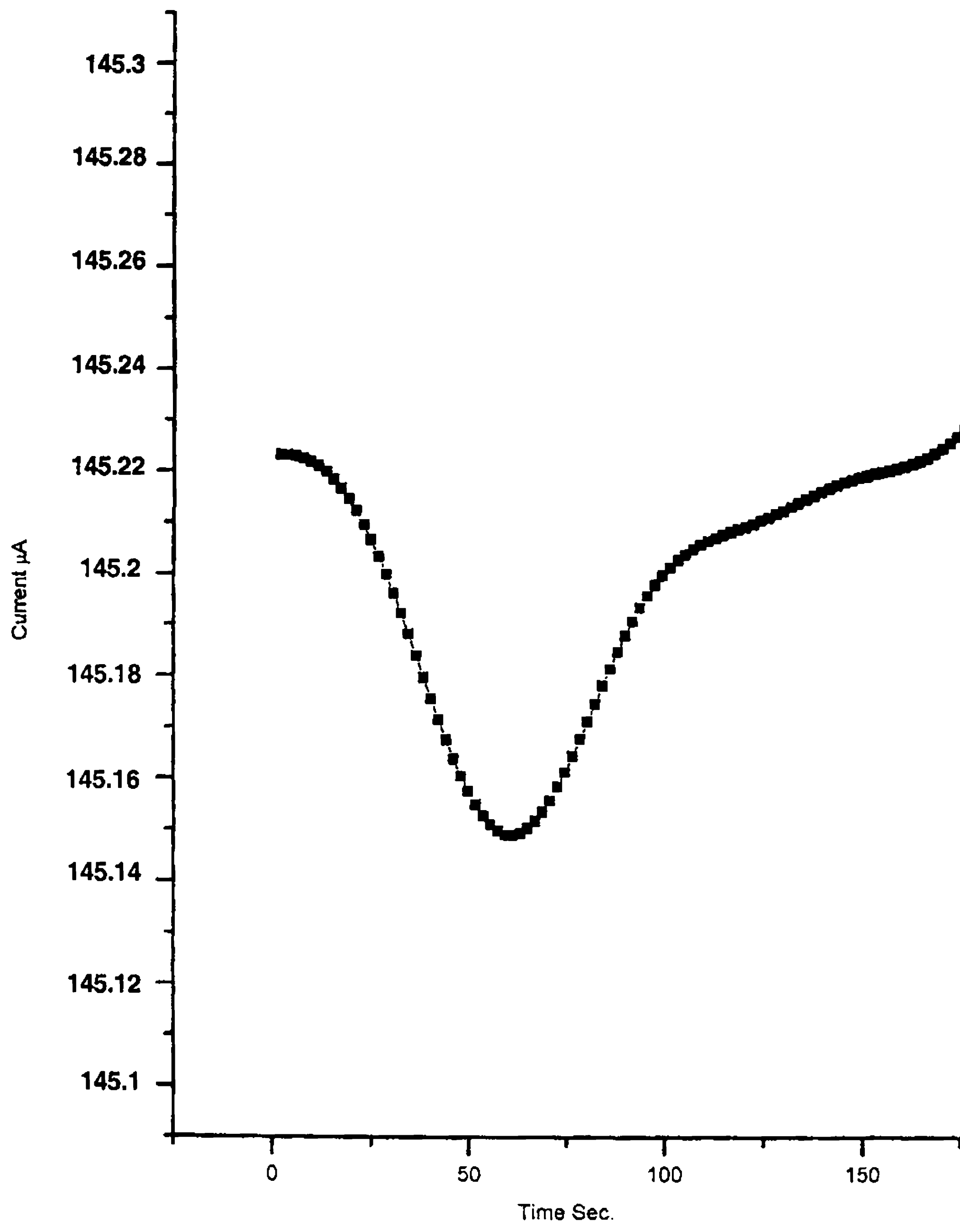

Fig.4.3 Negative photoconductivity of the sample 'CIS 1.22'

which act as donor level contributing n-type carriers. S. B. Zhang et al. reported that defect formation energies vary considerably with the electrical potential and chemical potential of the atomic species (28). The order of formation of energies in Cu rich In poor p-type $CuInSe_2$ are

$$Cu_{In} < V_{Cu} < V_{In} < Cu_i < In_{Cu}$$

So Cu_{In} (antisite of Cu on In site) is the most abundant defect in Cu rich In poor p-type $CuInSe_2$. On illuminating the sample, the other donor type defect - Cu_i (Cu interstitial), may donate electrons and recombine with the holes from Cu_{In} defect and that may be the reason for the negative photoconductivity in p-type $CuInSe_2$ thin films.

Positive photoconductivity

'CIS 0.9' is slightly Copper deficient but it is p-type (30). It shows a positive photoconductivity and its PCD curve at 300 K is shown in Fig 4.3. At this temperature, increase in current on illumination is only 6.5 nA and the decay time of charge carriers is 1.04 Sec. Decay time decreased as sample temperature decreased from 300 K to 250 K. Variation of decay time with sample temperature is shown in Fig 4.4. Measurements could not be done below 250 K, as the photoconductivity was negligibly small.

'CIS 0.45' shows positive photoconductivity and its PCD curve at 300 K is shown in Fig. 4.4. The increase in photocurrent on illumination is 15.5 nA but decay time is only 402 mSc. at 300 K. Variation of decay time with sample temperature is shown in Fig. 4.5. There is an increase in decay around 150 K and 300 K, which indicates that charge carriers are released from two defects at these two temperatures. The increase of defect density due to In_{Cu} as Cu/In decreases may be the reason for the increase in photoconductivity of the sample 'CIS 0.45'. But there is a probability of formation of vacancy of Cu as Cu/In ratio decreases, which is a single acceptor (12). The holes from this defect may recombine with the electrons from In_{Cu} antisite and reduces the decay time.

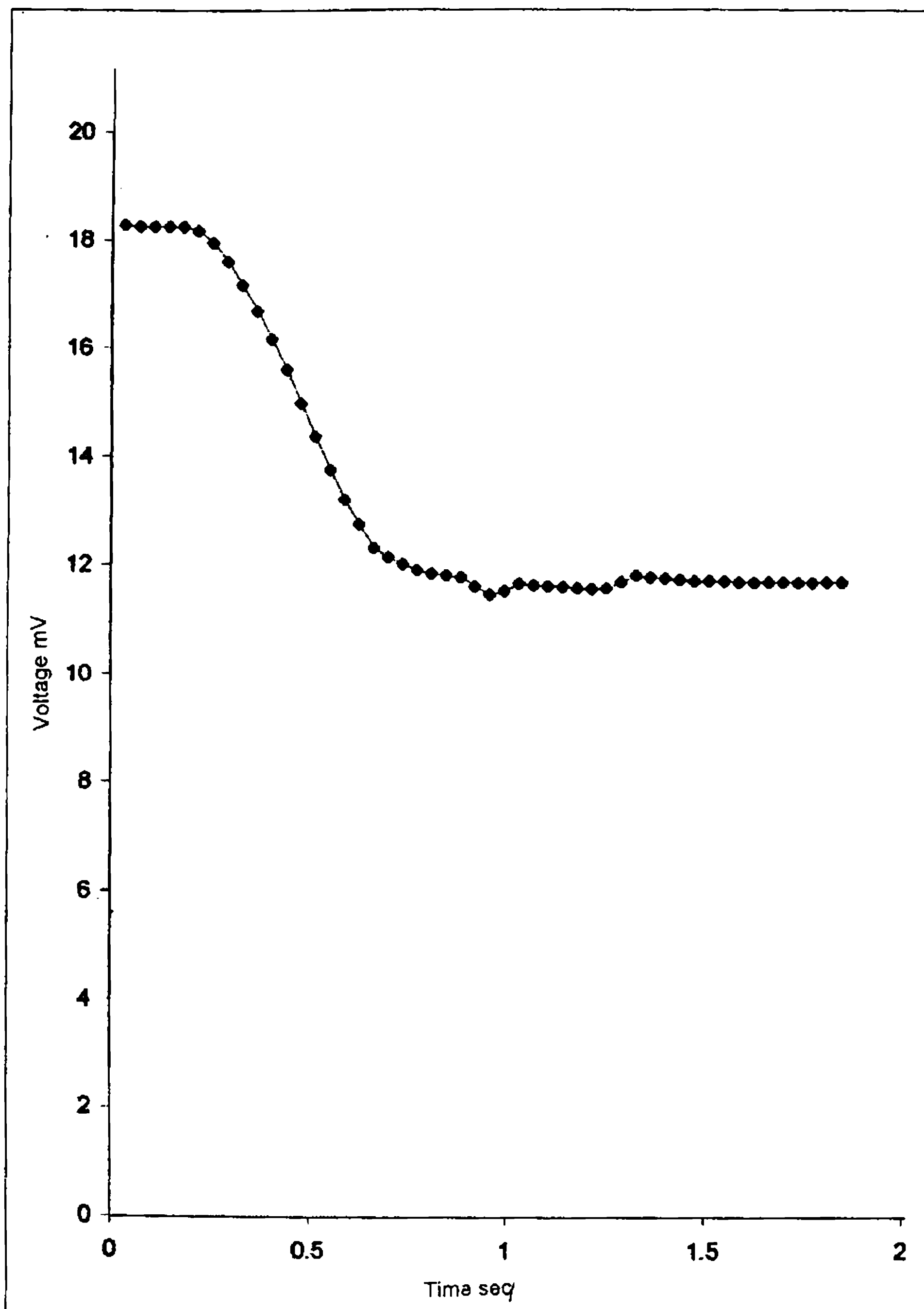

Fig.4.4 PCD curve for sample 'IS 0.9' at 300 K

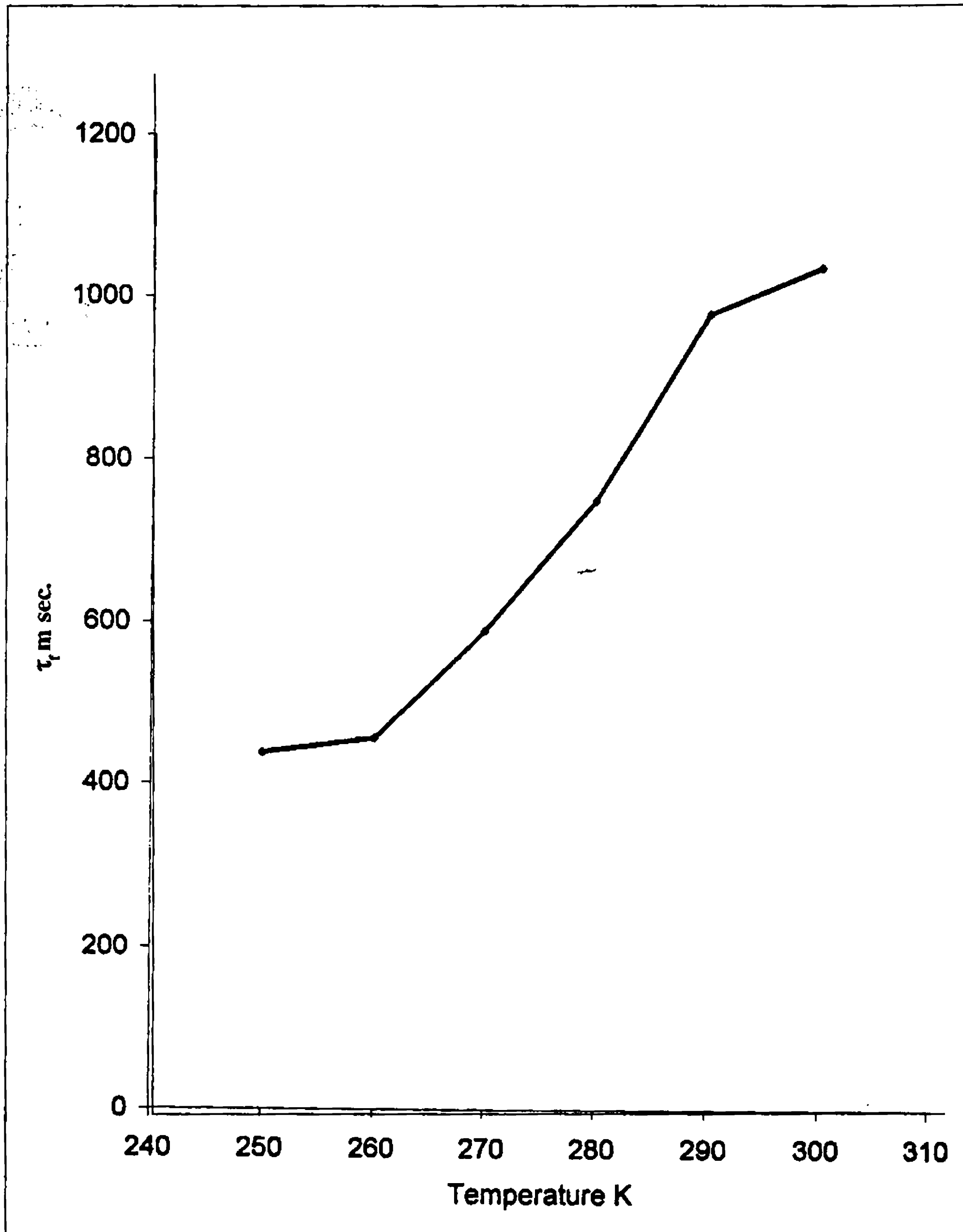

Fig.4.5. Variation of τ_r with temperature for sample 'CIS 0.9'

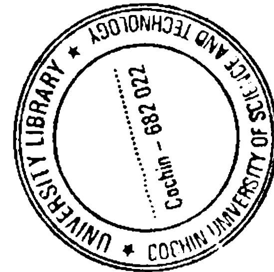

Voltage mV

19
18
17
16
15
14
13
12

0.0 0.2 0.4 0.6 0.8 1.0 1.2

Time Sec.

Fig.4.6. PCD curve for sample 'CIS 0.45' at 300 K

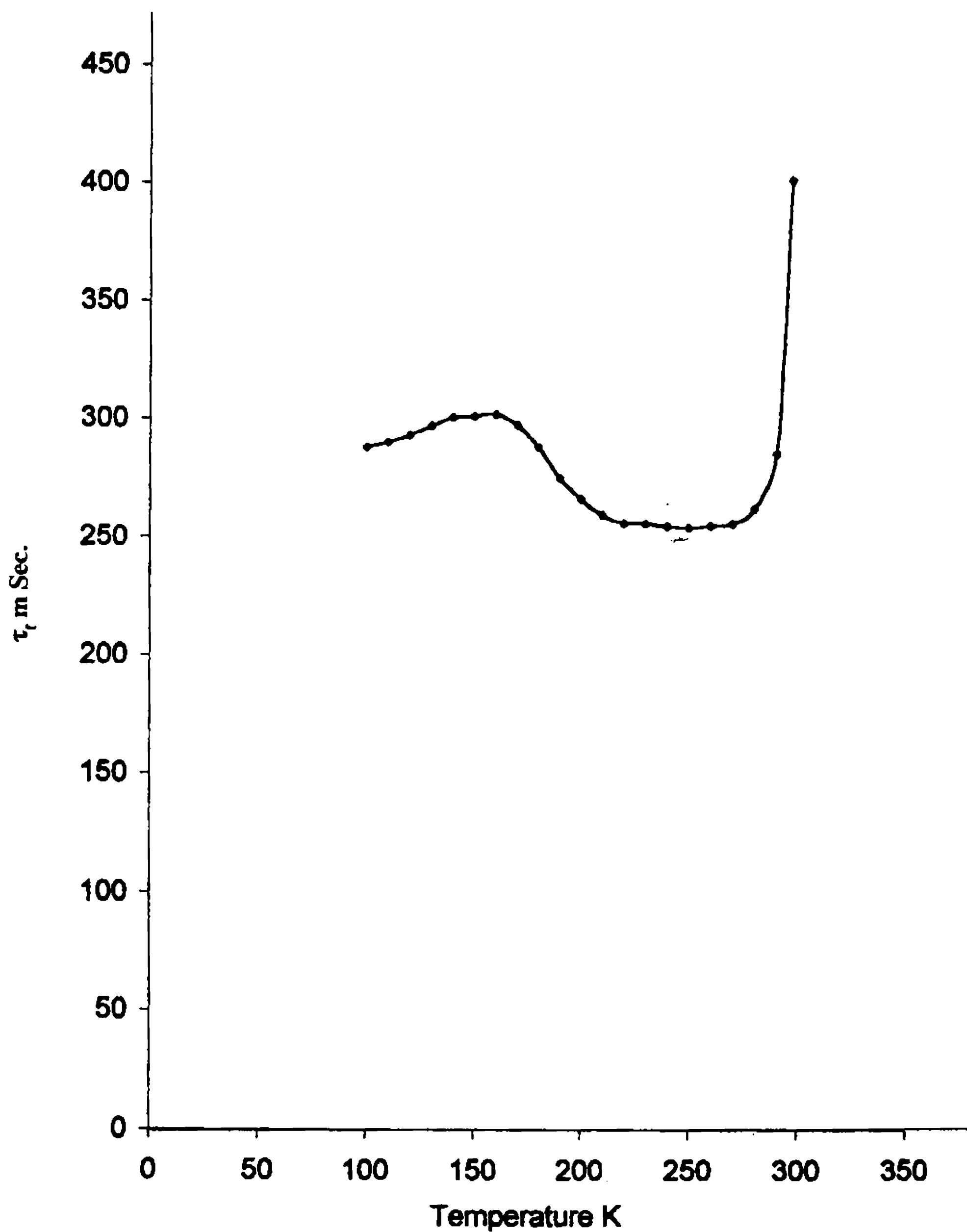

Fig.4.7. Variation of τ_r with temperature for sample 'CIS 0.45' at 300 K

4.5 Conclusion

Photoconductivity measurements are done on CIS films having different Cu/In ratio. As the Copper content in the film decreased, photoconductivity changed from negative to positive. Photoconductivity was more for 'CIS 0.45' than 'CIS 0.9'. Variation of decay time with temperature measurements of 'CIS 0.45' shows an increase of decay time around 150 K and 300 K indicating release of charge carriers from two defects at these temperatures.

References

1. Neelkanth. G. Dhere, M. Cristina Lourenco, Remesh. G. Dhere and Lawrence. L. Kazmerski, Solar Cells, 16 (1986) 369
2. R. J. Matson, R. Noufi, K. J. Bachmann and D. Cahen, Appl. Phys. Lett., 50 (3) (1987) 158
3. Y. Horikoshi, M. Kawasimha and Y.Yamaguchi, Jpn. J. Appl. Phys., 25 (1986) 68
4. A. Goetzberger and Hebling, Sol. Energy Mater. Sol. Cells, 62 (2000) 1
5. Shalini Menezes, Appl. Phys. Lett., 61 (13) (1992) 1564
6. R. Noufi, R. Axton, C. Herrington and S. K. Deb, Appl. Phys. Lett., 45 (1984) 668
7. H. Neumann and R. D. Tomlinson, Solar Cells, 28 (1990) 301
8. J. Herrero and C. Jullien, J. Appl. Phys., 69 (1991) 429
9. J. R. Tuttle, D. Albin, R. J. Matson and F. Noufi, J. Appl. Phys., 66 (1989) 4405
10. L. Y. Sun, L. L. Kazmerski, A. H. Clark, P. J. Ireland and D. W. Morton, J. Vac. Sci. Techn., 15 (1978) 265
11. J. Klais, H. J. Moller, R. Krause-Rehbery, D. Cahen, V. Lyakhovitskaya, Inst. Phys. Conf. Ser. No. 152 Section E: Surfaces and Interfaces Proc. I (TMC-11, Salford 1997) P. 741 (1998)

12. C. Rincon and R. Marquez, J. Phys. Chem. Solids, 60 (1999) 1865

13. J. A. Groenink, P. H. Janse, Z. Phys. Chem. Neue Folge, 110 (1978) 17

14. L.Essaleh, S. M. Wasim and J. Galibert, J. Appl. Phys., 90 (8) (2001) 3993

15. M. Igalson, Phys. Stat. Sol. (a), 139 (1993) 481

16. K. Puech, S. Zott, K. Leo, M. Ruckh and H. W. Schock, Appl. Phy. Lett., 69 (22) (1996) 3375

17. B. Ohnesorge, R. Weigand, G. Bacher, A. Forchel, W. Riedl and F. H. Karg., Appl. Phys. Lett., 73 (9) (1998) 1224

18. L. L. Kazmerski, P. J. Iveland, P. R. White and R. B. Cooper, Proc. 13th IEEE Photovoltaic Specialists Conf., Washington DC, (1978) 18

19. Clayron W. Bates, JR, Kim F. Nelson, S. Atiq Raza, John B. Mooney, Jutta M. Recktenwald, Loren Macintosh and Robert Lamoreaux, Thin Solid Films, 88 (1982) 279

20. S. Isomura, A. Nagamatsu, K. Shinohara and T. Aono, Solar Cells, 16 (1986) 143

21. Toshiyuki Yamaguchi, Jiro Matsufusa, Hideki Kabasawa and Akira Yoshida, J. Appl. Phys., 69 (1991) 7714

22. Gary Hodes and David Cahen, Solar Cells, 16 (1986) 245

23. P. K. Vidyadharan Pillai, K. P. Vijayakumar and P. S. Mukherjee, J. Mater. Sci. Lett., 13 (1994) 1725

24. Mikihiko Nishitani, Takayuki negami, Masaharu Terauchi and Takashi Hirao, Jpn. J. Appl. Phys., 31 (1992) 192

25. F. O. Adurodija, M. J. Carter and R. Hill, Sol. Ener. Mater. and Sol. Cells, 37 (1995) 203

26. K. Bindu, M. Lakshmi, S. Bini, C. Sudha Kartha, K. P. Vijayakumar, T. Abe and Y. Kashiwaba, Semicond. Sci. and Tech., 17 (2002) 270

27. N. V. Joshi, L. Mogollon, J. Sanchez and J. M. Martin, Solid State Commun., 65 (1988) 151

28. S. B. Zhang, Su-Huai Wei, Alex Zunger and H. Katayama-Yoshida, Physical Review. B, 57 (16) (1998) 9642

29. T. L. Chu, Shirley S. Chu, S. C. Lin and J. Yue, J. Electrochem. Soc: Solid State Sci. Technol., 131 (1984) 2182

30. K. Bindu, Ph. D. Thesis, Cochin University of Science and Technology, Kochi, (2002) 144

Chapter 5

Photoconductivity studies in $CuInS_2$

5.1 Introduction

$CuInS_2$ is an I-III-VI semiconductor, which belongs to the tetragonal chalcopyrite structure (1). It also crystallizes in sphalerite structure (2). The optical absorption coefficient is 10^5 cm^{-1} in the visible and near infrared region (2, 3). Its band gap is 1.55 eV at 300 K. Due to its optimum band gap and high absorption coefficient it has great potential for photovoltaic applications. The highest reported conversion efficiency for recent $CuInS_2$ – based solar cells is 12.5 % (4).

By making deviation from molecularity and stoichiometry, in terms of the ratios [Cu]/[In] and [S]/[Cu] in the film, $CuInS_2$ can be made n- or p-type so that homojunction solar cell is possible with this material (5,6). In_2S_3-rich $CuInS_2$ is obtained as p-type and Cu_2S-rich $CuInS_2$ is obtained as n-type (7). Hsu. H. J et al reported that $CuInS_2$ crystals grown in excess Indium were n-type and those grown in excess Sulphur were p-type (8). The electrical conducting phenomena are mainly affected by the intrinsic defects of the material (9). It has a compatible lattice structure with the binary compound semiconductor CdS with acceptable lattice mismatches and differences in electron affinity for the formation of hetero junction devices. The advantage of this material over $CuInSe_2$ is the reduced toxicity and abundance of its constituents.

In 1975 two deposition methods for producing $CuInS_2$ thin films – single and double source methods, were reported for the first time by Kazmerski et al. (10). For the single source method, single-phase $CuInS_2$ was used as the starting material. The second, a more controllable and reproducible method, involved a two-source arrangement. Since then, $CuInS_2$ thin film has been prepared by a variety of methods viz. three sources evaporation (11, 2 and 12), rf-sputtering (13, 14), close spaced chemical transport (15), chemical deposition (16,17), electro deposition (18-20), flash evaporation (21, 22), painting (23), spray pyrolysis (24-26) and stacked elemental layer deposition technique (27). S. Bini et al. reported the conversion of Cu_xS films prepared using CBD technique into $CuInS_2$ films (28). For the present study, samples are prepared using spray pyrolysis technique. Photoconductivity studies are done on different samples having different Cu/In ratio and Cu/S ratio.

5.2 Preparation of $CuInS_2$ thin films

Cleaned glass slides were placed on a thick iron block (15x9x1 cm^3), which can be heated to the required temperature with a controlled heater. Temperature of substrate holder was measured using a digital thermometer (Thermins, series 4000) and temperature control was achieved using variable transformer. Spray head and heater with substrate were kept inside a chamber provided with an exhaust fan for removing gaseous by-products and vapor of the solvent (water). During spray, the temperature of substrate was kept constant with an accuracy of ± 5°C. The pressure of carrier gas was noted using a manometer and was kept at 90 ± 0.5 cm of Hg. Spray rate was 15 ml/min., and the distance between spray head and the substrates was ~15 cm. In order to get uniform composition and thickness, spray head was moved to either side manually with uniform speed. $CuInS_2$ thin films were deposited over glass substrates from aqueous solutions of cupric chloride ($CuCl_2$, 2 ½ H_2O), Indium tri chloride and thiourea using compressed air as the carrier gas. Thiourea was chosen as the source of sulfur ions in spray solution because it avoids precipitation of metallic sulfides and hydroxides since it forms complexes with copper and indium ions easily (7). Aqueous solutions of these salts were prepared in distilled water, and Cu/In ratio and S/Cu ratio in spray solutions were varied. The deposition temperature was always fixed at 300 °C. A set of samples was prepared by varying Cu/In molar ratio 0.5, 1 and 1.5 in the solution, keeping S:Cu molar ratio constant at 4 (samples 'CIS0.5,SC4', 'CIS1,SC4' and 'CIS1.5,SC4'). An-

other set was prepared by varying S/Cu molar ratio from 5 to 8 (samples 'CIS0.5,SC5' to 'CIS0.5,SC8') keeping Cu/In molar ratio at 0.5.

5.3 Experimental set up

Experimental set up was explained in detail in chapter 2. For photoconductivity measurements in $CuInS_2$, a constant dc voltage of 0.1 V and a resistance R_L (10 MΩ) were connected in series with the sample. Duration of illumination was different for each sample. Care was taken to get steady value for dark conductivity before illuminating the sample for each measurement. Voltage across the resistance after switching off the illumination was measured using Kiethely 2000 multimeter. All the measurements were done at room temperature.

5.4 Nature of photoconductivity in $CuInS_2$ thin films

Photoconductivity measurements were done on two sets of samples 'CIS0.5,SC4' to 'CIS1.5,SC4', and 'CIS0.5,SC4' to 'CIS0.5,SC8'. Among the first set of samples, 'CIS0.5,SC4' is most photo conducting. Its PCD curves in air and vacuum are shown in Fig. 5.1. For sample 'CIS1,SC4' photoconductivity was negligibly small and could not be measured, where as 'CIS1.5,SC4' did not show photo-conducting property. On illuminating the sample in air (curve-1, at A), photoconductivity increased (up to B) and immediately afterwards it decreased while the illumination is on (BC). On switching off the illumination (at C), photoconductivity decreased even below the dark value (up to D) and then increased to the equilibrium dark value. This oscillating nature of photoconductivity could not be observed while taking the measurements in vacuum. Another observation is that the photo conducting nature of the material decreased on keeping the sample in vacuum for a long time Fig (5.2). It is also observed that it regained the nature of photoconductivity on admitting air. Similar nature of photoconductivity could be observed in samples 'CIS0.5,SC5' to 'CIS0.5,SC8' also (Fig. 5.3 to Fig. 5.6). D. Cahen and R.Noufi reported that post deposition annealing of $CdS/CuInS_2$ solar cell in air or O_2 optimizes the photovoltaic performance (29). Koichi Fukuzaki et al. reported that incorporation of Oxygen with the $CuInS_2$ results in a new $CuIn(S,O)_2$ phase at the $CuInS_2$ surface which is responsible for the elevated open-circuit voltage (V_{oc}) and efficiency (30). J. Grzanna et al. reported a chemical analysis, performed in a quater-

nary system - Cu-In-S-O at different partial pressures of Oxygen and observed that $CuInS_2$ is unstable in air and form $In_2(SO_4)_3$, and CuS at Oxygen pressures larger than log *p*(pascal) = - 51.5 (31). Instability of $CuInS_2$ in the presence of Oxygen may be the reason for the instability in photoconductivity.

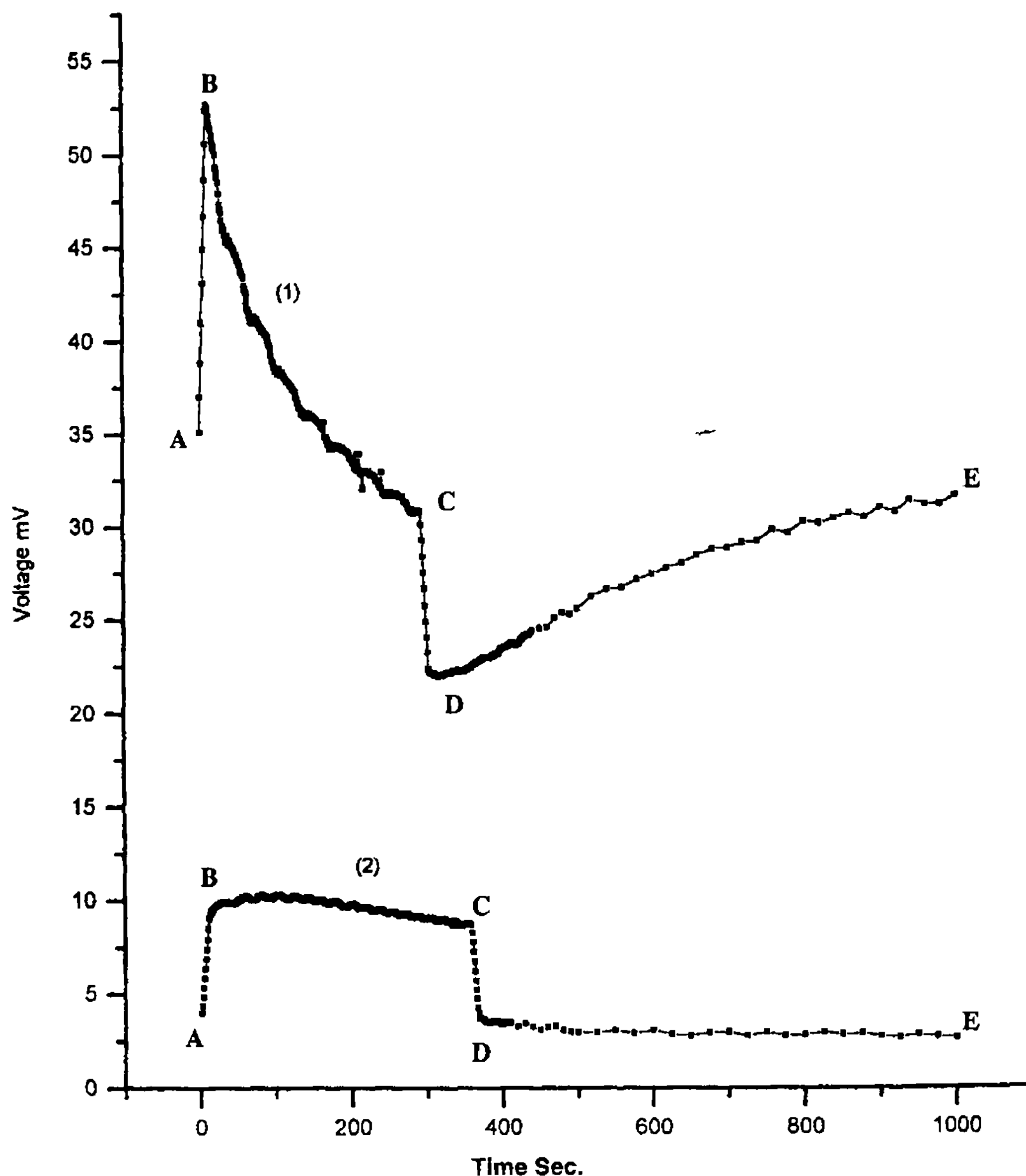

Fig. 5.1 PCD curves for 'CIS 0.5, SC4' at 300k in air (1) and vacuum (2)

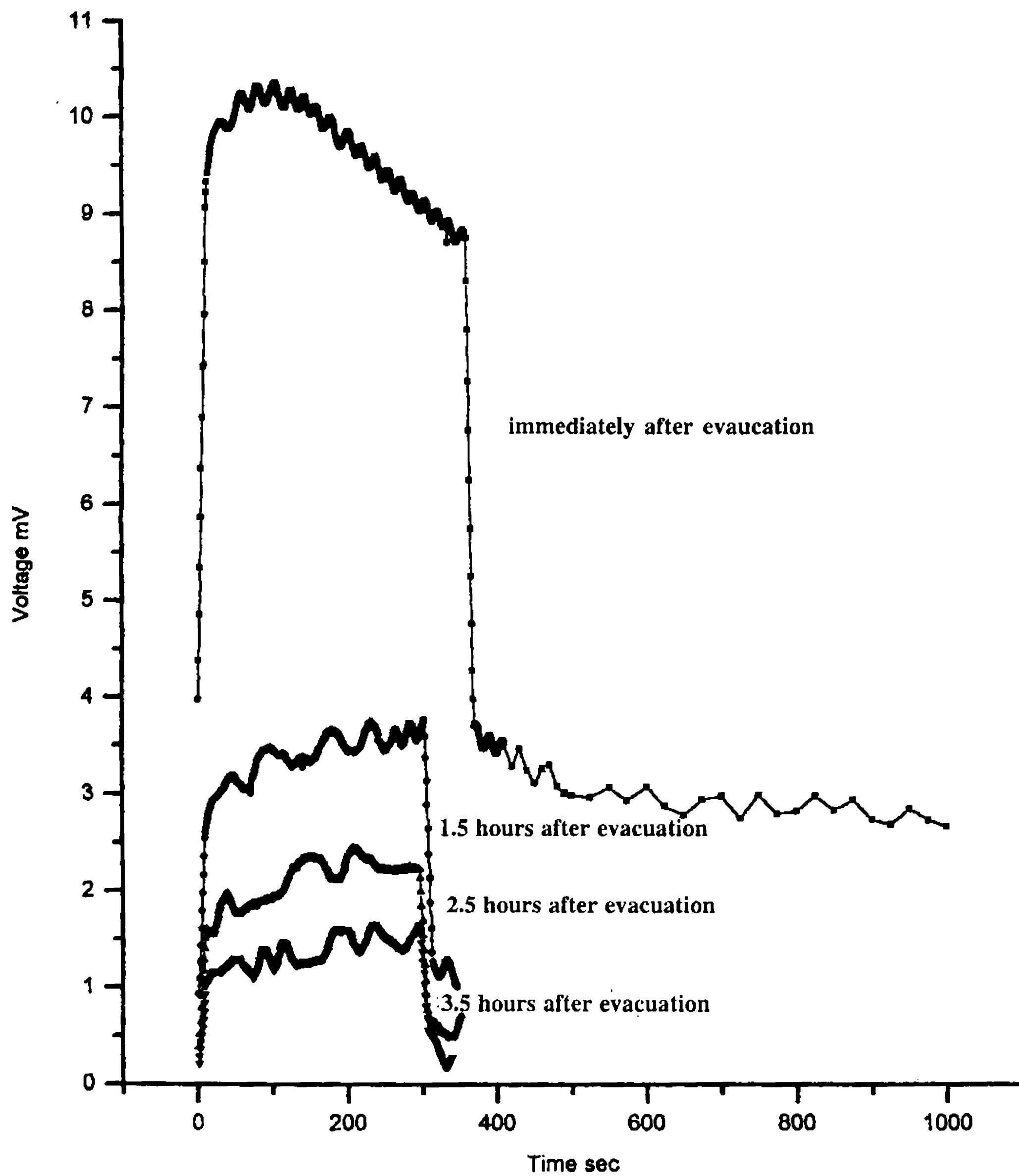

Fig. 5.2 PCD curves for 'CIS 0.5, SC4' at 300 K in vacuum for different duration of time

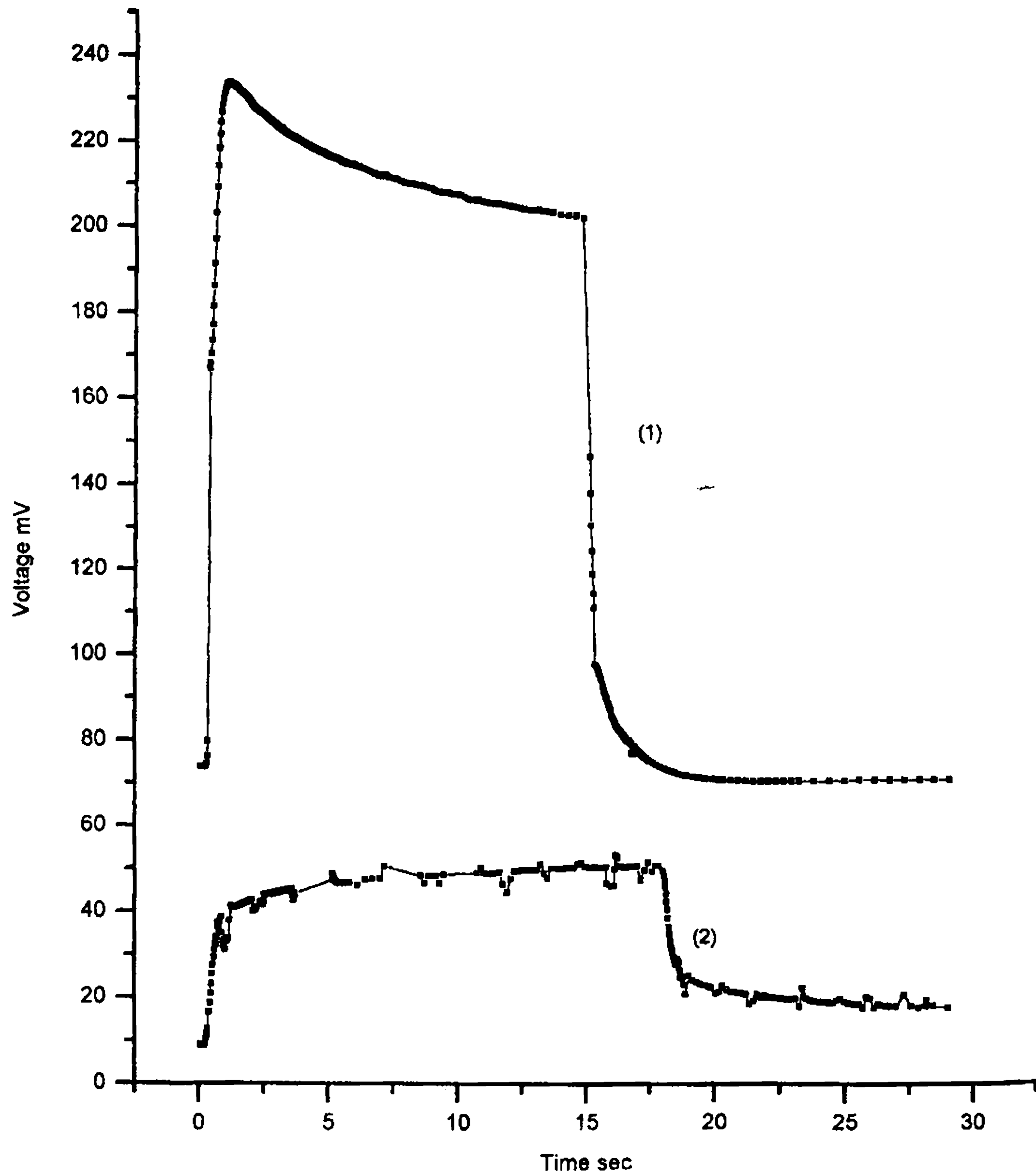

Fig. 5.3 PCD curves for 'CIS 0.5, SC5' at 300 K in air (1) and vacuum (2)

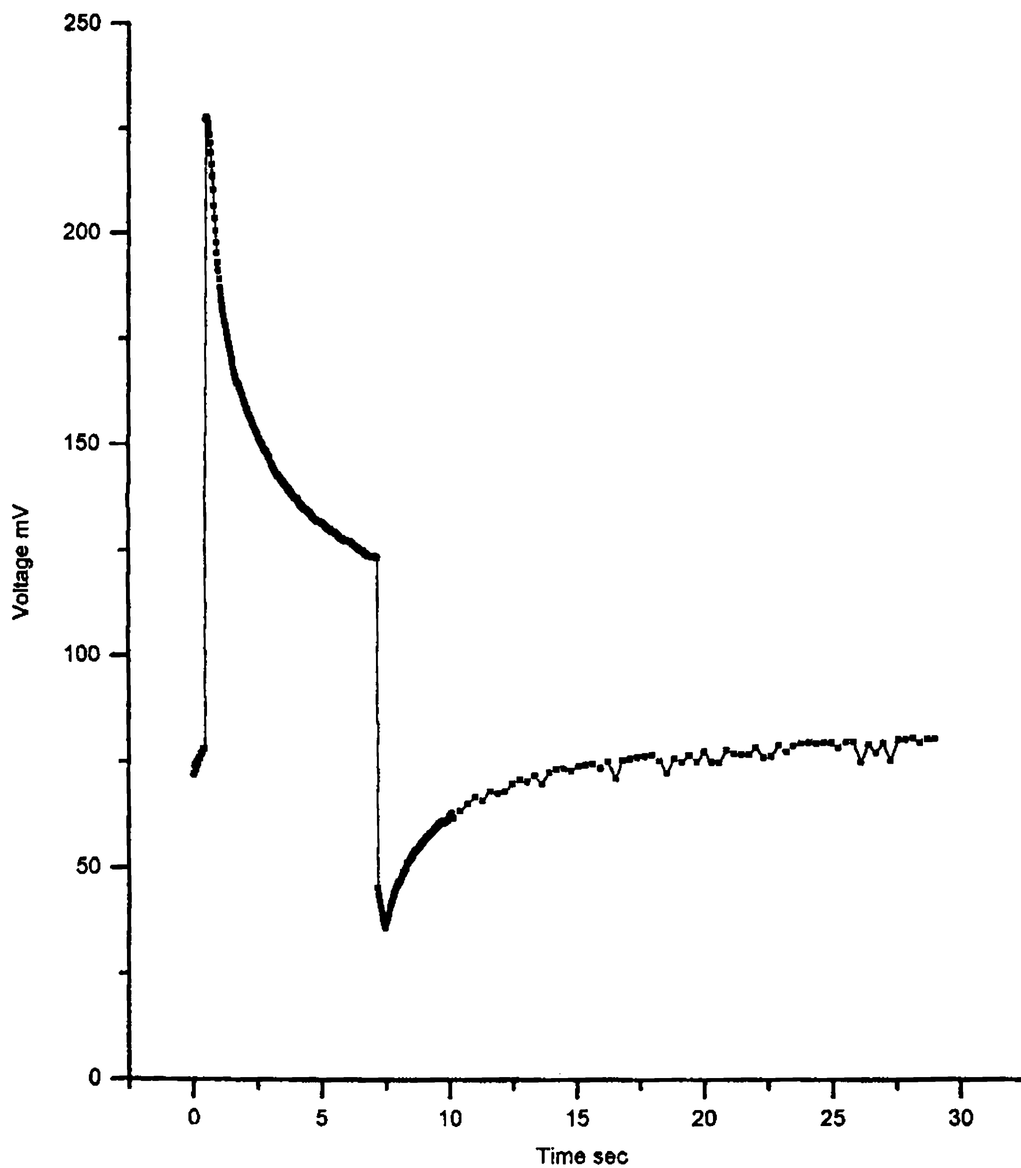

Fig. 5.4 PCD curve for 'CIS 0.5_SC6' at 300 K in air

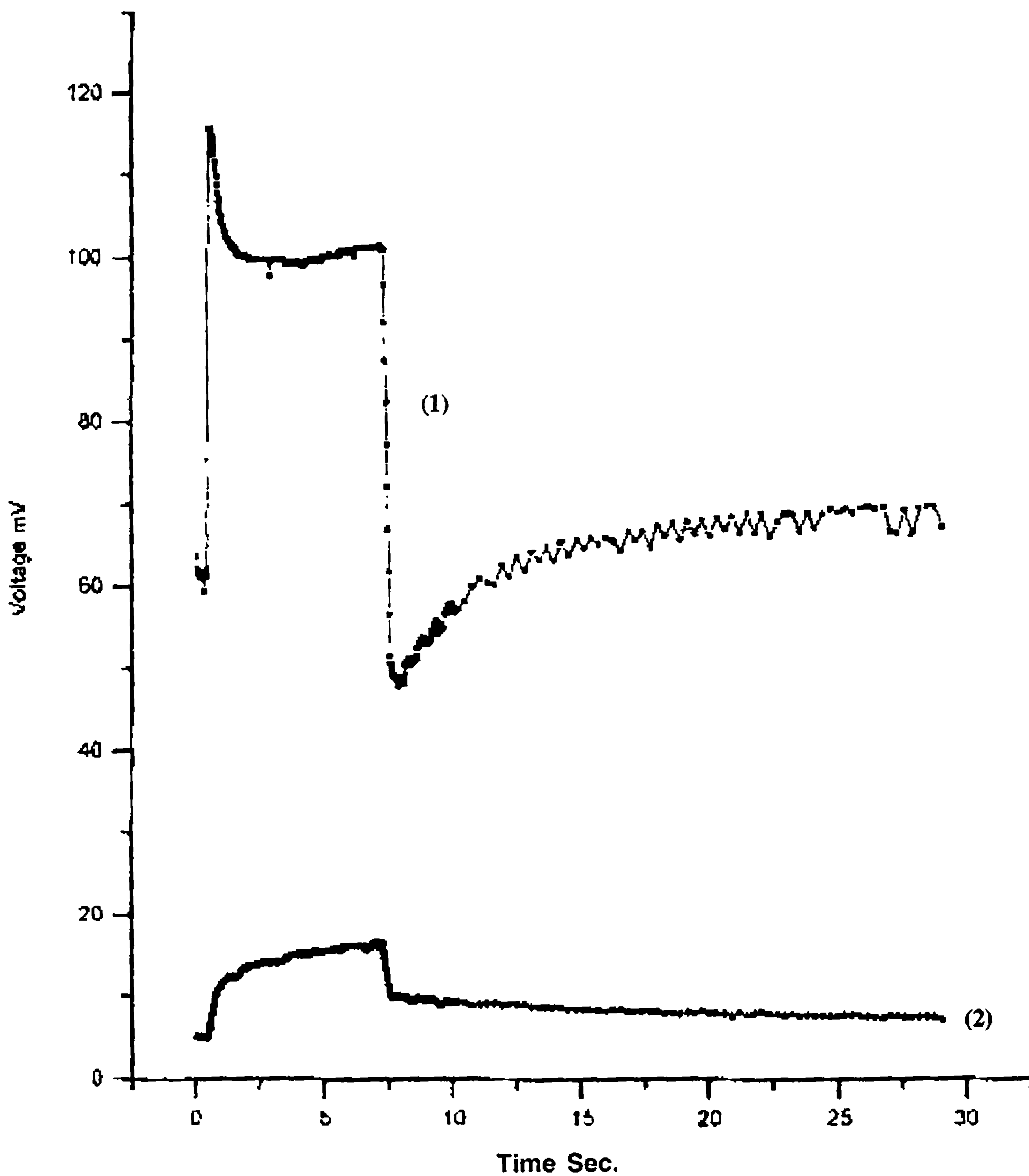

Fig. 5.5 PCD curves for 'CIS 0.5, SC 7' at 300 K in air (1) and vacuum (2)

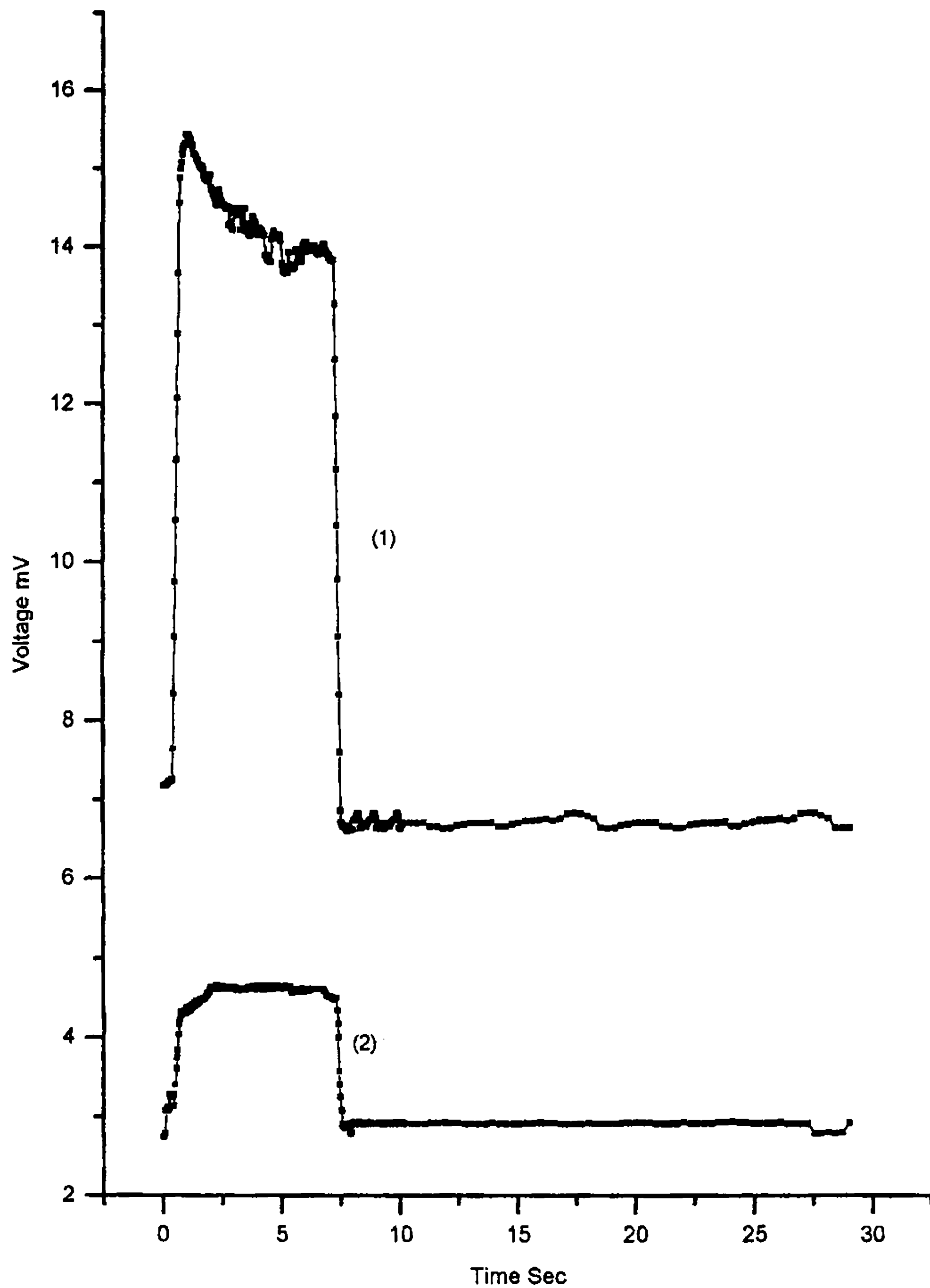

Fig. 5.6 PCD curves for 'CIS 0.5, SC 8' at 300 K in air (1) and vacuum (2)

5.5 Variation of photoconductivity with Cu/In and S/Cu molar ratio in the solution

Photoconductivity measurements done on samples 'CIS0.5,SC4' to 'CIS1.5,SC4' showed that 'CIS0.5,SC4' was most photo conducting (Fig. 1). For this film Cu:In ratio in the film was found to be nearly 1:1 from XPS analysis. But crystallinity was poor. S. Bini reported that as Copper content in the film increased crystallinity improved (32). For sample 'CIS1,SC4' photoconductivity was negligibly small and could not be measured, where as 'CIS1.5,SC4', did not show photoconducting property at all. From this study it is clear that film having Cu:In ratio 1:1 in the film is most photoconducting and as Copper increased in the film, photoconductivity decreased.

Photoconductivity studies done on samples 'CIS0.5,SC4' to 'CIS0.5,SC8' (Fig. 5.1 and Figs.5.3 to 5.6) revealed that photoconductivity was maximum for sample 'CIS0.5,SC5'. Another observation was that dark conductivity also was maximum for this sample and as Sulphur content in the film increased dark conductivity decreased. The oscillatory nature was minimum for this sample. Decay time was different for different duration of illumination for all samples.

5.6 Conclusion

Photoconductivity measurements were done on $CuInS_2$ films prepared from solutions with different Cu/In and S/Cu molar ratios. It was found that film prepared from solution having Cu/In molar ratio 0.5 (Cu/In ratio 1:1 in the film) is most photo conducting. On varying S/Cu molar ratio from 4 to 8 in the solution, it was found that the film prepared from the solution having molar ratio S/Cu=5 is most photo conducting. All the films showed an oscillatory nature in photoconductivity when the measurements were taken in air, whereas this nature disappeared when the measurements were done in vacuum. On keeping the sample in vacuum for longer time, photoconductivity was found to decrease.

References

1. J. L. Shay and J. H. Wernick, Ternary Chalcopyrite Semiconductors: Growth, Electronic properties and Applications, Pergamon Press, Oxford (1975) 4
2. R. Scheer, K. Diesner, H. J. Lewerenz, Thin Solid Films, 268 (1994) 130
3. L. I. Gurinovich, V. S. Gurin, V. A. Ivanov, I. V. Bodnar, A. P. Molochko and N. P. Solovei, Phys. Stat. Sol. (b), 208 (1998) 533
4. J. Klaer, J. Bruns, R. Henninger, K. Siemer, R. Klenk, K. Ellmer and D. Braunig, Semicond. Sci. Technol., 13 (1998) 1456
5. D. C. Look and J. C. Manthuruthil, J. Phys. Chem. Solids 37 (1976) 173
6. B. Tell, J. L. Shay and H. M. Kasper, Phys. Rev. B4 (1971) 2463
7. J. J. M. Binsma, L. J. Giling and J. Bloem, J. Luminescence, 27 (1982) 35
8. H. J. Hsu, N. H. Yang, R. S. Tang, T. M. Hsu and H. L. Hwang, Crystal Growth, 20 (1984) 83
9. H. L. Hwang, L. M. Liu, M. H. Yang, P.Y. Chen, J. R. Chen and C. Y. Sun, Sol.Energy Mater. 7 (1982) 237
10. L.L Kazmerski, M. S. Ayyagari and G. A Sanborn, J. Appl. Phys, 46 (1975) 4865
11. J. Alvarez-Garcia, A. Perez-Rodriguez, A. Romana-Rodrigues, J. R. Morante, L. Calvo-Barrio, R. Scheer and R. Klenk, J. Vac. Sci. Technol. A, 19 (2001) 232
12. Y. L. Wu, H. Y. Lin, C.Y. Sun, M. H. Yang and H. L. Hwang, Thin Solid Films, 168 (1989) 113
13. A. N. Y. Samaan, S. M. Wasim, A. E. Hill, D. G. Armour and R. D. Tomlinson, Phys. Stat. Sol. (a), 96 (1986) 317
14. H. L. Hwang, C. Y. Sun, C. Y. Leu, C. L. Cheng and C. C. Tu, Revue De Physique Appliquee, 13 (1978) 745
15. K. Djessas, G. Masse and M. Ibannaim, J. Electro. Chem. Soc., 147 (200) 1235
16. G. K. Padam and S. U. M. Rao, Solar Energy Materials, 13 (1986) 297

17. Siham Mahmoud and Abdel- Hamid Eid, Fizika A, 6 (1997) 171

18. R. N. Bhattacharya, David Cahen and Gary Hodes, Solar Energy Mater., 10 (1984) 41

19. Gary Hodes, Tina Engelhard, David Cahen, L. L. Kazmerski and Charles R. Herrington, Thin Solid Films, 128 (1985) 93

20. Sigeyuki Nakamura and Akio Yamamoto, Sol. Energy Mat. Sol. Cells, 49 (1997) 415

21. M. K. Agarwal, P. D. Patel, Sunil H. Chaki and D. Lakshminarayana, Bull. Mater. Sci., 21 (1998) 291

22. H. Neumann, W. Horig, V. Savelev, J. Lagzdonis, B. Schumann and G. Kuhn, Thin Solid Films, 79 (1981) 167

23. G. Hodes, D. Cahen, J. Manassen and M. David, J. Electrochem. Soc., 127 (1980) 2252

24. B. Pamplin and R. S. Feigelson, Thin Solid Films, 60 (1979) 141

25. P. Rajaram, R. Thangaraj, A. K. Sharma, A. Raza and O. P. Agnihotri, Thin Solid Films, 100 (1983) 111

26. A. N. Tiwari, D. K. Pandya and K. L. Chopra, Thin Solid Films, 130 (1985) 217

27. S. K. Kim, W. J. Jeong, G. C. Park, Y. G. Back, Y. G. Jeong and Y. T. Yoo, Synthetic Metals, 71 (1995) 1747

28. S. Bini, K. Bindu, M. Lakshmi, C. Sudha Kartha, K. P. Vijayakumar, Y. Kashiwaba, T. Abe, Renewable Energy, 20 (2000) 405

29. D. Cahen and R. Noufi, A. Phys. Lett., 54 (1989) 558J.

30. Koichi Fukuzaki and Shigemi Kohiki, A. Phys. Lett. 77(17) (2000) 2713

31. Grzanna and H. Migge, J. Mat. Research, 12(2) (1997) 355

32. S. Bini, Ph. D Thesis, Cochin University of Science and Technology, Kochi (2003)

Chapter 6

Summary and conclusions

This chapter summarises the entire work discussed in the earlier chapters. The objective of the work is to characterize semiconducting thin films prepared in our laboratory for photovoltaic applications using Photoconductive Decay technique. PCD method is a simple and powerful technique to study energy levels in the band gap of semiconducting material. A major effect of trapping is to make the experimentally observed decay time of photocurrent, longer than carrier lifetime. If no trapping centers are present, observed photocurrent will decay in the same way as the density of free carriers and the observed decay time will be equal to carrier lifetime. If the density of free carriers is much less than the density of trapped carriers, the entire decay of photocurrent is effectively dominated by the rate of trap emptying rather than by rate of recombination. At a fixed temperature, the rise or decay of photoconductivity is controlled by the density of imperfections involved, capture cross-section and activation energy at that temperature. Hence presence of traps and trap parameters could be studied from lifetime measurements.

In the present study, the decay time of charge carriers was measured using photoconductive decay (PCD) technique. For the measurements at different temperatures, film was loaded in a liquid Helium cryostat and temperature was controlled using Lakshore Auto tuning temperature controller (Model 321). White light was used to illuminate the required area of the sample. Heat radiation from the light source was avoided by passing the light beam through a water filter. The decay current after switching off the illumination was

measured using a Kiethely 2000 multimeter. Sets of PCD measurements were taken by varying sample temperature, sample preparation temperature, thickness of the film, partial pressure of Oxygen and concentration of a particular element in a compound. Decay times were calculated using the rate window technique, which is a decay sampling technique particularly suited to computerized analysis. For PCD curves with two well-defined regions, two windows were chosen, one at the fast decay region and the other at the slow decay region. The curves in a particular window were exponentially fitted using Microsoft Excell 2000 programme.

PCD measurements were done on CdS, In_2Se_3, $CuInSe_2$ and CuInS thin films. CdS thin films were prepared using CBD technique. A set of three samples having thickness 1, 1.3 and 2 μm was used for the present study. Studies on these samples were categorized into two. The first category was the room temperature measurement of photoconductivity and photoconductivity decay time in vacuum and air. The second category was the study of variation of photoconductivity decay time with sample temperature. It was observed that there was two decay regions for the PCD curves: fast decay and slow decay regions. The corresponding decay times were named 'τ_f' and 'τ_s' respectively. Room temperature measurements revealed that for single and double dip films, surface recombination was more, where as it was less for triple dip film. Photoconductivity also increased as the film thickness increased. From the photoconductivity study at 300 K in air and vacuum, it was found that fast decay time was reduced (probably due to diffusion of Oxygen) when exposed to air. XPS analysis was done on this sample and was found that Oxygen was present only on the surface of the film. Fast decay time and photoconductivity increased when PCD measurements were done in vacuum. Again in vacuum measurements, both these parameters increased as the thickness increased, whereas thickness dependence was lost when the measurements were done in air.

Decay time variation with temperature was studied in a temperature range 100 – 300 K using rate window technique. Variation of τ_f and τ_s with temperature showed three well-defined peaks at 190 K, 250 K and 273 K with a shoulder around 295 K. The increase in

decay time was due to the release of carriers from different traps having activation energy corresponding to that temperature. Activation energies of these defects were calculated using TSC technique. Comparing with earlier reports, these defects were identified to be due to charge release from grain boundary defects, chloride ion in sulphide ion vacancy and cadmium sulphur vacancy complex. The significance of decay time variation study is that the prominence of defects at the surface and bulk can be understood. In most of the earlier reports, the initial fast decay region was neglected for the calculation of decay time stating that it was merely due to surface recombination. But our study revealed that this region gives information not only about surface recombination but also about other traps at the surface. The variation of the prominence of traps from surface to bulk and with thickness of the film was also reported in this study.

γ-In_2Se_3 thin films were prepared using Stacked Elemental Layer (SEL) technique. This preparation technique was very simple and non hazardous as Selenium was deposited using CBD technique. In this technique even the unreacted Selenium remaining in the solution, used for the preparation of Selenium film can be reused. In this experiment two sets of films were prepared – one set was prepared by varying sample preparation temperature, keeping all other preparation conditions same and the other set, by varying the amount of Indium in film, keeping preparation temperature and other parameters same.

In the first part of the work, room temperature measurements were done on samples prepared at different temperatures. In the second part, variation of decay time with sample temperature was studied on two sets of samples – one set, prepared at different preparation temperatures and other having different amount of Indium in the film. Photoconductivity studies revealed that 'is373' was most photo conducting. Steady state photocurrent and photoconductivity decay time at 300 K decreased as the sample preparation temperature increased. It is to be concluded that the density of traps decreased as the sample preparation temperature increased. Decay time measurement on samples indicated that here also there were two decay times τ_f and τ_s. Decay time variation with temperature showed that charge carriers were released from two defects having activation energy corresponding to

temperatures around 150 K and 300 K. The density of the defects, releasing charge carrier at 300 K was found to decrease on increasing sample preparation temperature. It was also observed that the release of charge carriers at 300 K increased with Indium concentration in the film. Dark conductivity measurements showed a sharp increase only at 300 K and activation energy of this defect is found to be 0.34 eV, while that of the defect, releasing charge carrier around 150 K was found to be 0.04 eV using TSC technique.

γ-In_2Se_3 film is a promising window material for solar cells. Its photoconductivity, decay time of charge carriers and resistance could be properly chosen by varying the sample preparation temperature. Through this study we found that the sample prepared at 373 K was most photoconducting.

$CuInSe_2$ was prepared using Stacked Elemental Layer (SEL) technique. Chemical Bath Deposited (CBD) amorphous Selenium thin film was used for the preparation of $CuInSe_2$ films, which avoided the use of Selenium vapor or H_2Se gas, which was highly toxic. Both p-type and n-type $CuInSe_2$ films could be prepared by varying the amount of Cu in the film. In this chapter the variation of nature of photoconductivity with Cu concentration in the film was studied. Room temperature photoconductivity and decay time of charge carriers in each sample were measured. The variation of decay time with sample temperature was measured in p-type samples.

Photoconductivity measurements done on $CuInSe_2$ films having different Cu/In ratio revealed that as the Copper content in the film decreased, photoconductivity changed from negative to positive. Photoconductivity was more for 'CIS 0.45' than 'CIS 0.9'. The variation of decay time with temperature measurements of 'CIS 0.45' showed an increase of decay time around 150 K and 300 K indicating the release of carriers from two types of defects at these temperatures.

$CuInS_2$ samples were prepared using spray pyrolysis technique A set of samples was prepared by varying Cu/In molar ratio 0.5, 1 and 1.5 in the solution, keeping S:Cu molar ratio constant at 4. Another set was prepared by varying S/Cu molar ratio from 5 to 8 keeping

Cu/In molar ratio at 0.5. Photoconductivity measurements revealed that the film prepared from the solution having Cu/In molar ratio 0.5 (Cu/In ratio 1:1 in the film) was most photo conducting. On varying S/Cu molar ratio from 4 to 8 in the solution, it was found that film prepared from solution having molar ratio S/Cu=5 was most photo conducting. All films showed an oscillatory nature of photoconductivity when the measurements were taken in air, whereas this nature disappeared when the measurements were done in vacuum. On keeping the sample in vacuum for longer time before measurement, photoconductivity was found to be decreasing.

The over all conclusion of the study is that PCD method is a simple and powerful technique to study levels in the band gap of a semiconducting material. The significance of decay time variation study with temperature is that the prominence of defects at the surface and bulk can be understood. Our study revealed that this region gives information not only about surface recombination but also about other traps at the surface. The variation of the prominence of traps from surface to bulk and with thickness of the film could be studied using this technique. The preparation conditions of the materials developed in our laboratory for photovoltaic applications could be optimized using the results obtained from these studies. The study of the effect of ambient conditions on photoconductivity and decay time helps in the designing of the solar cell.

List of Publications

1. Minority carrier lifetime variation study in CBD CdS thin films by photoconductive decay method.

   S. B. Syamala, K. P. Vijayakumar, C. Sudha Kartha.

   Solid State Physics Symposium – 2000, Guru Ghasidas University, Bilaspur.

2. Photo electronic investigation of traps in CBD CdS thin films using thermally stimulated conductivity.

   R. R. Pai, **S. B. Syamala**, K. P. Vijayakumar, C. Sudha Kartha. Mo-P 47, Tenth International Conference on II-VI compounds, Bremen, Germany 2001.

3. Effect of impurities and temperature on photoconductivity and carrier lifetime in CBD CdS thin films.

   S. B. Syamala, Rupa R. Pai, K. P. Vijayakumar, C. Sudha Kartha, T. Abe, Y. Kashiwaba.

   Workshop on Complete cycle characterization of materials 2001, MRSI and IGCAR, Kalpakkam, India.

4. Photo conductivity measurements on γ-$In_2 Se_3$ thin films.

   S. B. Syamala, K. Bindu, K. P. Vijayakumar, C. Sudha Kartha.

   Symposium on perspectives in materials characterization 2002, MRSI and DMRL Hyderabad, India.

5. Effect of trap levels on photo conductivity decay time in CdS thin films prepared using CBD technique.

   S. B. Syamala, Roopa R. Pai, K. P. Vijayakumar, C. Sudha Kartha.

   National Seminar on Recent Trends in Optoelectronic materials and devices 2002, Sri Venkateswara University, Thirupathi.

6. Thermally stimulated conductivity studies on γ-In_2Se_3 thin films.

   Roopa R.Pai, K. C. Wilson, **S. B. Syamala**, K. Bindu, K. P. Vijayakumar, C. Sudha Kartha

   National Seminar on Recent Trends in Optoelectronic materials and devices 2002, Sri Venkateswara University, Thirupathi.

7. Effect of preparation temperature on photoconductivity and photoconductivity decay time in γ-$In_2 Se_3$ thin films.

   S. B. Syamala, K. Bindu, Roopa R Pai, K. P. Vijayakumar, C. Sudha Kartha. International Conference, 2nd Mongolian Photovoltaic Conference, Ulaanbaatar, Mongolia, 2003.

Papers communicated

1. Photoconductivity studies on γ-$In_2 Se_3$ thin films prepared at different temperatures using CBD Se films.

   S. B. Syamala, K. Bindu, Rupa. R. Pai, K. P. Vijayakumar and C. Sudha Kartha, Semicon. Sci. and Technology.

2. Photoconductivity decay studies on $CuInS_2$ thin films varying Cu/In and S/Cu ratio.

   S. B. Syamala, S. Bini, Teny Theresa John, K. P. Vijayakumar and C. Sudha Kartha, Semicon. Sci. and Technology.

3. Negative photoconductivity studies on $CuInSe_2$ thin films prepared using SEL technique.

   S. B. Syamala, K. Bindu, K. P. Vijayakumar and C. Sudha Kartha, Renewable Energy.

List of symbols and abbreviations

α	absorption coefficient
β	capture coefficient
ϕ_o	number of photons
η	solar cell efficiency
μ	mobility
μ_n	mobility of electron
μ_p	mobility of hole
μ_g	effective mobility
μ_{gn}	effective mobility of electron
μ_{gp}	effective mobility of hole
ν	frequency
ρ	resistivity
σ	conductivity
$\Delta\sigma$	change in conductivity
τ	lifetime
τ_n	lifetime of electrons
τ_p	lifetime of holes
τ_f	fast decay time
τ_s	slow decay time
ω	angular modulation frequency
a -Se	amorphous Selenium
B	applied magnetic field
D_n	diffusion coefficient
d	thickness
E	applied electric field

E_c	energy corresponding to the bottom of the conduction band
E_v	energy corresponding to the top of the valence band
E_F	Fermi energy
E_g	band gap energy
E_{Gd}	direct band gap energy
E_{Gi}	indirect band gap energy
E_{phonon}	energy of phonon
E_1, E_2	impurity levels above valence band or below conduction band
e	electron charge
G	rate of generation
I	intensity of light
i_{po}	steady state photo current
J_{sc}	current density
K	Kelvin
k	Boltzman's constant
L	diffusion length
N_a	density of absorbing centers at the surface
N_c	density of states in conduction band
N_v	density of states in valence band
n	density of electron/density of photo excited charge carriers
Δn	change in density of electron
n_t	density of traps that must empty in order for the steady state Fermi energy to drop by kT
p	density of hole
Δp	change in density of hole
S	capture cross-section
S_a	rate of recombination of electrons and holes at surface
S_o	optical cross-section

s	surface recombination velocity
R	rate of recombination
R_c	capture rate
R_d	thermal detrapping rate
R_o	reflection coefficient
R_L	high resistance
R_d	dark resistance of the sample
R_{ill}	resistance of the sample on illumination
$S(V)$	signal response
T	temperature
t	time
V_{oc}	open circuit voltage
v	thermal velocity
ac	alternating current
CBD	Chemical Bath Deposition
DC	Dark Current
dc	direct current
DLTS	Deep Level Transient Spectroscopy
MBE	Molecular Beam Epitaxy
OCVD	Open Circuit Voltage Decay
PCD	Photoconductive Decay
PEM	Photo Electromagnetic Effect
PPC	Persistent Photoconductivity
I_{PEM}	increase of current due to PEM effect
V_{PEM}	open circuit voltage due to PEM effect
RFPCD	Radio Frequency Photoconductive Decay
SEL	Stacked Elemental Layer
TSC	Thermally Stimulated Current
XPS	X-ray Photo electron Spectroscopy